

Open camera or QR reader and
scan code to access this article
and other resources online.



REVIEW

Imaging Findings in Acute Traumatic Brain Injury: a National Institute of Neurological Disorders and Stroke Common Data Element-Based Pictorial Review and Analysis of Over 4000 Admission Brain Computed Tomography Scans from the Collaborative European NeuroTrauma Effectiveness Research in Traumatic Brain Injury (CENTER-TBI) Study

Thijs Vande Vyvere,^{1,2,*,**} Dana Pisciă,^{3,4,**} Guido Wilms,⁵ Lene Claes,⁶ Pieter Van Dyck,^{1,2} Annemiek Snoeckx,^{1,2} Luc van den Hauwe,¹ Pim Pullens,⁷ Jan Verheyden,⁶ Max Wintermark,⁸ Sven Dekeyzer,^{1,9} Christine L. Mac Donald,^{10,11} Andrew I.R. Maas,^{12,13,***} and Paul M. Parizel^{14,***},
and The CENTER-TBI Participants and Investigators^{****}

Abstract

In 2010, the National Institute of Neurological Disorders and Stroke (NINDS) created a set of common data elements (CDEs) to help standardize the assessment and reporting of imaging findings in traumatic brain injury (TBI). However, as opposed to other standardized radiology reporting systems, a visual overview and data to support the proposed standardized lexicon are lacking. We used over 4000 admission computed tomography (CT) scans of patients with TBI from the Collaborative European NeuroTrauma Effectiveness Research in Traumatic Brain Injury (CENTER-TBI) study to develop an extensive pictorial overview of the NINDS TBI CDEs, with visual examples and background information on individual pathoanatomical lesion

¹Department of Radiology, ¹²Department of Neurosurgery, Antwerp University Hospital, Antwerp, Belgium.

²Department of Molecular Imaging and Radiology (MIRA), ¹³Department of Translational Neuroscience, Faculty of Medicine and Health Science, University of Antwerp, Antwerp, Belgium.

³Department of Neurosurgery, ⁴Department of Public Health, Erasmus MC - University Medical Center Rotterdam, Rotterdam, the Netherlands.

⁵Department of Radiology, University Hospitals Leuven, Leuven, Belgium.

⁶icomatrix, Research and Development, Leuven, Belgium

⁷Department of Imaging, University Hospital Ghent; IBITech/MEDISIP, Engineering and Architecture, Ghent University; Ghent Institute for Functional and Metabolic Imaging, Ghent University, Belgium.

⁸Department of Neuroradiology, University of Texas MD Anderson Center, Houston, Texas, USA.

⁹Department of Radiology, University Hospital Ghent, Belgium.

¹⁰Department of Neurological Surgery, School of Medicine, Harborview Medical Center, Seattle, Washington, USA.

¹¹Department of Neurological Surgery, School of Medicine, University of Washington, Seattle, Washington, USA.

¹⁴Department of Radiology, Royal Perth Hospital (RPH) and University of Western Australia (UWA), Perth, Australia; Western Australia National Imaging Facility (WA NIF) node, Australia.

**Shared first authors.

***Shared last authors.

****The CENTER-TBI Participants and Investigators may be found at the end of this article.

*Address correspondence to: *Thijs Vande Vyvere, PhD, Department of Radiology, Antwerp University Hospital, Drie Eikenstraat 655, Edegem 2650, Belgium* E-mail: thijs.vandevyvere@uza.be

© Thijs Vande Vyvere et. al 2024; Published by Mary Ann Liebert, Inc. This Open Access article is distributed under the terms of the Creative Commons License (CC-BY) (<http://creativecommons.org/licenses/by/4.0>), which permits unrestricted use, distribution, and reproduction in any medium, provided the original work is properly credited.

types, up to the level of supplemental and emerging information (e.g., location and estimated volumes). We documented the frequency of lesion occurrence, aiming to quantify the relative importance of different CDEs for characterizing TBI, and performed a critical appraisal of our experience with the intent to inform updating of the CDEs. In addition, we investigated the co-occurrence and clustering of lesion types and the distribution of six CT classification systems. The median age of the 4087 patients in our dataset was 50 years (interquartile range, 29-66; range, 0-96), including 238 patients under 18 years old (5.8%). Traumatic subarachnoid hemorrhage (45.3%), skull fractures (37.4%), contusions (31.3%), and acute subdural hematoma (28.9%) were the most frequently occurring CT findings in acute TBI. The ranking of these lesions was the same in patients with mild TBI (baseline Glasgow Coma Scale [GCS] score 13-15) compared with those with moderate-severe TBI (baseline GCS score 3-12), but the frequency of occurrence was up to three times higher in moderate-severe TBI. In most TBI patients with CT abnormalities, there was co-occurrence and clustering of different lesion types, with significant differences between mild and moderate-severe TBI patients. More specifically, lesion patterns were more complex in moderate-severe TBI patients, with more co-existing lesions and more frequent signs of mass effect. These patients also had higher and more heterogeneous CT score distributions, associated with worse predicted outcomes. The critical appraisal of the NINDS CDEs was highly positive, but revealed that full assessment can be time consuming, that some CDEs had very low frequencies, and identified a few redundancies and ambiguity in some definitions. Whilst primarily developed for research, implementation of CDE templates for use in clinical practice is advocated, but this will require development of an abbreviated version. In conclusion, with this study, we provide an educational resource for clinicians and researchers to help assess, characterize, and report the vast and complex spectrum of imaging findings in patients with TBI. Our data provides a comprehensive overview of the contemporary landscape of TBI imaging pathology in Europe, and the findings can serve as empirical evidence for updating the current NINDS radiologic CDEs to version 3.0.

Keywords: neuroimaging; NIH/NINDS Common Data Elements; structured reporting; traumatic brain injury

Introduction

Patients who suffer a traumatic brain injury (TBI) are initially assessed clinically using the Glasgow Coma Scale (GCS), which broadly categorizes them into “mild TBI” (GCS score 13-15), “moderate TBI” (GCS score 9-12) or “severe TBI” (GCS score <9; Supplementary Table S1).¹ Despite its utility in the clinical and research setting,² this classification is unidimensional and relatively crude. The terms mild, moderate, and severe TBI may lead to treatment bias (e.g., nihilism in severe TBI and disregard for the adverse long-term consequences of mild TBI). Importantly, patients and their families object to the use of these terms. A more refined and multi-dimensional approach to characterization of TBI is required.

Neuroimaging studies play a pivotal role in the diagnosis, management, and clinical outcome prediction of brain-injured patients, and can contribute to a better characterization of TBI.³ In the acute phase post-injury, non-contrast computed tomography (CT) is the preferred imaging modality in adults, primarily due to its cost-effectiveness, speed, widespread accessibility, and sensitivity in detecting a broad spectrum of injuries affecting the skull, brain, and blood vessels.³ CT is eminently suited to identify pathological conditions that may require surgery or other urgent interventions, such as intracranial pressure (ICP)-lowering therapies. Magnetic

resonance imaging (MRI), however, is more sensitive in detecting subtle hemorrhagic lesions such as microbleeds, small traces of subarachnoid hemorrhage, as well as certain non-hemorrhagic abnormalities such as edema, ischemia, and distinct forms of axonal injuries and contusions.³ As a consequence, it can better reveal the full lesion burden of TBI.

Depending on the magnitude and direction of external forces to the head, a vast spectrum of findings can be encountered on both standard and advanced neuroimaging.⁴⁻⁹ Individual findings may vary according to location (e.g., temporal, frontal), anatomical compartment (e.g., intra-axial, extra-axial), pattern (focal vs. diffuse), temporality (primary vs. secondary injury) and extent (e.g., small vs. large) and may be solitary or coexist in various combinations with other findings. In the clinical setting, the interpretation of neuroimaging studies is predominantly visual, qualitative, and subjective. Findings are reported in narrative form, with different physicians often using different terminology for the same pathoanatomic lesion type (e.g., extradural collection, epidural hematoma, extradural hematoma, etc.). Substantial observer differences have been reported, even between expert neuroradiologists.^{10,11} Such reporting inconsistencies are then perpetuated and potentially enhanced when transferring imaging reports in study databases for research purposes, with negative

implications for data sharing, harmonization, aggregation, and interpretation across studies.

To address these issues, a multi-disciplinary task force, led by the National Institutes of Health (NIH)-National Institute of Neurological Disorders and Stroke (NINDS), created in 2010 a set of common data elements (CDEs) with practical operational definitions and standardized terminology for reporting imaging findings in TBI.^{12,13} These data elements were then updated to version 2 (v.2) in 2013.¹⁴ A structured interpretation scheme was proposed, with an outside-in approach (i.e., from the skull inward) of inspecting and reporting findings. Information on each individual lesion or encountered abnormality can be reported by tiers of increasing detail and complexity: 1) core information, relating to whether the lesion or abnormality in question is present, absent or indeterminate; 2) supplemental-highly recommended information, relating to extent and anatomic location; and 3) emerging information, relating to in-depth measurements of specific features, often performed with computer-aided image analysis.^{12,13} We note that, in contrast to the clinical TBI CDEs, these designations relate to the detail of scoring, and not to the relative importance of radiologic CDEs.

Standardized reporting of neuroimaging findings, using the CDE recommendations, substantially minimizes inter- and intra-observer variability in research settings, for both CT and MRI.^{15,16} Moreover, with adequate training by experienced neuroradiologists, non-physician researchers (e.g., neuropsychologists, neuroscientists, etc.) can also reliably interpret and report CDEs.¹⁶ As such, TBI CDEs have a great potential to increase neuroimaging reporting quality, in both clinical and research settings. However, the CDE recommendations were published strictly as a written guide, without the support of illustrated cases and data. This is in contrast to other imaging classification systems, such as the widely used BI-RADS (Breast Imaging-Reporting and Data System), or PI-RADS (Prostate Imaging Reporting and Data System), which are supported by visual examples to increase clarity, maximize adoption, and further decrease reporting variability.¹⁷⁻²⁰

The large-scale Collaborative European NeuroTrauma Effectiveness Research in Traumatic Brain Injury (CENTER-TBI) study has created one of the largest neuroimaging repositories in the world and implemented scan interpretation and reporting according to the CDEs. Based on this experience we aim to: 1) present an extensive pictorial overview of TBI neuroimaging CDEs, with visual examples and background information; 2) report the frequencies of core, supplemental, and emerging CDEs of observed findings on more than 4000 admission CTs of patients with acute TBI; and 3) explore clustering of core CDEs (pathoanatomic

entities) across TBI severities (mild TBI, defined by baseline GCS score 13-15, and moderate-severe TBI defined by baseline GCS score 3-12). This empirical evidence will provide both an educational resource for clinicians and researchers, and a comprehensive overview of the neuroimaging case-mix of contemporary TBI patients in the European landscape. Further, it provides an empirical evidence base to inform updating of the CDEs to version 3.0.

Methods

Study population

The CENTER-TBI study was a prospective, longitudinal, observational study (ClinicalTrials.gov, NCT02210221), conducted between December 2014 and December 2017 in over 60 centers across Europe and Israel.²¹ The study recruited patients within 24h of injury, with a clinical diagnosis of TBI, a clinical indication for CT imaging based on the judgment of the treating team, and no severe pre-existing neurologic disorders that could confound outcome assessment.²¹ The majority of participating centers were referral centers for neurotrauma. Consequently, the population studied may not be readily generalizable to community hospital settings. Further, pediatric patients are underrepresented, as most centers mainly focused on adult TBI.

Central scan interpretation and reporting process

Interpretable admission CT datasets were forwarded to a neuroimaging repository and centrally assessed by trained investigators using NINDS CDE-based standardized templates, under the supervision of an expert neuroradiologist. The central review methodology has been described in detail elsewhere.¹⁶ The pathoanatomic lesion types assessed are listed in Table 1. Apart from the NINDS CDEs, the CENTER-TBI CDE reporting template included brain herniation and cortical sulcus effacement as distinct lesion types, and an extra item to record incidental neuroimaging findings, of potential interest in the context of TBI. Some types of incidental findings were preset choices (e.g., old stroke, prior TBI, normal/abnormal prominent ventricles), but reviewers could also add free text remarks. Free text was mostly used to give extra information regarding interpretation decisions or to add information when the readers felt that certain options were lacking in the standard CDE templates. As part of the structured reporting in CENTER-TBI, we also graded the admission CTs according to the Rotterdam, Marshall and Helsinki classification systems, and the Fisher, Morris-Marshall, and Greene CT grading systems for quantification of traumatic subarachnoid hemorrhage (tSAH).

Table 1. Occurrence of Pathoanatomic Lesion Types on Admission CT in CENTER-TBI

Pathoanatomic lesion type (TBI CDE core information)	NIH/NINDS CDE ID	All TBIs	Mild TBI*	Moderate-severe TBI*	χ^2 p value	Classification	
		N = 4087	N = 2744	N = 1193		Primary/ secondary	Focal/ diffuse
Skull fracture (%)	C02463	1529 (37.4)	728 (26.5)	731 (61.3)	< 0.001	Primary	Focal/diffuse
Epidural hematoma (%)	C02427	463 (11.3)	228 (8.3)	214 (17.9)	< 0.001	Primary	Focal
Extraxial hematoma (%)	C02430	24 (0.6)	8 (0.3)	13 (1.1)	0.003	Primary	Focal/diffuse
Subdural hematoma, acute (%)	C02472	1183 (28.9)	500 (18.2)	633 (53.1)	< 0.001	Primary	Focal/diffuse
Subdural hematoma, subacute or chronic (%)	C02476	22 (0.5)	16 (0.6)	5 (0.4)	0.681	Primary	Focal/diffuse
Subdural hematoma, mixed density (%)	C02480	86 (2.1)	43 (1.6)	39 (3.3)	0.001	Primary	Focal/diffuse
Traumatic subarachnoid hemorrhage (%)	C02469	1852 (45.3)	840 (30.6)	927 (77.7)	< 0.001	Primary	Focal/diffuse
Vascular dissection (%)	C02489	2 (0.0)	1 (0.0)	0 (0.0)	1.000	Primary	Focal
Traumatic aneurysm (%)	C02484	1 (0.0)	1 (0.0)	0 (0.0)	1.000	Primary	Focal
Venous sinus injury (%)	C02491	0 (0.0)	0 (0.0)	0 (0.0)	NA	Primary	Focal
Midline shift (%)	C02455	470 (11.5)	107 (3.9)	341 (28.6)	< 0.001	Secondary	Focal
Cisternal compression (%)	C02410	652 (16.0)	130 (4.7)	485 (40.7)	< 0.001	Secondary	Focal
Ventricular shift/effacement (%)	C02435	591 (14.5)	129 (4.7)	431 (36.1)	< 0.001	Secondary	Focal
Contusion (%)	C02414	1280 (31.3)	540 (19.7)	677 (56.7)	< 0.001	Primary	Focal/diffuse
Intracerebral hemorrhage (%)	C02440	126 (3.1)	39 (1.4)	80 (6.7)	< 0.001	Primary	Focal
Intraventricular hemorrhage (%)	C02446	491 (12.0)	121 (4.4)	347 (29.1)	< 0.001	Primary/ secondary	Focal
Diffuse and traumatic axonal injury (%)	C02420/21	336 (8.2)	104 (3.8)	216 (18.1)	< 0.001	Primary	Focal/diffuse
Penetrating injury (%)	C02459	18 (0.4)	5 (0.2)	12 (1.0)	0.001	Primary	Focal/diffuse
Cervicomedullary/brainstem injury (%)	C02407	5 (0.1)	0 (0.0)	5 (0.4)	0.004	Primary/ secondary	Focal/diffuse
Cerebral edema (%)	C02424	56 (1.4)	4 (0.1)	49 (4.1)	< 0.001	Secondary	Focal/diffuse
Brain swelling/hyperemia (%)	C02404	14 (0.3)	0 (0.0)	14 (1.2)	< 0.001	Secondary	Focal/diffuse
Ischemia (%)	C02451	4 (0.1)	0 (0.0)	4 (0.3)	0.013	Secondary	Focal/diffuse
Pathoanatomic lesion types currently not in the CDEs but collected extra in CENTER-TBI							
Brain herniation (%)		390 (9.5)	85 (3.1)	285 (23.9)	< 0.001	Primary/ secondary	Focal/diffuse
Cortical sulcus effacement (%)		459 (11.2)	113 (4.1)	319 (26.7)	< 0.001	Secondary	Focal/diffuse
Incidental findings (%)		622 (15.2)	451 (16.4)	155 (13.0)	0.007		

The data contains no missing values.

*Mild TBI was defined by baseline Glasgow Coma Scale (GCS) score 13-15, regardless of presence of CT abnormalities. Moderate-severe TBI was defined by baseline GCS score 3-12. The baseline GCS score used for classification was a derived variable calculated centrally for baseline risk adjustment. It represents the post-stabilization GCS value, which was imputed when absent using IMPACT methodology: work back in time towards pre-hospital value until a non-missing value is found.

CDE, common data element; CENTER-TBI, Collaborative European NeuroTrauma Effectiveness Research in Traumatic Brain Injury; CT, computed tomography; NA, not applicable; NIH/NINDS, National Institutes of Health/National Institute of Neurological Disorders and Stroke; TBI, traumatic brain injury.

For pathoanatomic lesion types with size as a supplemental CDE, the recommendations state reporting volume or length, width, and maximal thickness. In CENTER-TBI, these lesions were measured by volume, calculated using the width \times depth \times length \times 0.5 formula (ABC/2; Supplementary Fig. S1). For subdural hematomas in particular, the width was chosen on an axial slice of average width, and not on the slice of largest width, to avoid overestimation of non-ellipsoid volumes. Data inconsistencies, such as discrepancies in timing and naming of the scans, were addressed through diligent data curation efforts.

Statistical analysis

Characteristics of the study sample. Demographic and injury characteristics are reported for the entire study sample and separately for patients with mild (defined

by baseline GCS score 13-15, regardless of presence of CT abnormalities) and moderate-severe TBI (defined by baseline GCS score 3-12).

Occurrence of pathoanatomic lesion types. The absolute and relative frequencies of pathoanatomic lesion types included in the TBI CDEs reporting scheme are reported for admission CTs of all patients and separately for patients with mild and moderate-severe TBI. Additionally, we reported the occurrence of pathoanatomic lesion types for patients at the extremes of the GCS-based severity spectrum: the subgroup of patients with baseline GCS score 3 and the subgroup with baseline GCS score 15.

Individual pathoanatomic lesion types. We then elaborated on each individual pathoanatomic lesion type,

following the proposed “outside-in” approach. For each type of lesion, we first provided background information, including definitions and aspects on non-contrast CT. Descriptive analyses for each type of lesion were reported and summarized following the CDEs information tiers, and are accompanied by definitions and typical pictorial examples, along with diagnostic insights, explanatory text on clinical implications of specific findings and imaging recommendations where appropriate. An initial set of pictorial examples was selected during the central review process in CENTER-TBI by the principal central reader and an expert neuroradiologist. Subsequently, this set of images was reviewed by a neurosurgeon with extensive expertise in TBI. In instances where the clarity or representativeness of the images was deemed insufficient, a consensus was reached to substitute with an alternative image. Subsequently, the refined set of images underwent final scrutiny and was disseminated to the remaining co-authors, including expert neuroradiologists, for approval.

Core information relating to lesion occurrence and multiplicity was provided for all patients, and separately for patients with mild and moderate-severe TBI. Because of lesion multiplicity for some types of findings (e.g., multiple contusions in a single patient), supplemental and emerging information was reported at lesion-level for individual lesions identified in all patients, and separately for lesions identified in patients with mild and moderate-severe TBI. Supplemental and emerging information was reported as absolute and relative frequencies for categorical variables and medians and interquartile ranges (IQR) for continuous variables. Often, supplemental and emerging information categories are not exclusive, so an individual lesion may present multiple such characteristics simultaneously (e.g., a lesion extending in multiple locations). Such information was depicted in UpSet and polar plots. UpSet plots show the combinations in which characteristics co-occur, the absolute frequencies of these combinations (vertical bars) and the absolute frequencies of each individual characteristic (horizontal bars). The polar plot can be seen as a circular bar chart, with variable categories listed on the circumference and the length of each sector corresponding to the number of lesions which display that characteristic. Supplemental information relating to lesion extent (volume) was visualized using histograms. No descriptive statistics were provided for pathoanatomic lesion types observed less than 20 times in the entire sample.

Co-occurrence and clustering of pathoanatomic lesion types. Correlations between pairs of pathoanatomic lesions in the CENTER-TBI dataset were depicted using a heatmap, with corresponding phi correlation coefficients. Pathoanatomic lesion co-occurrence was visualized using UpSet plots, separately for patients with mild

and moderate-severe TBI. For a summary description of the most frequent findings, combinations of the four most frequently observed lesion types across all severities and the corresponding 6-months post-injury Glasgow Outcome Scale-Extended (GOSE)²² scores of patients exhibiting these combinations were visualized using an UpSet plot.

In addition, hierarchical cluster analysis was performed to identify clusters of pathoanatomic lesions that tend to co-exist in the mild and moderate-severe TBI subgroups with positive CT findings, using the R package ClustOfVar.²³ Each core CDE (as a binary variable, lesion present/absent) was first set in its own cluster. The algorithm performed ascendant hierarchical clustering, selecting at each step the two most similar clusters to merge. Similarity between any two clusters was measured by the loss of homogeneity if the two were merged. Cluster homogeneity (i.e., how strongly the variables inside a cluster are related to its center) was calculated as the sum of the correlation ratios between all the cluster variables and the cluster center. The cluster center, a synthetic quantitative variable, is the first principal component from multiple correspondence analysis applied to all the variables in the cluster.²³ Results of the cluster analyses were summarized using dendrograms.

The relative distribution of admission CT scores according to the Rotterdam, Marshall, Helsinki, Fisher, Morris-Marshall, and Greene CT systems in mild and moderate-severe TBI was visualized using bar plots. The relative distribution of 6 months post-injury GOSE scores within the categories of each CT score was visualized using bar plots.

Differences in demographic and injury characteristics, and pathoanatomic lesion occurrence between patients with moderate-severe TBI and patients with mild TBI were tested using Mann-Whitney U tests for continuous variables and χ^2 statistics for categorical variables. The same respective tests were used to test differences in the distribution of supplemental and emerging characteristics at lesion-level, between individual lesions observed in patients with moderate-severe TBI and individual lesions observed in patients with mild TBI.

Analyses were performed using R (version 4.0.3) and RStudio (version 2022.7.1.554). When testing differences between patient and lesion subgroups, two-sided $p < 0.05$ was considered statistically significant. Given the exploratory nature of our study, no corrections for multiple comparisons were made.

Results

Characteristics of the study sample

Of 4509 patients enrolled in CENTER-TBI, 4087 had an available and interpretable admission CT and were included in the analysis. The median age was 50 years (IQR, 29-66; range, 0-96) and 238 patients were under

the age of 18 (5.8%). Two-thirds of patients were male, the most common cause of injury was an incidental fall (46%), and the most common mechanism of injury was a ground level fall (24%). A major extracranial injury (any extracranial injury with an Abbreviated Injury Scale score ≥ 3) was present in 37% of patients. The majority of patients were admitted to hospital, either to the ward (34%) or intensive care unit (ICU; 46%).

Based on the recorded baseline GCS score, 2744 patients had mild TBI (of whom 77% with GCS 15, 17% with GCS 14, and 6% with GCS 13) and 1193 moderate-severe TBI (of whom 72% with GCS 3-8 and 28% with GCS 9-12). Patients with moderate-severe TBI were on average younger (median 47 years, IQR 27-64 vs. median 52 years, IQR 31-67, $p < 0.001$), more frequently male (73% vs. 64%, $p < 0.001$), had different distributions of injury causes and mechanisms (Table 2), as well as more frequent major extracranial injury (57% vs. 28%, $p < 0.001$), compared with patients with mild TBI. The most frequent cause of injury was a road traffic incident in the moderate-severe TBI subgroup (47%) and an incidental fall in the mild TBI subgroup (50%). The most frequent mechanism of injury was

high velocity (acceleration/deceleration) trauma in the moderate-severe TBI subgroup (28%) and ground level fall in the mild TBI subgroup (28%). The vast majority of patients with moderate-severe TBI were admitted to the ICU (94%). Of the patients with mild TBI, 47% were admitted to the ward, 29% were discharged home from the emergency department and 24% were admitted to the ICU (Table 2).

Occurrence of pathoanatomic lesion types

Of the 4087 admission CTs we reviewed, 1520 (37%) were negative, with none of the NINDS TBI core CDEs observed. These included 221 scans with isolated incidental findings, such as (abnormal) prominent ventricles, old strokes, and anatomical variants. While the proportion of negative scans was low in patients with moderate-severe TBI (81/1193, 7%), more than half of patients with mild TBI had a negative admission CT scan (1399/2744, 51%).

Considering both negative scans and those on which only isolated skull fracture(s) were reported, a total of 1652/4087 admission CTs (40%) were negative for intracranial pathology. The proportion of scans negative for intracranial pathology was considerably lower in patients

Table 2. Characteristics of the Study Sample

	All TBIs N = 4087	Mild TBI* N = 2744	Moderate-severe TBI* N = 1193	p value**	Missing
Age, years (median [IQR])	50 [29, 66]	52 [31, 67]	47 [27, 64]	< 0.001	0.0
Male sex (%)	2735 (66.9)	1767 (64.4)	868 (72.8)	< 0.001	0.0
Cause of injury (%)				< 0.001	2.3
Road traffic incident	1539 (38.5)	946 (34.9)	546 (47.4)		
Incidental fall	1850 (46.3)	1349 (49.8)	445 (38.6)		
Other non-intentional injury	221 (5.5)	153 (5.7)	51 (4.4)		
Violence/assault	206 (5.2)	158 (5.8)	42 (3.6)		
Act of mass violence	4 (0.1)	4 (0.1)	0 (0.0)		
Suicide attempt	45 (1.1)	15 (0.6)	27 (2.3)		
Other	128 (3.2)	82 (3.0)	42 (3.6)		
Mechanism of injury (%)				< 0.001	4.8
High velocity trauma (acceleration/deceleration)	772 (19.9)	428 (16.1)	311 (28.1)		
Direct impact: blow to head	337 (8.7)	269 (10.1)	60 (5.4)		
Direct impact: head against object	338 (8.7)	251 (9.5)	72 (6.5)		
Ground level fall	923 (23.7)	729 (27.5)	179 (16.2)		
Fall from height >1 m/5 stairs	716 (18.4)	453 (17.1)	232 (20.9)		
Other closed head injury	94 (2.4)	57 (2.2)	35 (3.2)		
Combined mechanism of injury	709 (18.2)	464 (17.5)	219 (19.8)		
Baseline GCS Score (median [IQR])	15 [10, 15]	15 [15, 15]	6 [3, 9]	< 0.001	3.7
Major extracranial injury*** (%)	1500 (36.7)	759 (27.7)	677 (56.7)	< 0.001	0.0
Admission stratum (%)				< 0.001	0.0
Emergency department	808 (19.8)	789 (28.8)	5 (0.4)		
Ward	1396 (34.2)	1298 (47.3)	69 (5.8)		
Intensive care unit	1883 (46.1)	657 (23.9)	1119 (93.8)		
Clinical deterioration**** (%)	982 (24.0)	322 (11.7)	612 (51.3)	< 0.001	0.0

*Mild TBI was defined by baseline GCS score 13-15, regardless of presence of computed tomography (CT) abnormalities. Moderate-severe TBI was defined by baseline GCS score 3-12. The baseline GCS score used for classification was a derived variable calculated centrally for baseline risk adjustment. It represents the post-stabilization GCS value, which was imputed when absent using IMPACT methodology: work back in time towards pre-hospital value until a non-missing value is found.

**p values derived from χ^2 statistics for categorical variables and Mann-Whitney U tests for continuous variables, comparing patients with mild TBI vs. patients with moderate-severe TBI.

***Any extracranial injury with an Abbreviated Injury Scale score ≥ 3 .

****Including GCS score deterioration of 1 point or more within 1 hour of presentation, any episode of neuroworsening during intensive care unit (ICU) or hospital stay and clinical deterioration as reason for ICU admission or surgical intervention.

GCS, Glasgow Coma Scale; IQR, interquartile range; TBI, traumatic brain injury.

with moderate-severe TBI compared with patients with mild TBI (98/1193 vs. 1508/2744; 8% vs. 55% respectively, $p < 0.001$).

In Table 1, we present the core TBI CDEs and their distribution, as well as three additional elements, in the entire CENTER-TBI dataset and separately for mild and moderate-severe TBI. The four most frequently observed lesion types across all severities were tSAH (45%), skull fracture (37%), contusion (31%), and acute subdural hematoma (aSDH; 29%). The frequency of occurrence of all other CDEs was much lower, ranging from 0 to 16%. For the top four CDEs, the order of frequencies was the same for patients with mild and those with moderate-severe TBI, but the relative frequencies were up to three times higher in moderate-severe TBI (Table 1). Of the 2567 patients with a positive scan (at least one core CDE present), only 89 (3%) did not exhibit any of the top four most common CDEs (Fig. 1). The majority of patients presented with various combinations of the top 4 CDEs, the most frequent of which was all 4 lesion types simultaneously present (20% of positive scans), followed by isolated tSAH (12% of positive scans). When looking at 6 months post-injury outcomes in subgroups of patients with each of the four top CDEs present (Fig. 1, horizontal bars), the highest percentages of mortality and GOSE scores ≤ 4 were observed in the subgroup of patients with aSDH present, isolated or in various combinations with other lesion types (23% mortality, 40% GOSE score ≤ 4).

Additional pathoanatomic findings related to mass effect were at least 7 to 8 times more frequent in moderate-severe TBI than mild TBI (e.g., midline shift [MLS] 29% in moderate-severe TBI vs. 4% in mild TBI, $p < 0.001$; cisternal compression 41% vs. 5%, $p < 0.001$; ventricular effacement 36% vs. 5%, $p < 0.001$; brain herniation 24% vs. 3%, $p < 0.001$). Certain lesion types occurred almost exclusively in moderate-severe TBI, such as cerebral edema, cervicomedullary/brainstem injury, ischemia, and brain swelling.

Some lesion types, such as traumatic (pseudo-)aneurysm, vascular dissection, and venous sinus injury, were very rarely observed on admission CT in our cohort. This may reflect a very low occurrence in the acute stage or indicate that non-contrast CT is not the optimal investigation to detect such lesions. We suggest a liberal indication for contrast enhanced CT scanning when any clinical suspicion for such lesions exists (e.g., fracture of the carotid canal, associated cervical spine injury, intracranial hematoma near major artery or venous sinus). Additionally, magnetic resonance angiography or venography can be beneficial in offering supplementary information, particularly in cases involving fractures over dural venous sinuses.

At the extremes of the severity spectrum, 428 patients had a baseline GCS score 3, and 2107 patients had base-

line GCS score 15 (Supplementary Table S2). Of patients with baseline GCS score 3, 83% presented with tSAH, 63% with skull fractures, 56% with aSDHs and 54% with contusions. Even though the GCS 3 subgroup represents around 10% of our entire TBI sample, it accounted for approximately a third of the total number of reported cases of MLS (139/470, 30%), cisternal compression (216/652, 33%), ventricular effacement (196/591, 33%) and brain herniation (121/390, 31%). At the other end of the severity spectrum, patients with baseline GCS score 15 presented less frequently with findings: tSAH 25%, skull fractures 22%, aSDHs 15% and contusions 15%. The GCS 15 subgroup represented more than half of our entire TBI sample, but accounted for approximately a tenth of reported cases of MLS (51/470, 11%), cisternal compression (51/652, 8%), ventricular effacement (48/591, 8%) and brain herniation (34/390, 9%). Nevertheless, these percentages are relatively high, illustrating how imaging characteristics can contribute to the characterization of patients with mild TBI.

Individual pathoanatomic lesion types

For each pathoanatomic lesion type, explanatory text on clinical implications of specific findings or imaging recommendations are included where appropriate.

Skull fracture

Background. Skull fractures are primary injuries where the neurocranium is broken in either partial or full thickness, often in the proximity of scalp injuries.^{12,13} A three-dimensional volume rendering of the non-contrast CT images is warranted for better visualization (Fig. 2 Panel 1 A2, A4, A6), as fractures that run parallel to the conventional two-dimensional planes can be easily missed.⁶ MRI is less sensitive for detecting fractures and is therefore not the modality of choice for detecting these lesions.^{3,4,6} The intricate anatomy of the skull base warrants thorough inspection for small fractures with potentially severe clinical complications, such as fractures of the internal carotid artery (ICA) canal (Fig. 3), that may be accompanied by vascular injury.²⁴ In the past, skull base fractures were considered a clinical diagnosis (e.g., cerebrospinal fluid [CSF] leakage from nose or ear, raccoon eyes, Battle's sign and blood leakage from the ear), as they were poorly visualized on conventional skull X-rays. The current generation of CT scanners, however, allows accurate radiologic detection of skull base fractures.

Core information: presence, multiplicity. Skull fractures were the second most common lesion type on admission CT in the CENTER-TBI dataset. They were encountered in 37% of patients (1958 fractures in 1529/4087 patients), and significantly more frequently in the

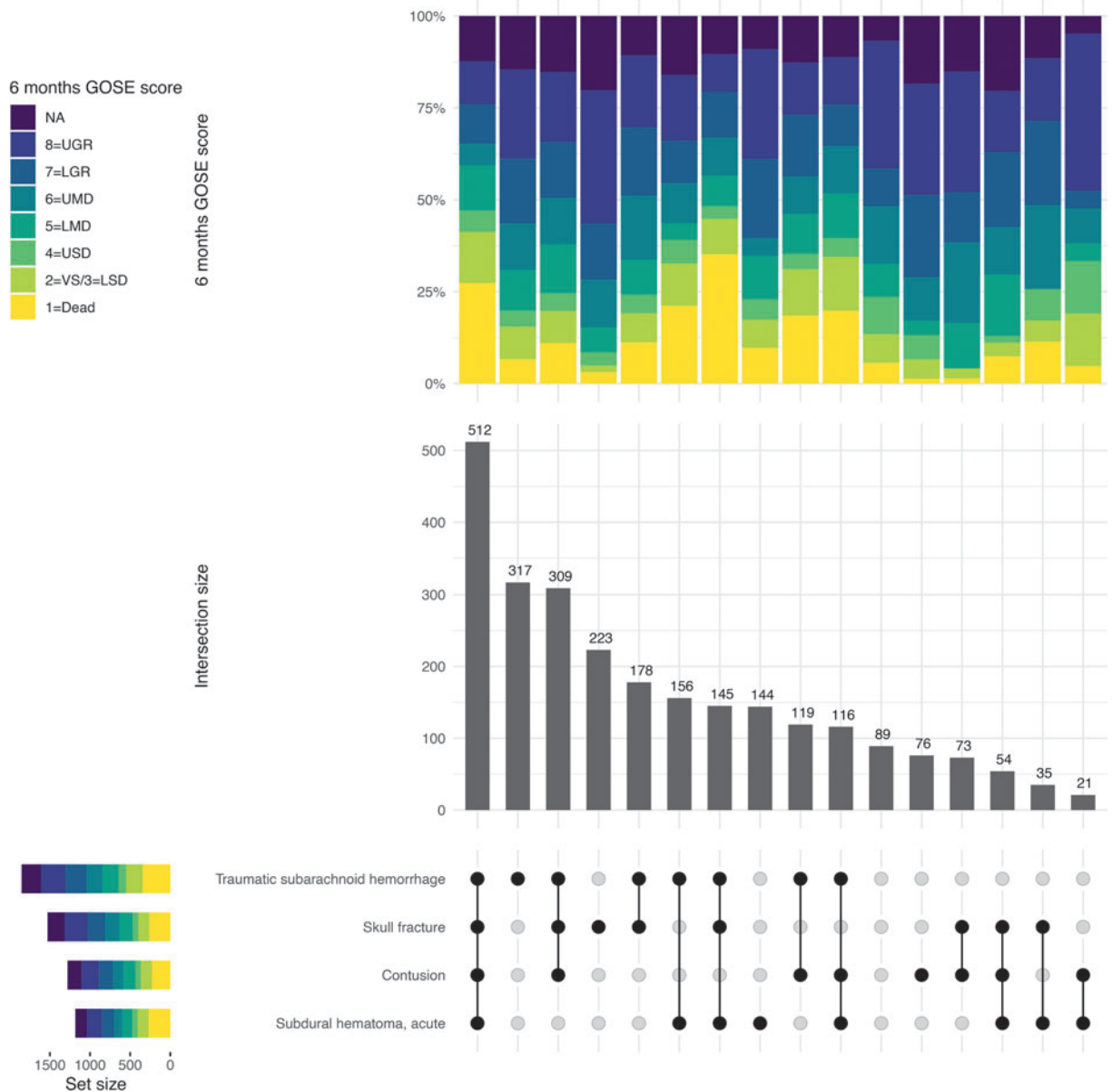


FIG. 1. UpSet plot of combinations of the four most frequent lesion types encountered on non-contrast computed tomography (CT) images. This figure depicts the combinations in which the four most frequent lesion types (traumatic subarachnoid hemorrhage, skull fracture, contusion, acute subdural hematoma) occur on admission CT. Combinations with other lesion types are not depicted here. Of all 2567 patients with positive CT findings, only 89 did not present with any of the four most frequent lesion types. The most common phenotype, present in a fifth of patients with positive CT findings, was all four lesion types simultaneously present. The mortality at 6 months post-injury was high (27%) in this group, and almost half of these patients had an unfavorable outcome at 6 months (47% Glasgow Outcome Scale-Extended [GOSE] score <5). We can also observe that almost a quarter of patients (23%) with an acute subdural hematoma died within 6 months of injury, regardless of the presence of other lesions. When possible, missing GOSE scores were imputed centrally from scores recorded at different time-points, using a multi-state model. GOSE scores were assessed by in-person/telephonic interviews or postal questionnaires, and as such a clear distinction between GOSE 2 (vegetative state) and GOSE 3 (lower severe disability) was not always possible. As a result of this, these two categories were combined, giving a seven-point ordinal scale. GOSE, Glasgow Outcome Scale-Extended; LGR, lower good recovery; LMD, lower moderate disability; LSD, lower severe disability; NA, not available; UGR, upper good recovery; UMD, upper moderate disability; USD, upper severe disability; VS, vegetative state.

moderate-severe TBI subgroup than in the mild TBI subgroup (1009 fractures in 731/1193 patients vs. 850 fractures in 728/2744 patients; 61% vs. 27% respectively; $p < 0.001$). Most patients with skull fractures presented with a single fracture (79%), while two or more concomitant fractures were present in 27% and 14% of skull fracture cases with moderate-severe and mild TBI respectively.

Supplementary information: location. A total of 568 fractures were restricted to the cranial vault (29% of skull fractures), and 190 to the skull base (10% of skull fractures). Most fractures (i.e., 1199) involved both the cranial vault and the skull base (61% of skull fractures), with the most common location being the middle fossa (41% of all fractures), with extension into the temporal and/or parietal bones or vice versa (Supplementary Fig. S2). Fractures in moderate-severe TBI more frequently involved the middle fossa (46% vs. 35%, $p < 0.001$), parietal bone (left 27% vs. 20%, $p < 0.001$; right 30% vs. 23%, $p = 0.001$) and temporal bone (left 25% vs. 17%, $p < 0.001$; right 28% vs. 23%, $p = 0.007$) compared with fractures in the mild TBI subgroup (Supplementary Table S3).

Emerging information: morphology. Skull fractures (Fig. 2 Panel 1 A1-A6; Fig. 3) can be further characterized based on morphological traits: linear, depressed, comminuted, diastatic, compound and penetrating.^{12,13} Often, fractures are complex, meaning they display various combinations of multiple morphological traits (Supplementary Fig. S3). In the CENTER-TBI dataset, over 90% of fractures had a linear component (Supplementary Table S3; Fig. 2 Panel 1 A1-A6). Linear skull fractures can be simple, but in many patients, they are branched or encompass multiple separated fracture lines.

After simple linear fractures, linear and compound fractures with pneumocephalus were most common (Supplementary Fig. S3). Compound fractures are fractures that communicate with the skin, mastoid air cells, or paranasal sinuses.^{12,13} In CENTER-TBI, around 30% of fractures were compound. These were mostly linear fractures in the middle fossa that extended into the mastoid air cells of the petrous bone or linear fractures in the anterior fossa that extended into the frontal sinus. Detecting such pathologic connections between the intracranial space and the outside environment is crucial, as they can be associated with CSF leakage and risk for infection, especially in the presence of intracranial air (i.e., pneumocephalus).²⁵

The third most common morphology was comminuted (28% of fractures), meaning fractures consisting of multiple fragments (Fig. 2 Panel 1 A3-A6). Diastatic fractures cause widening of a cranial su-

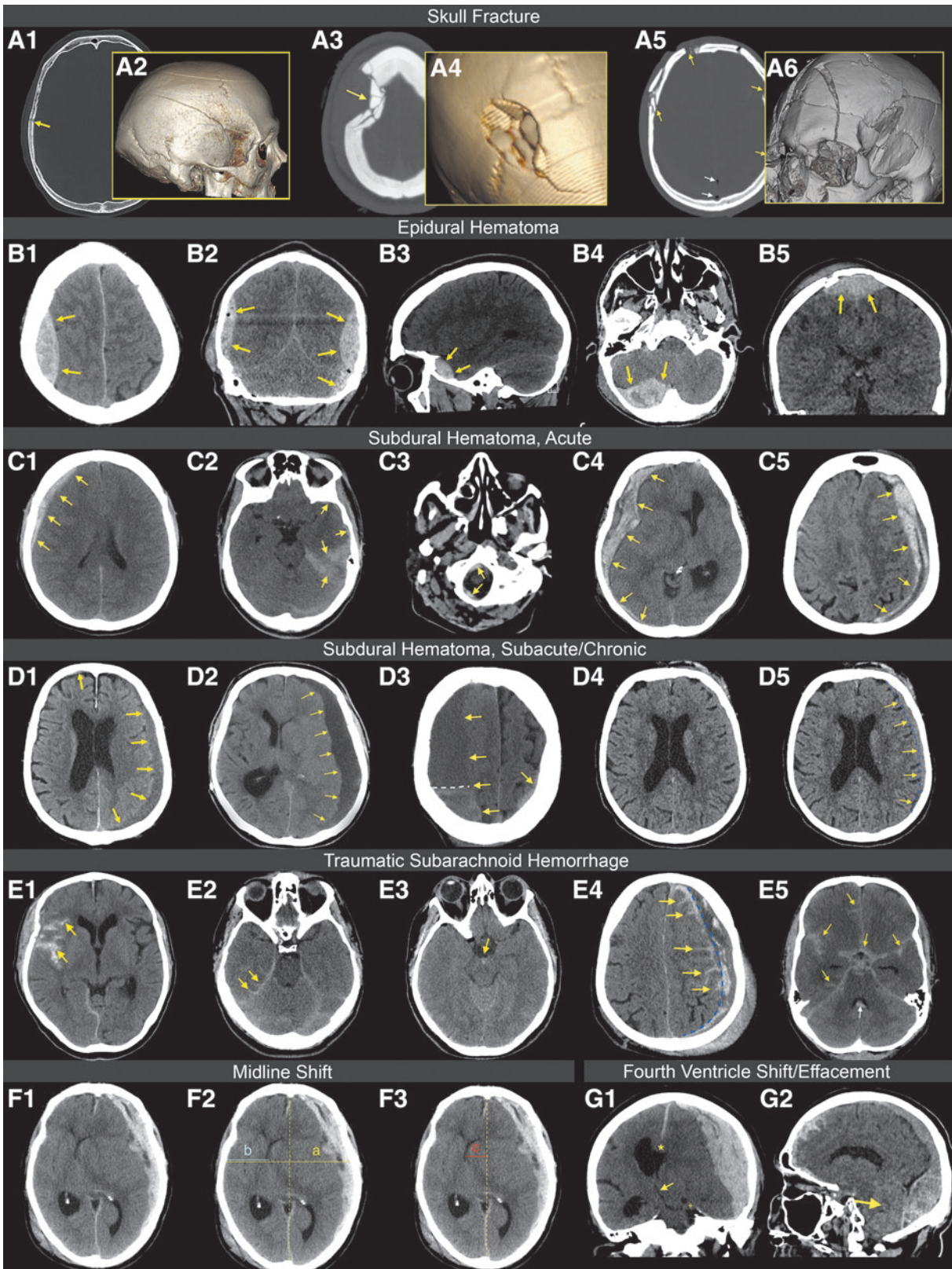
ture or have bone fragments separated by more than 3 mm, according to the CDE definition.^{12,13} Diastatic involvement occurred in 21% of fractures. Depressed skull fractures are fractures where bone fragments are driven inward by >1 cm or by the full thickness of the skull in that location.^{12,13} These fractures were less common (Fig. 2 Panel 1 A3, A4), representing 13% of observed fractures, and can be associated with underlying parenchymal and/or vascular injury. They may require surgery to elevate or remove bone fragments and reconstruct the underlying dura if torn.²⁶ In particular, compound depressed skull fractures underlying scalp lacerations are considered a potential surgical indication. Of the 105 patients with compound depressed skull fractures, 56 (53%) were treated surgically, often in combination with removal of a hematoma. Penetrating fractures, resulting from indriven foreign bodies (e.g., missile, blade), were the least common morphology type (4%). Suspected “probable fractures” are cases in which the fracture itself cannot be detected definitively, but is suspected due to pneumocephalus, and were rarely encountered in this predominantly adult population. Accompanying pneumocephalus was very common and found alongside 48% of fractures. Further description of the location of pneumocephalus can be relevant to determine patient management.²⁷

Fractures in patients with moderate-severe TBI, compared with fractures in patients with mild TBI, were significantly more often compound (36% vs. 27%, $p < 0.001$), comminuted (32% vs 23%, $p < 0.001$), diastatic (24% vs. 18%, $p = 0.002$), depressed (14% vs. 11%, $p = 0.04$) and accompanied by pneumocephalus (52% vs. 42%, $p < 0.001$).

Epidural hematoma

Background. Epidural hematomas (EDHs; Fig. 2 Panel 1 B1-B5) are predominantly focal primary injuries that typically occur at the site of impact (i.e., the “coup” site).²⁸ A large force is needed to cause this kind of injury in adults, which is reflected by the fact that an overlying skull fracture is present in over 90% of cases.²⁸ Epidural hematomas are generally caused by a fracture lacerating or rupturing extradural blood vessels, with blood filling the space between the dura mater and the tabula interna of the skull.⁴ EDHs do not typically cross sutural margins because the periosteal layer of the dura adheres very tightly to the sutures.⁶ On non-contrast CT, EDHs are hyperdense in the acute phase, but may include mixed density components in the case of active ongoing bleeding. Over time, EDHs become isodense or hypodense. Hypodense areas within the predominantly hyperdense bleeding on non-contrast CT represent unclotted blood and are referred to as “swirl

FIG. 2 Panel 1. Examples of imaging findings in acute traumatic brain injury patients. Skull Fractures. **(A1)** Shows a right parietal linear skull fracture (arrow) on the axial non-contrast computed tomography (CT) images with bone window, which is better appreciated on the three-dimensional reconstruction **(A2)**. **(A3, A4)** Show a right frontoparietal depressed and comminuted skull fracture (arrow), possibly from blunt-force trauma. In cases like this, underlying parenchymal injury should always be ruled out on the soft tissue window. **(A5)** Shows extensive frontotemporoparietal (arrows) and craniofacial fractures **(A6)**. The cranial fractures are morphologically depressed, comminuted, and compound. The white arrows indicate the presence of pneumocephalus. Epidural hematomas (EDHs). Non-contrast CT images with soft tissue window show an arterial EDH **(B1)**, arrows, estimated [est.] 71 cm^3) with a typical biconvex shape. Note the swelling in the right cerebral hemisphere, indicated by cortical sulcus effacement, but preserved gray-white matter differentiation. In these cases, it is important to inspect underlying midbrain structures for mass effect (i.e., midline shift and cisternal compression or obliteration). **(B2)** Shows three distinct EDHs (arrows) in a single TBI patient: one right parietal EDH, likely arterial, one left parietal EDH, also likely arterial and one EDH in the left posterior fossa, which is likely venous (combined volumes, est. 108 cm^3). Note the presence of pneumocephalus. **(B3)** Shows a small temporal EDH (arrows, est. 5.50 cm^3). In this case, the location is suggestive of injury to the sphenoparietal sinus, and the EDH is therefore most likely of venous origin. **(B4)** Shows a large underlying EDH (arrows, est. 50.80 cm^3), likely venous. The location is suggestive of injury to the right transverse sinus or one of its tributaries. **(B5)** Shows a vertex EDH (arrows, est. 32.40 cm^3), likely venous in nature. Note the distortion and displacement of the superior sagittal sinus. Subdural hematoma (SDH), acute. **(C1)** Shows a right frontoparietal homogeneous acute SDH (arrows, est. 10 cm^3). **(C2)** Shows a typical hyperdense left temporal and tentorial acute SDH (arrows), often distinguishable from tentorial traumatic subarachnoid hemorrhage due to its thickness. **(C3)** Shows an acute SDH in the infratentorial compartment. Infratentorial involvement of an SDH in the posterior fossa should be carefully examined in multiple directions, especially in the sagittal plane, to inspect the retroclival area for bleedings (arrows). **(C4)** Right frontotemporoparieto-occipital acute heterogeneous SDH (arrows, est. 158 cm^3), causing mass effect with extensive midline shift, brain herniation, ipsilateral ventricular compression, and contralateral obstructive hydrocephalus. **(C5)** Left frontotemporoparieto-occipital laminated acute atypical mixed SDH (arrows, est. 99 cm^3), causing midline shift and secondary mass effect. The hypodense areas within the hematoma can indicate active bleeding or chronic components, which makes it very difficult to distinguish atypical SDH from acute-on-chronic SDH. Note the hypodense aspect of the left hemisphere and part of the right hemisphere, with preservation of gray-white matter differentiation, indicative of local ischemia or possibly vasogenic edema. Subdural hematoma, subacute/chronic. **(D1)** Left frontotemporoparieto-occipital and small right frontal subacute/chronic SDHs (arrows, total est. 74 cm^3). **(D2)** Left frontotemporoparieto-occipital chronic SDH (arrows, est. 126 cm^3), with midline shift and cortical sulcal effacement. **(D3)** Organized right frontotemporoparieto-occipital acute-on-chronic SDH (arrows, total est. 168 cm^3). Note a sediment of high density below the white dashed line in the chronic collection. **(D4)** Shows a difficult-to-detect small isodense bleeding consistent with subacute SDH close to the cortex. **(D5)** Shows the same patient, but with the SDH delineated using blue dashed lines (arrows, est. 6 cm^3). Traumatic subarachnoid hemorrhage (tSAH). **(E1)** Shows the right Sylvian cistern that is filled with tSAH (arrows), as opposed to a normal-appearing left side. **(E2)** Shows typical traces of tentorial tSAH (arrows). **(E3)** Shows a small focal trace of perimesencephalic tSAH in the interpeduncular fossa (arrow). Small traces in this area can easily be missed. **(E4)** Shows diffuse left hemispheric tSAH (arrows) adjacent to an acute-on-chronic SDH (blue dashed lines). **(E5)** Shows diffuse, full tSAH in the basal and Sylvian cisterns, with traces of interhemispheric and bilateral cortical blood (arrows). Note the trace of intraventricular hemorrhage (IVH) in the 4th ventricle (white arrow). Midline shift (MLS). **(F1)** Shows a patient with left frontotemporoparieto-occipital SDH, causing a significant shift of the midline structures. **(F2)** Shows the (A/2-B) method to measure MLS, where A is the width of the intracranial space and B is the distance from the tabula interna to the septum pellucidum at the level of the foramen of Monro (MLS = 1.94 cm). This method can also be used to measure MLS at the level of the largest displacement and is the preferred method according to the National Institute of Neurological Disorders and Stroke Common Data Elements. **(F3)** An alternative method is commonly used in routine radiological practice, where the ideal midline (dashed yellow line) is drawn between the most anterior and posterior part of the falx cerebri. A perpendicular line c is drawn to the septum pellucidum and is then measured as shift (MLS = 2.09 cm). In some cases, these methods can lead to quite different results. Third/fourth ventricle shift/effacement. **(G1)** Shows a large left SDH (est. 173 cm^3) causing MLS with subfalcine (*) and downward transtentorial (+) herniation. This causes a compression of the third ventricle from left to right (arrow). **(G2)** Shows a large posterior fossa EDH (est. 170 cm^3) causing upward transtentorial herniation and obliteration or effacement of the fourth ventricle (arrow).

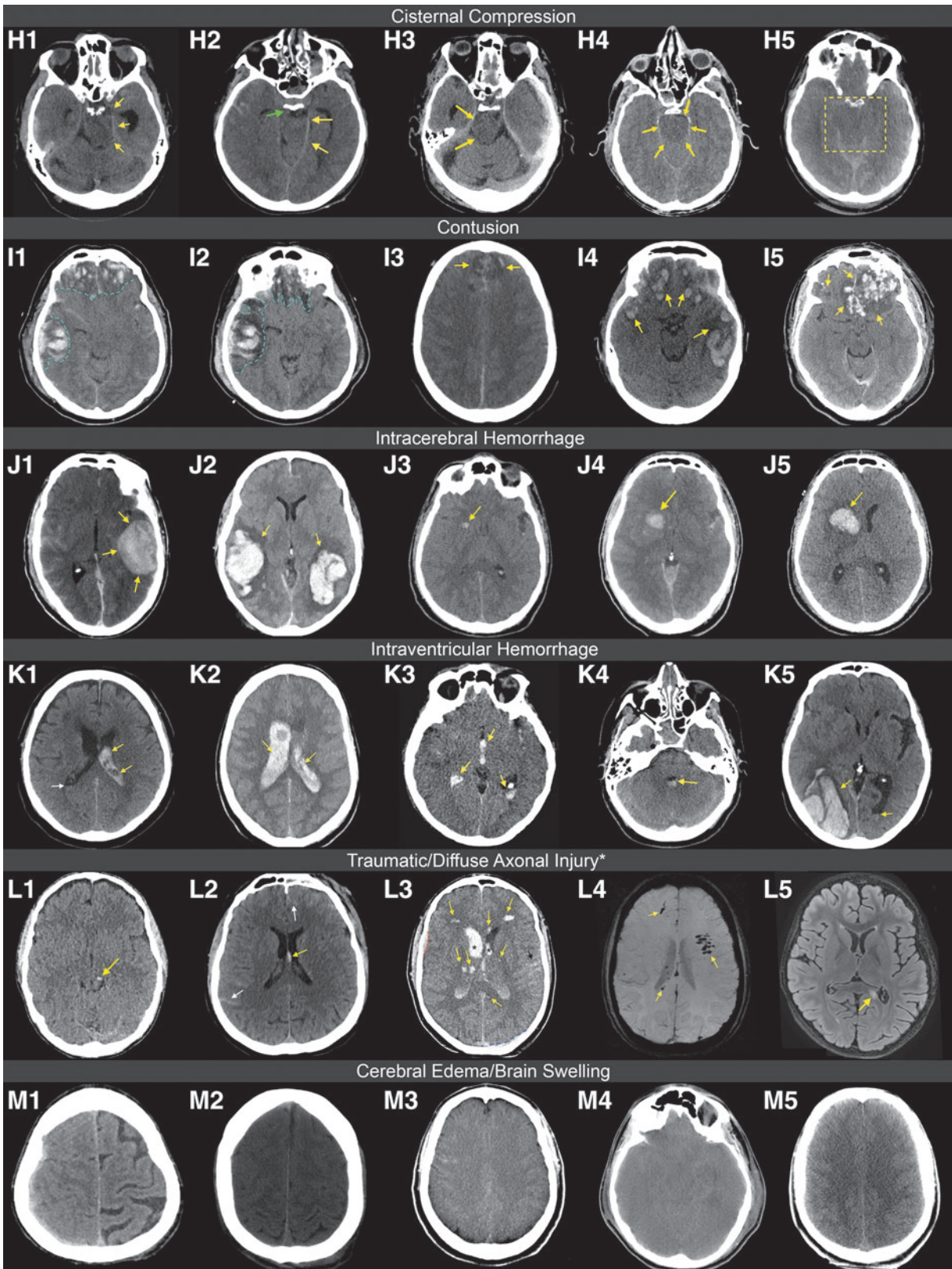


signs".²⁹ Bleedings with swirl signs are often, though not always, associated with active arterial bleeding and a worse clinical outcome, and most require immediate surgical intervention.^{29,30}

Core information: presence, multiplicity. Epidural hematomas were not very common in the CENTER-TBI dataset (589 EDHs in 463/4087 patients, 11%) and

occurred significantly more frequently in the moderate-severe TBI subgroup than in the mild TBI subgroup (291 EDHs in 214/1193 patients vs. 273 EDHs in 228/2744 patients; 18% vs. 8%, respectively; $p < 0.001$). Most EDHs were solitary (78% of patients with EDH), with multiple EDHs occurring simultaneously in 28% and 17% of EDH cases with moderate-severe and mild TBI respectively.

FIG. 2 Panel 2. Examples of imaging findings in acute traumatic brain injury patients continued. Cisternal compression. **(H1)** Shows a patient with a right epidural hematoma (EDH), causing compression of the contralateral ambient and quadrigeminal cisterns (arrows). **(H2)** Shows a patient with compression of the prepontine, ambient (arrows), and quadrigeminal cisterns. Note the downward transtentorial herniation of the uncus of the right temporal lobe into the prepontine cistern (green arrow) and the trace of temporal cortical traumatic subarachnoid hemorrhage (tSAH). **(H3)** Shows a left acute subdural hematoma (SDH) causing compression of the contralateral ambient and quadrigeminal cisterns (arrows). **(H4-5)** Show two patients with global edema and brain swelling, causing complete obliteration of all basal subarachnoid cisterns (arrows in H4, area between yellow dashed lines in H5). Contusion. **(I1-2)** Show how peri-contusional edema (blue dashed lines) in a patient with typical frontotemporal contusions expands over the next few days following injury and becomes more hypodense. Note the contralateral shift and severe compression of the basal cisterns, with some traces of cortical/convexal tSAH. **(I3)** Shows bilateral parasagittal contusions, also sometimes referred to as "gliding contusions" (arrows). **(I4)** Shows typical bilateral frontotemporal contusions (arrows, total estimated [est.] 88 cm³), and **(I5)** shows typical bilateral frontal contusions (arrows, total est. 58 cm³). Intracerebral hemorrhage (ICH). **(J1)** Shows a patient with a temporal left ICH (arrows, est. 27 cm³). Note the contralateral diffuse tSAH. The third ventricle is slightly shifted but still open. **(J2)** Shows a patient with bilateral temporal ICHs (arrows, total est. 120 cm³), with some traces of bilateral tSAH. Note the surrounding rings of edema. **(J3-5)** Show growing intracerebral bleeding in a patient where the lesion was initially classified as focal traumatic axonal injury (TAI) at time-point one (J3, arrow, est. 0.3 cm³). However, at time-point two (J4, 2 h later) the lesion grew into an ICH (arrow, 3 cm³) and continued growing (J5, 2 days later, arrow, 8 cm³). In retrospect, the initial lesion was therefore likely a small intracerebral hemorrhage. Intraventricular hemorrhage (IVH). **(K1)** Shows acute, mostly hyperdense, blood in the left lateral ventricle (arrows) and a right, more isodense, horizontal sedimentation (white arrow). **(K2)** Shows lateral ventricles filled with intraventricular blood (arrows). **(K3)** Shows IVH in both lateral ventricles (arrows) and in the third ventricle (top arrow), with traces of co-occurring bilateral tSAH. **(K4)** Shows a typical horizontal sedimentation level in the fourth ventricle (> 50% filled, arrow). **(K5)** Shows a right temporo-occipital ICH (est. 41 cm³), connecting to the right lateral ventricle. There is also a horizontal sedimentation level of blood in the left lateral ventricle (arrow). Traumatic and diffuse axonal injury. *Terminology under debate. **(L1)** Shows a typical focal traumatic axonal injury (TAI) in the left midbrain (arrow). **(L2)** Shows an isolated TAI in the fornix (arrow) and bilateral traces of frontal and parietal tSAH (white arrows). **(L3)** Shows a complex case with diffuse axonal injury (DAI) in the frontal hemispheres, the right thalamus, the left genu, the left splenium of the corpus callosum, and the left internal capsule. Note the bilateral IVH (asterisks) extending into the third ventricle, the moderate amount of left frontotemporal tSAH (black arrow), the small right frontal EDH (red dashed line) and left occipital SDH (blue dashed line). **(L4)** Magnetic resonance (MR) susceptibility-weighted image (SWI) of a patient showing diffuse hypointense foci in the frontal lobes and splenium of the corpus callosum (arrows), consistent with DAI. **(L5)** MR fluid-attenuated inversion recovery (FLAIR) image showing a patient with a focal axonal injury in the left splenium of the corpus callosum (arrow), not visible on SWI (not shown), indicative of a non-hemorrhagic lesion. Cerebral edema/brain swelling. **(M1)** Shows a patient with right hemispheric cerebral edema, swelling, and cortical sulcal effacement, with preservation of gray-white matter differentiation. **(M2)** Shows a patient with bilateral hemispheric cerebral edema, swelling, and cortical sulcal effacement, also with preservation of gray-white matter differentiation. **(M3-4)** Show patients with global edema. In both cases, there is an obliteration of the basal cisterns, cortical sulcal effacement, and loss of gray-white matter differentiation. **(M5)** Shows a patient with bilateral hemispheric swelling, cortical sulcal effacement, and preservation of gray-white matter differentiation, consistent with possible cerebral hyperemia.



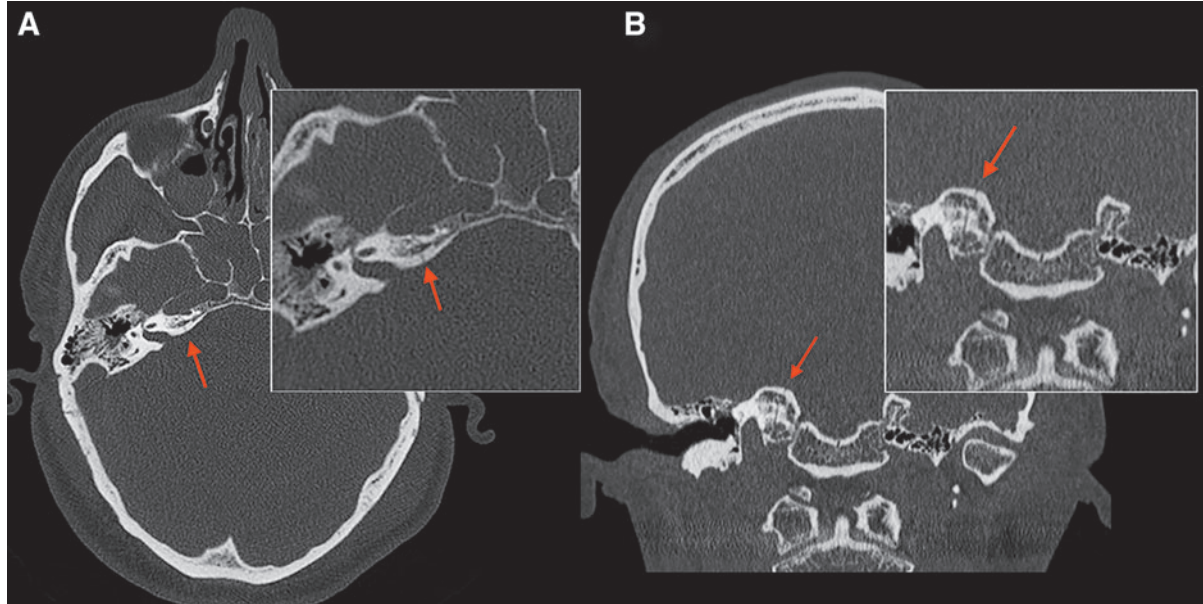


FIG. 3. Axial and coronal non-contrast computed tomography images with bone window of a patient with skull base fractures. Fractures at the level of the skull base, especially in the sphenoid bone and the petrous part of the temporal bone, may be difficult to detect. **(A)** Shows a fracture at the level of the horizontal (arrow, **A**) and vertical segment (arrow, **B**) of the internal carotid artery (ICA) canal. It is crucial not to miss these fractures, as they can be associated with vascular dissection.

Supplementary information: size. Most epidural hematomas in the CENTER-TBI dataset were relatively small (median volume 3.7 cm³, IQR, 1.4-13.9), with no significant volume differences between EDHs in patients with moderate-severe versus mild TBI (Table 3). EDHs of similar volume were relatively equally distributed between patients with moderate-severe and mild TBI, except for large EDHs above 80 cm³ which occurred more often in patients with moderate-severe TBI (60%; Fig. 4). A total of 90 patients (19% of patients with EDH) had an EDH volume higher than 25 cm³, thus qualifying as a mass lesion according to the Marshall CT Clas-

sification.³¹ Of these, 80 patients (89%) were treated surgically for the EDH mass lesion and/or other co-existing lesions, including 34/41 (83%) patients with EDH mass lesion who were classified as having a mild TBI.

Supplementary information: location. The most common location where EDHs were encountered was temporal (51%), followed by frontal (34%) and parietal (27%). In contrast, occipital EDHs (8%) or in the posterior fossa (6%) were quite rare. Most EDHs were confined to a single location (Supplementary Fig. S4), which underscores the

Table 3. Characteristics of Epidural Hematomas on Admission CT

	<i>EDHs in all TBIs</i>	<i>EDHs in mild TBI</i>	<i>EDHs in moderate-severe TBI</i>	<i>p value*</i>	<i>Missing</i>
	N = 589	N = 273	N = 291		
Number of EDHs (%)				< 0.001	0.0
1	361 (61.3)	189 (69.2)	154 (52.9)		
2	164 (27.8)	70 (25.6)	90 (30.9)		
3-5	64 (10.9)	14 (5.1)	47 (16.2)		
Supplementary CDEs: size				0.956	0.0
Volume, cm ³ (median [IQR])	3.74 [1.38, 13.85]	3.92 [1.47, 12.19]	3.58 [1.32, 14.87]		
Supplementary CDEs: location (Table S4)					
Emerging CDEs: likely source					
Likely venous (%)	174 (31.1)	84 (32.2)	81 (29.6)	0.574	5.1
Likely arterial (%)	388 (69.4)	179 (68.6)	194 (70.8)	0.642	5.1

* *p* values derived from χ^2 statistics for categorical variables and Mann-Whitney U tests for continuous variables, comparing EDHs encountered in patients with mild TBI vs. EDHs in patients with moderate-severe TBI.

CDE, common data element; CT, computed tomography; EDH, epidural hematoma, IQR, interquartile range; TBI, traumatic brain injury.

typical focal nature of this type of lesion, bound by sutural margins. Overall, the locations of EDHs encountered in patients with moderate-severe and mild TBI were distributed similarly (Supplementary Table S4).

Emerging information: likely source. EDHs can also be classified based on the suspected origin of the bleeding, either arterial or venous. Arterial EDHs result from a laceration of the middle meningeal artery (MMA) or its branches (Fig. 2 Panel 1 B1, B2).^{4,9} More than two thirds of EDHs in CENTER-TBI had suspected arterial origin, which could also explain the observed frequent localization of EDHs temporally, frontally and/or parietally (Supplementary Fig. S5). Monitoring the size of arterial bleedings is of paramount importance, as they can evolve into space-occupying mass lesions that increase ICP to a life-threatening level (Supplementary Fig. S6). Sometimes multiple MMA branches can be affected in a single patient (Fig. 2 Panel 1 B2).

Venous EDHs may result from the disruption of venous sinuses or blood leaking from a skull fracture and are often associated with occipital fractures or fractures of the greater wing of the sphenoid bone (Fig. 2 Panel 1 B3, B4).⁴ These bleedings are less prone to progression, and do not always warrant surgical intervention.³² Some venous EDHs can cross the dural folds, as they are not limited by the falx cerebri and tentorium cerebelli. For example, vertex hematomas caused by a laceration of the superior sagittal sinus can cross the midline and are typically associated with skull fractures along the sagittal suture (Fig. 2 Panel 1 B5). In general, a more conservative approach to the management of such lesions is recommended, given the high risk of profuse bleeding during surgery. In our cohort, suspected venous EDHs were mostly localized temporally, although the majority of temporal EDHs had a suspected arterial origin. Occipital EDHs and EDHs in the posterior fossa were more frequently of suspected venous origin. No significant difference was observed in the suspected origin of EDHs diagnosed in patients with moderate-severe versus mild TBI (likely arterial origin 71% vs. 69%, $p=0.642$).

Extra-axial hematoma

Background. Sometimes it is difficult to determine whether a bleeding is epidural, subdural, or subarachnoid in nature (Supplementary Fig. S7). When the exact anatomical compartment cannot be determined and the bleeding does not fit the description of another patho-anatomic entity specified elsewhere, it can be classified as extraaxial.^{12,13} Extra-axial hematoma (EAH) refers to the bleeding being inside of the skull, but external to the brain parenchyma.^{12,13}

Core information: presence, multiplicity. EAHs were rarely reported on acute CT in the CENTER-TBI dataset (28 EAHs in 24/4087 patients, 0.6%). These lesions were more often diagnosed in patients with moderate-severe TBI than with mild TBI (15 EAHs in 13/1193 patients vs. 8 EAHs in 8/2744 patients; 1.1% vs. 0.3% respectively, $p=0.003$). A single EAH was usually present (88% of cases).

Supplementary information: size. EAHs reported in the CENTER-TBI dataset were small (median volume 4.7 cm³, IQR 1.5-10), with the ones diagnosed in patients with moderate-severe TBI being significantly larger than those diagnosed in patients with mild TBI (median 6.2 cm³, IQR 2.8-10.9 vs. median 0.9 cm³, IQR 0.6-3.6, $p=0.03$; Supplementary Table S5; Fig. 4).

Supplementary information: location. The most common locations where EAHs were encountered were frontal (64%), followed by parietal (36%) and temporal (32%), with few lesions in the posterior fossa, occipital region or interhemispheric. Most EAHs were confined to a single location (Supplementary Fig. S8).

Subdural hematoma, acute

Background. Acute subdural hematomas (aSDHs; Fig. 2 Panel 1 C1-C5) are primary injuries that are most often caused by acceleration-deceleration forces with rotational components that rupture one or more so-called “bridging” veins,^{33,34} or result from temporobasal contusions with rupture of draining veins. Bridging veins traverse the potential space between the dura mater and arachnoid membrane and drain into the dural sinuses. Because of their thin walls, they are fragile to laceration caused by inertial forces.^{35,36} especially in older people, where progressive cerebral atrophy can create tension on these bridging veins. This frequent aSDH structural injury pattern, involving bridging or draining veins, is one of the reasons for recommending the use of a large trauma flap in surgery for an aSDH, to ensure proper visualization of the parasagittal and temporobasal regions. aSDHs commonly have a crescent shape that can span the entire cerebral convexity and typically cross suture lines, in contrast to most EDHs. The meningeal layer of the dura mater and the arachnoid membrane are not as firmly attached as the periosteal layer of the dura mater to the tabula interna of the skull. Generally, aSDHs are limited by dural reflections (i.e., the falx cerebri and tentorium cerebelli), which often, but not always, confine them to the supra- or infratentorial compartment.⁶ In the acute phase after injury (<1 week), aSDHs predominantly appear hyperdense on non-contrast CT (Fig. 2 Panel 1 C1-C4).

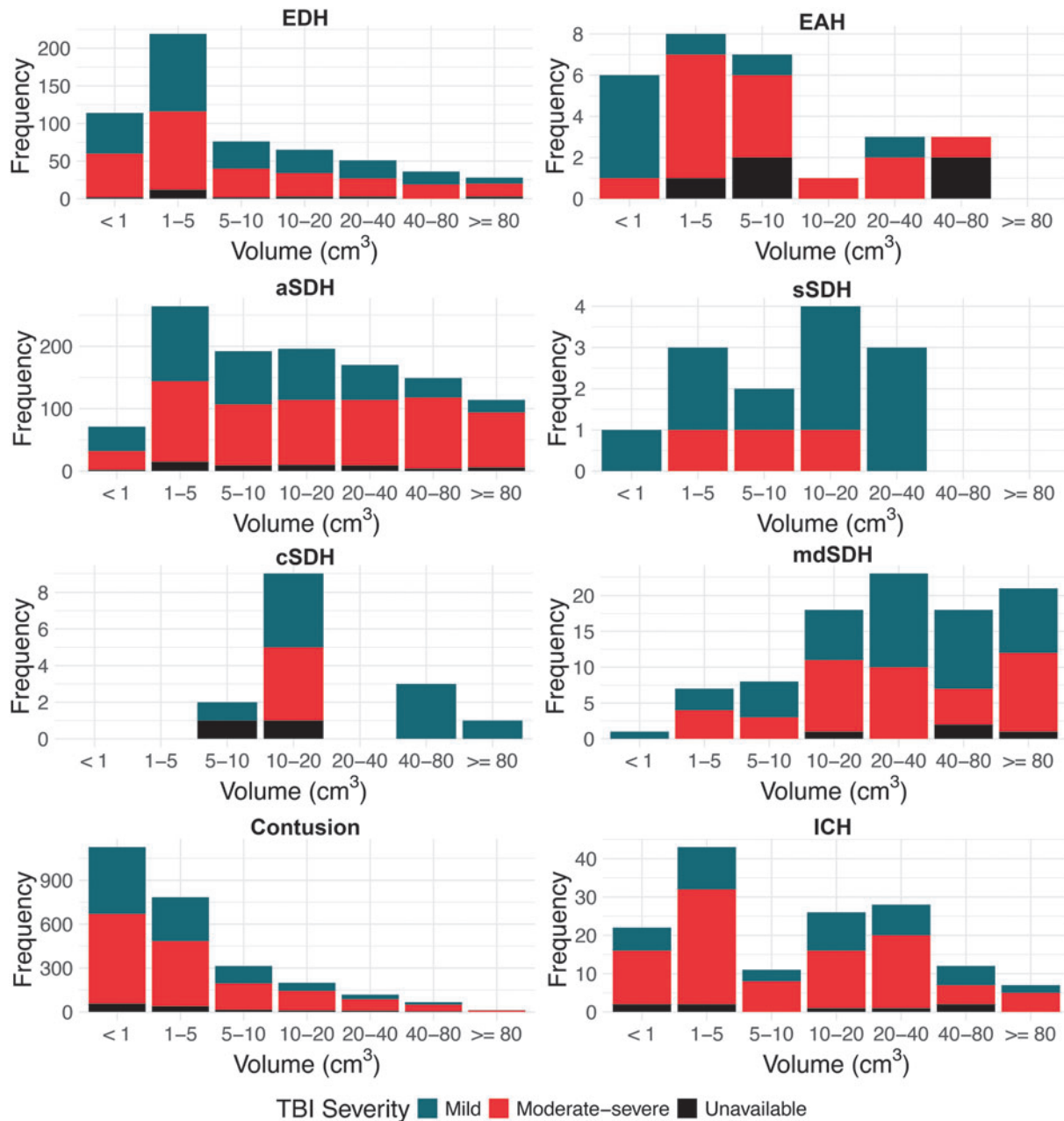


FIG. 4. Histograms, showing the volume distributions of hematomas and contusions in Collaborative European NeuroTrauma Effectiveness Research in Traumatic Brain Injury (CENTER-TBI), differentiated by TBI severity. aSDH, acute subdural hematoma; cSDH, chronic subdural hematoma; EAH, extra-axial hematoma; EDH, epidural hematoma; ICH, intracerebral hemorrhage; mdSDH, mixed density subdural hematoma; sSDH, subacute subdural hematoma.

Core information: presence, multiplicity. Acute subdural bleedings were relatively common in the CENTER-TBI dataset (1374 aSDHs in 1183/4087 patients, 29%) and were encountered almost three times as often in patients with moderate-severe TBI compared with patients with mild TBI (762 aSDHs in 633/1193 patients vs. 552 aSDHs in 500/2744 patients; 53% vs. 18% respectively, $p < 0.001$). In most cases, only one aSDH

was present (85% of all patients with aSDH). Multiple aSDHs occurring simultaneously were encountered in 19% of patients with aSDH in the moderate-severe TBI subgroup and in 10% of patients with aSDH in the mild TBI subgroup.

Supplementary information: size. The median aSDH volume in the CENTER-TBI dataset was 12.8 cm^3

(IQR, 4.1-35.8), with aSDHs encountered in patients with moderate-severe TBI being significantly larger compared with those in patients with mild TBI (median volume 17 cm³, IQR 5.3-49.4 vs. 7.9 cm³, IQR 3.0-19.6, $p < 0.001$; Table 4). Moreover, the majority of large aSDHs above 40 cm³ were diagnosed in moderate-severe TBI (77%; Fig. 4). In general, aSDHs in the CENTER-TBI cohort were larger than EDHs (median volume 12.8 cm³, IQR, 4.1-35.8 vs. 3.7 cm³, IQR, 1.4-13.9). A total of 352 patients (30% of patients with aSDH) had an aSDH volume higher than 25 cm³, thus qualifying as a mass lesion according to the Marshall CT Classification.³¹ Of these, 229 patients (65%) were treated surgically for the aSDH mass lesion and/or other co-existing lesions, including 44/80 (55%) patients with aSDH mass lesion who were classified as having a mild TBI. Of note, given the limitations of the width×depth×length×0.5 formula, lesion volumes were not recorded for tentorial or interhemispheric aSDH components.

Supplementary information: location. As mentioned, aSDHs usually span an entire hemisphere, so a single lesion may extend to multiple anatomical locations. In our cohort, the locations where aSDHs were most frequently recorded were frontal (69% of all aSDHs extended frontally), parietal (61%) and temporal (55%). Unilateral fronto-parieto-temporal aSDH was the most common presentation, followed by aSDHs confined to the frontal region and those confined to the tentorium (Supplementary Fig. S9). Interhemispheric involvement was also frequent (48% of all aSDHs), with or without extension to the convexity and/or tentorium (Supplementary Fig. S9). Although infrequent, infratentorial aSDHs were encountered, warranting inspection of the region (Fig. 2 Panel 1 C3).

aSDHs observed in patients with moderate-severe TBI were reported more frequently in almost all possible locations, compared with aSDHs observed in patients with mild TBI (e.g., frontal left region was reported in 37% vs. 28% of aSDHs in patients with moderate-severe and

mild TBI respectively, $p = 0.001$; Supplementary Table S6). This is to be expected given the larger average volume of aSDHs in more severe patients. A larger aSDH spreads across a larger surface and thus interests multiple anatomical locations at once.

Emerging information: homogeneous or heterogeneous. Acute SDHs can also be described according to their aspect on non-contrast CT imaging (i.e., hypodense or hyperdense).^{12,13} Although aSDHs predominantly appear hyperdense on acute non-contrast CT, many times a mix of hypodense and hyperdense areas can be observed. This heterogeneous aspect may be due to active bleeding, underlying coagulopathy and/or CSF admixture (Fig. 2 Panel 1 C4, C5).⁴ The majority of aSDHs observed in CENTER-TBI were homogenous (58%), with bleedings in patients with moderate-severe TBI being heterogeneous significantly more frequently than those of patients from the mild subgroup (48% vs. 34%, $p < 0.001$; Table 4).

Subdural hematoma, subacute, or chronic

Background. In the subacute phase after injury (1-3 weeks), cellular elements are degraded and removed, gradually rendering the hyperdense aSDH into an isodense or hypodense subacute SDH (sSDH) on non-contrast CT (Fig. 2 Panel 1 D1-D5).⁴ In the chronic phase after injury (> 3 weeks), the subacute SDH typically becomes a homogeneously hypodense collection (cSDH) on CT (Fig. 2 Panel 1 D2).⁴

Core information: presence, multiplicity. Subacute or chronic SDHs (s-cSDHs) on the admission CT were very rarely encountered in CENTER-TBI (28 s-cSDHs in 22/4087 patients, 0.5%). They were the only pathoanatomic lesion type not to occur significantly more often in patients with moderate-severe TBI compared with patients with mild TBI (7 s-cSDHs in 5/1193 patients vs. 19 s-cSDHs in 16/2744 patients; 0.4% vs. 0.6% respectively, $p = 0.68$). This could be explained by the fact

Table 4. Characteristics of Acute Subdural Hematomas on Admission CT

	aSDHs in all TBIs N = 1374	aSDHs in mild TBI N = 552	aSDHs in moderate-severe TBI N = 762	p value*	Missing
Number of aSDHs (%)				< 0.001	0.0
1	1002 (72.9)	449 (81.3)	513 (67.3)		
2	346 (25.2)	100 (18.1)	226 (29.7)		
3-4	26 (1.9)	3 (0.5)	23 (3.0)		
Supplementary CDEs: size					
Volume, cm ³ (median [IQR])	12.84 [4.12, 35.82]	7.94 [3.02, 19.63]	16.98 [5.30, 49.41]	< 0.001	15.9
Supplementary CDEs: location (Table S6)					
Emerging CDEs: homogeneous or heterogeneous					
Homogeneous (%)	797 (58.0)	366 (66.3)	399 (52.4)	< 0.001	0.0

*p values derived from χ^2 statistics for categorical variables and Mann-Whitney U tests for continuous variables, comparing aSDHs encountered in patients with mild TBI vs. aSDHs in patients with moderate-severe TBI.

aSDH, acute subdural hematoma; CDE, common data element; CT, computed tomography; IQR, interquartile range; TBI, traumatic brain injury.

that CENTER-TBI only included patients within 24 h of injury, so the s-cSDHs seen on acute CT potentially originated during previous TBIs, before enrollment in the study, and so may have had limited influence on the clinical status at enrollment. Approximately half of lesions observed were subacute and the rest chronic, with no difference between severity subgroups (Supplementary Table S7). Similar to aSDHs, most s-cSDHs were solitary (73%, of all patients with s-cSDHs; 60% and 81% of patients with s-cSDHs in the moderate-severe and mild TBI subgroups respectively, $p=0.46$). Of the six patients with two lesions simultaneously present on acute CT, only one had both a subacute and a chronic lesion, with the rest having both lesions of the same chronicity. Despite the low frequency of occurrence of subacute and chronic SDHs in our predominantly adult population, we consider it relevant to record their presence, because of a potential decrease in intracranial volume-buffering capacity.

Supplementary information: size. The median s-cSDHs volume in the CENTER-TBI dataset was 12.3 cm^3 (IQR, 9.2-20.0), with no significant difference in size between lesions encountered in patients with moderate-severe vs. mild TBI (median volume 12 cm^3 , IQR 8.1-12.3 vs. 13.9, IQR 9.7-33.2, $p=0.285$; Supplementary Table S7). All large s-cSDHs above 20 cm^3 were diagnosed in mild TBI (Fig. 4), suggesting once again that these lesions preceded the acute TBI. Chronic lesions had on average slightly larger volumes than subacute lesions (median volume 12.5, IQR 10.8-29.4 vs. 10.1 cm^3 , IQR 4.4-14, $p=0.08$; Fig. 4). Location and emerging information can be found in the supplemental materials (Supplementary Text File; Supplementary Fig. S10; Supplementary Fig. S11).

Subdural hematoma/mixed density subdural collection/CSF-like collections

Background. For some subdural collections and in certain research settings, like the CENTER-TBI study, when reviewers are blinded to clinical information, the chronicity is sometimes difficult to determine. In these cases, a SDH can be referred to as a subdural collection, with or without mixed density.^{12,13} In CENTER-TBI, central reviewers recorded subdural collections under the variable “mixed density SDHs (mdSDHs)”, mainly when the timing of these lesions was difficult to determine based on admission CTs. Suspected subdural hygromas with no hemorrhagic components in the subdural space (i.e., subdural collections without mixed density) and CSF-like collections were recorded under incidental findings. Based on CT alone, it can be very difficult to determine whether a collection is caused by changes in CSF dynamics or because of progressive atrophy (e.g., in

elderly patients). In these cases, MRI can be useful to differentiate between chronic SDH, subdural hygroma and atrophic changes.³⁷

Core information: presence, multiplicity. Mixed density SDHs were rarely reported on acute CT in CENTER-TBI (96 mdSDHs in 86/4087 patients, 2.1%). They were reported twice as often in patients with moderate-severe TBI compared with patients with mild TBI (43 mdSDHs in 39/1193 patients vs. 49 mdSDHs in 43/2744 patients; 3.3% vs. 1.6%, respectively; $p=0.001$). Like aSDHs and s-cSDHs, most mdSDHs were solitary (88% of all patients with mdSDHs; 90% and 86% of patients with mdSDHs in the moderate-severe and mild TBI subgroups respectively, $p=0.67$). While we observed no cases of mdSDHs in younger patients (< 18 years), this lesion type is presumed to be more prevalent in infants and young children.^{12,13}

Supplementary information: size. The median mdSDH volume in the CENTER-TBI dataset was 26.9 cm^3 (IQR, 13.4-66.2; Supplementary Table S8), considerably larger than the median volumes of s-cSDHs (median 12.3 cm^3 , IQR, 9.2-20.0) and aSDHs (median 12.8 cm^3 , IQR 4.1-35.8). More information on size, location and characteristics can be found in the supplementary materials (Supplementary Text File; Supplementary Fig. S12; Supplementary Fig. S13).

Traumatic subarachnoid hemorrhage

Background. Traumatic subarachnoid hemorrhage (tSAH; Fig. 2 Panel 1 E1-E5) is a common primary injury resulting in blood between the brain surface and the arachnoid membrane. It is caused by cerebral abrasions, tearing of small pial or arachnoidal cortical vessels, or results from intraventricular hemorrhage (IVH) with reflux into the subarachnoid space via the lateral apertures of the fourth ventricle (i.e., foramina of Luschka).⁴ On non-contrast CT, acute tSAH appears as hyperdense and is often quite straightforward to detect. However, the combination of fluid-attenuated inversion recovery (FLAIR) and susceptibility weighted imaging (SWI) MRI is more sensitive than non-contrast CT in detecting this kind of bleeding.³⁸ In contrast to non-traumatic subarachnoid hemorrhage, it is less frequently located in the basal cisterns, and mainly located in the cortical region. The presence of tSAH is an important prognostic factor and should ideally always be reported.

Core information: presence. Traumatic SAH was the most common pathoanatomic lesion type encountered on acute CT in the CENTER-TBI dataset (1852/4087 patients, 45%). Traumatic SAH was present in over three quarters of patients with moderate-severe TBI, significantly more frequently than in patients with mild TBI

(927/1193 patients vs. 840/2744 patients; 78% vs. 31% respectively, $p < 0.001$).

Supplementary information: location. Traumatic SAH is commonly classified based on location. Often, a distinction is made between cortical and basal tSAH.^{39,40} Cortical tSAH can be recognized by blood following the contours of the sulci or large fissures (Fig. 2 Panel 1 E1, E4), although “convexal” tSAH might be a better term to describe the location. Basal tSAH occurs mainly in the perimesencephalic subarachnoid cisterns (Fig. 2 Panel 1 E3, E5). A mixture of tSAH and contusion or subdural hematoma at the cortical surface is frequently encountered, making it sometimes difficult, if not impossible, to distinguish the borders between these distinct pathoanatomic entities (Fig. 2 Panel 1 E4). Perimesencephalic tSAH can also be easily missed, especially when only small traces are present (Fig. 2 Panel 1 E3).⁹ Careful inspection of the interpeduncular fossa is therefore warranted. Subarachnoid blood on the tentorium is sometimes difficult to distinguish from subdural blood. Subdural blood in this location is generally thicker and spans a larger space (Fig. 2 Panel 1 C2 vs. E2). Nevertheless, a combination of subdural and subarachnoid blood in this location may also occur.

In CENTER-TBI, central reviewers recorded the presence, but not the precise location of cortical/convexal tSAH (e.g., frontal, temporal), and instead elaborated on hemispheric involvement (i.e., unilateral versus bilateral). Cortical involvement was reported in 92% of patients with tSAH, unilaterally (43%) or bilaterally (49%). After the convexities, the most common locations were interhemispheric (38% of tSAH cases) and in the basal cisterns (38%), with tentorial tSAH being less common (19%). Traumatic SAH restricted to a single hemispheric convexity was the most frequent presentation (24% of tSAH cases), followed by tSAH restricted to both convexities (14%), but most cases had bleeding in multiple regions simultaneously, in various combinations (Supplementary Fig. S14).

Of patients with tSAH, those with moderate-severe TBI had tSAH located on the convexity bilaterally, interhemispheric, on the tentorium and in the basal cisterns significantly more frequently than those with mild TBI (Supplementary Table S9). This suggests that in more severe patients, tSAH is more diffuse, and spreads across multiple regions. Unilateral cortical tSAH was the only location that was reported significantly less often in patients with tSAH and moderate-severe TBI compared with patients with tSAH and mild TBI (34% vs. 53%, $p < 0.001$), indicating that in the mild TBI patients tSAH may be more focal (see next section).

Supplementary and emerging information not (systematically) recorded in CENTER-TBI. Traumatic SAH can

also be subdivided into focal (1-2 locations or lobes of the brain) or diffuse (involving more than two contiguous lobes or brain regions, supra- and infratentorial compartments, or multiple basal cisterns).^{12,13} In CENTER-TBI, tSAH locations were subdivided in cortical and basal and graded based on the amount of blood present (see the “Extra information” section below). The presence of acute hydrocephalus as a consequence of tSAH can also be recorded. This CDE was rarely observed in the context of acute tSAH, which is to be expected, as it typically evolves over several days or weeks. Besides location, the thickness of tSAH can be used for subclassification.^{12,13} Thresholds of >5 mm, >3 mm (specified in the CDEs) have been proposed to distinguish between linear and thick or “mass-like” tSAH.^{12,13,41,42} However, a consensus is lacking about what constitutes “thick” tSAH and how and where to measure it (e.g., in the coronal, sagittal and/or axial plane). For instance, in the Fisher grading system, vertical layers of tSAH or clots of tSAH >1 mm are considered “thick” and used as a predictor of vasospasm.³⁹ In CENTER-TBI, a thickness >5 mm was recorded, but was only observed in a minority of tSAH cases (7%), with similar proportions between patients with tSAH and moderate-severe vs. mild TBI (8% vs. 6%, $p = 0.19$).

Extra information: amount of tSAH per location. To facilitate the calculation of Morris-Marshall, Fisher, and Greene CT scores (see CT classification scores), the amount of tSAH (graded as a trace, moderate or full) present in a given location was recorded in CENTER-TBI, despite not being mentioned in the TBI CDEs. For every location, trace was the most frequent and full the most uncommon reported tSAH amount (Supplementary Table S9; Supplementary Fig. S15). In patients with unilateral convexal tSAH, those with moderate-severe TBI tended to have larger amounts of tSAH (i.e., more full and moderate) compared with patients with mild TBI ($p < 0.001$). Tentorial tSAH was almost never full, supporting the above-described distinction with aSDH.

Vascular dissection, traumatic aneurysm and venous sinus injury

In the CENTER-TBI study, these three pathoanatomic lesion types were very rarely encountered ($< 0.10\%$) or not encountered at all (i.e., venous sinus injury). The low frequency observed in our dataset should, however, not be construed as an indication that these lesions lack clinical significance, as these are often not visible on non-contrast CT or are delayed diagnoses that may be linked to preventable neurological catastrophes in individual patients. They are discussed individually in further detail in the supplementary materials (Supplementary Text File; Supplementary Fig. S16-S18).

Midline shift

Background. Midline shift (MLS) occurs when there is a displacement of the supratentorial midline structures, particularly the septum pellucidum, due to mass effect of a focal traumatic lesion or swelling of the brain.^{12,13} The shift is measured at the foramen of Monroe or where it is most significant (Fig. 2 Panel 1 F1-F3) and, according to the CDEs, reported when greater than 2 millimeters (mm).^{12,13} MLS is a relatively frequent occurrence in severe TBI and is often an indication of raised ICP.^{43,44} In the presence of other abnormalities with mass effect, MLS greater than 5 mm is often used by neurosurgeons as a sign to consider surgery.^{45,46} Moreover, as we will see later, this threshold is also often used in prognostic classification schemes. Given this consideration, and acknowledging the proximity of 2 mm to potential measurement errors, MLS was exclusively documented for individuals exhibiting shifts surpassing a 5 mm threshold. Only a minority of cases (i.e., 3%), distinguished by evident subfalcine herniation and marginal proximity to the designated 5 mm threshold, were also included in the analysis.

Core information: presence. In CENTER-TBI, a shift of 5 mm or more was observed on the admission CT in 470/4087 patients (12%). Although MLS was significantly more often encountered in patients with moderate-severe TBI, it was also observed in more than 100 patients with mild TBI (341/1193 patients vs. 107/2744 patients; 29% vs. 4% respectively, $p < 0.001$).

Supplementary information: degree. MLS can be classified according to the degree of shift in millimeters.^{12,13} Its presence indicates potentially dangerous tissue shifts, which can cause brain herniation and subsequent brainstem compression. Brainstem compression constitutes a medical emergency and serves as an indication for neurosurgeons to intervene, monitor and control ICP. Other thresholds than an MLS >5 mm have also been used in the past. For instance, decades ago, Ropper found that a horizontal shift of the pineal body >3 mm was associated with changes in consciousness that ultimately can lead to coma when the shift is >8 mm.⁴⁷

Supplementary information: side. MLS can be classified according to the direction of the shift.^{12,13} In CENTER-TBI, MLS was observed from right-to-left in 56% of MLS cases (54% in the moderate-severe TBI subset and 62% in the mild TBI subset, $p = 0.19$).

Cisternal compression

Background. The subarachnoid cisterns are expansions of the subarachnoid space between the pia mater and the arachnoid membrane (Supplementary Fig. S19; Supple-

mentary Fig. S20).⁴⁸ Although they are described as different compartments, they are interconnected and not truly anatomically distinct. Compression encompasses any asymmetry or obliteration of the normal configuration of the ambient, suprasellar, prepontine, superior cerebellar cisterns, and/or cisterna magna due to mass effect and/or brain swelling in the setting of trauma (Fig. 2 Panel 2 H1-H5).^{12,13} Compression or absence of the basal cisterns on the admission CT scan has been associated with raised ICP and unfavorable outcome.⁴⁹

Core information: presence. In CENTER-TBI, cisternal compression was observed on the admission CT in 652/4087 patients (16%), significantly more often in patients with moderate-severe TBI than in patients with mild TBI (485/1193 patients vs. 130/2744 patients; 41% vs. 5%, respectively; $p < 0.001$).

Supplementary information: amount. Cisternal compression can be classified based on the degree of compression: 1) visible but compressed (which can be further described as asymmetric/symmetric); 2) mixed (some cisterns open, others compressed/obliterated); or 3) obliterated (all cisterns).^{12,13} However, there are no clear operational definitions for compressed, partially compressed, or absent/obliterated cisterns. Therefore, knowledge of the cisterns' normal appearance in relation to age is crucial for a correct assessment. In CENTER-TBI, 77% of patients in whom cisternal compression was observed had mixed compression, with some cisterns open and others compressed/absent (Fig. 5). In 153 patients (23%), all 5 cisterns were compressed to some degree: 45 patients had all cisterns absent, meaning cisterns obliterated (7%), 27 patients had all cisterns visible but compressed (4%) and the rest had various combinations of cisterns compressed and absent (category not specified in CDEs).

Supplementary information: side of compression (not recorded in CENTER-TBI). Cisternal compression can also be classified based on the side of compression (left, right, midline or bilateral).^{12,13}

Emerging information: site. Cisternal compression can be described in further detail by specifying which cisterns are abnormal.^{12,13} The ambient cistern was abnormal in almost all patients with cisternal compression (92%), followed by the suprasellar and quadrigeminal cisterns (each abnormal in 78% of cases; Supplementary Table S10). The cisterna magna was less commonly affected (27% of cases). As mentioned earlier, the majority of patients have some degree of compression in 1-4 of the five cisterns, in various combinations (Fig. 2 Panel 2 H1-H5).

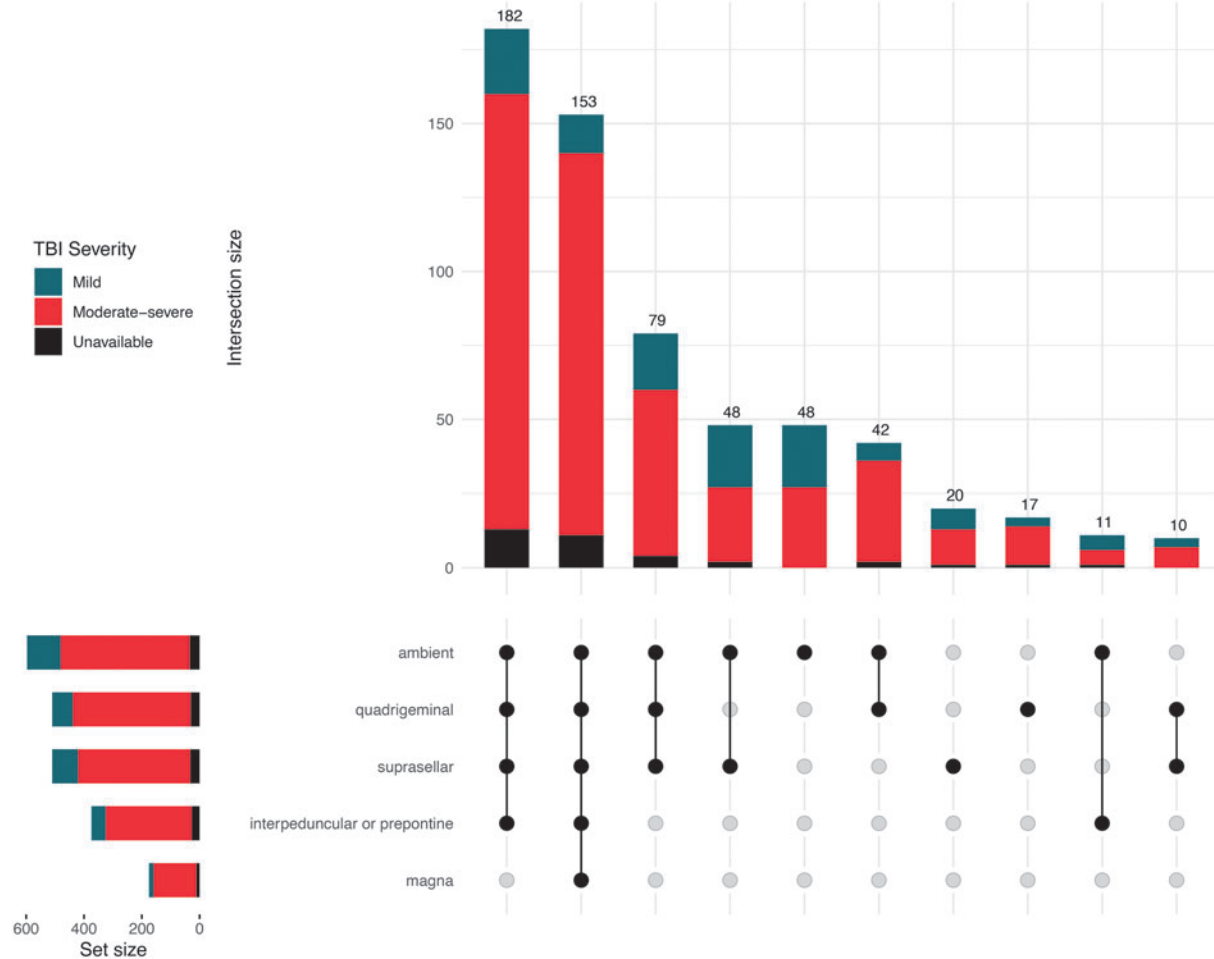


FIG. 5. UpSet plot of cisternal compression locations. The plot depicts any degree of compression (cistern compressed or obliterated) per location. Combinations with less than 10 occurrences not shown.

In CENTER-TBI, the degree of compression was also recorded, for each affected cistern (Supplementary Table S10). When abnormal, each cistern was more often compressed than completely obliterated (across the five locations, 27-45% of abnormal cisterns were absent; Supplementary Fig. S21). Whenever a specific cistern was abnormal, it tended to be absent more frequently in those patients with moderate-severe TBI than in those patients with mild TBI (Supplementary Table S10).

Fourth ventricle shift/effacement

Background. Ventricular shift or effacement (Fig. 2 Panel 1 G1, G2) occurs when there is a displacement, narrowing, or effacement of a ventricle due to adjacent mass lesions or brain swelling.^{12,13} TBI core CDEs include fourth ventricle shift/effacement, but in the CENTER-TBI study we additionally reported the status of the

third ventricle. Some authors combine the status of the third ventricle and the status of the basal cisterns because this has strong prognostic power.⁵⁰ Cerebral herniation is often associated with compression or effacement of the third and fourth ventricles.⁵¹

Core information: presence. Any ventricular shift/effacement (third and/or fourth) was reported on the admission CT in 591/4087 patients (15%), significantly more often in patients with moderate-severe TBI than in patients with mild TBI (431/1193 patients vs. 129/2744 patients; 36% vs. 5%, respectively; $p < 0.001$). Fourth ventricle shift/effacement (Fig. 2 Panel 1 G2) was reported in 146/4087 patients (4%), while third ventricle shift/effacement was much more common (Fig. 2 Panel 1 G1), occurring in 565/4087 patients (14%). In 82% of patients with fourth ventricle shift/effacement, the third ventricle was simultaneously compressed (Supplementary Table S11; Supplementary Fig. S22).

Supplementary information: amount. Ventricular compression can be classified based on the amount of displacement (maximal distance in mm from expected location in any direction).^{12,13} In the CENTER-TBI study, we recorded the degree of compression as ventricle compressed vs. obliterated/absent. In a fifth of cases of fourth ventricle effacement, the ventricle was completely obliterated (Supplementary Fig. S23). The proportion of complete obliteration when the third ventricle was compressed was much larger, at 42% of cases (Supplementary Fig. S23). Moreover, of patients with third ventricular compression, the proportion of complete obliteration was significantly larger in the moderate-severe compared with the mild TBI subgroup (48% vs. 23%, $p < 0.001$; Supplementary Table S12).

Emerging information: direction. The direction of shift/effacement can also be specified: left-to-right, right-to-left, anterior, posterior.^{12,13} In CENTER-TBI, ventricular compression was distributed relatively equally between left-to-right and right-to-left (Supplementary Tables S11 and S12).

Brain herniation (extra core CDE recorded in CENTER-TBI)

Background. Brain herniation is a consequence of mass effect, acute brain swelling or other aspects of acute injury that displace parts of the cerebrum or cerebellum through paths of least resistance. Although not part of the core TBI CDEs, this type of injury was recorded in CENTER-TBI, because of its relevance for diagnosis and surgical decision-making.⁵¹

Presence. Brain herniation was observed on the admission CT in 390/4087 patients (10%) in CENTER-TBI. Like MLS, brain herniation was significantly more often encountered in patients with moderate-severe TBI, compared with patients with mild TBI (285/1193 patients vs. 85/2744 patients; 24% vs. 3%, respectively; $p < 0.001$).

Location. Brain herniation can be classified according to location (Supplementary Table S13). Subfalcine herniation is the most commonly encountered radiological form of cerebral herniation, but lacks a clear clinical correlate other than symptoms of raised intracranial pressure. It occurs when one of the frontal hemispheres, specifically the cingulate gyrus, is pushed under the falx cerebri (Fig. 2 Panel 1 G1).⁵¹ It is sometimes used synonym for MLS. However, in CENTER-TBI, although we found that all patients with subfalcine herniation had MLS, not all patients with MLS had subfalcine herniation (i.e., 77%). Almost all patients with brain herniation had subfalcine herniation (93%), either on the left or right side, isolated or with additional herniation in other locations (Fig. 6).

Downward transtentorial or uncal herniation occurs when the uncus of the temporal lobe is pushed under the tentorium cerebelli (Fig. 2 Panel 1 G1; Fig. 2 Panel 2 H2).⁵¹ This type of herniation can cause compression of cranial nerves, in particular the oculomotor nerve, leading to pupillary dilation and loss of light reactivity. Moreover, it can cause compression of blood vessels that can lead to infarction and often requires immediate surgical and/or medical intervention to decrease ICP.^{51,52} Uncal herniation was the second most frequent type of herniation observed in CENTER-TBI (75% of cases). Simultaneous unilateral subfalcine and uncal herniation was the most common presentation in patients with brain herniation (Fig. 6). Of 293 patients with uncal herniation, 285 (97%) also had cisternal compression.

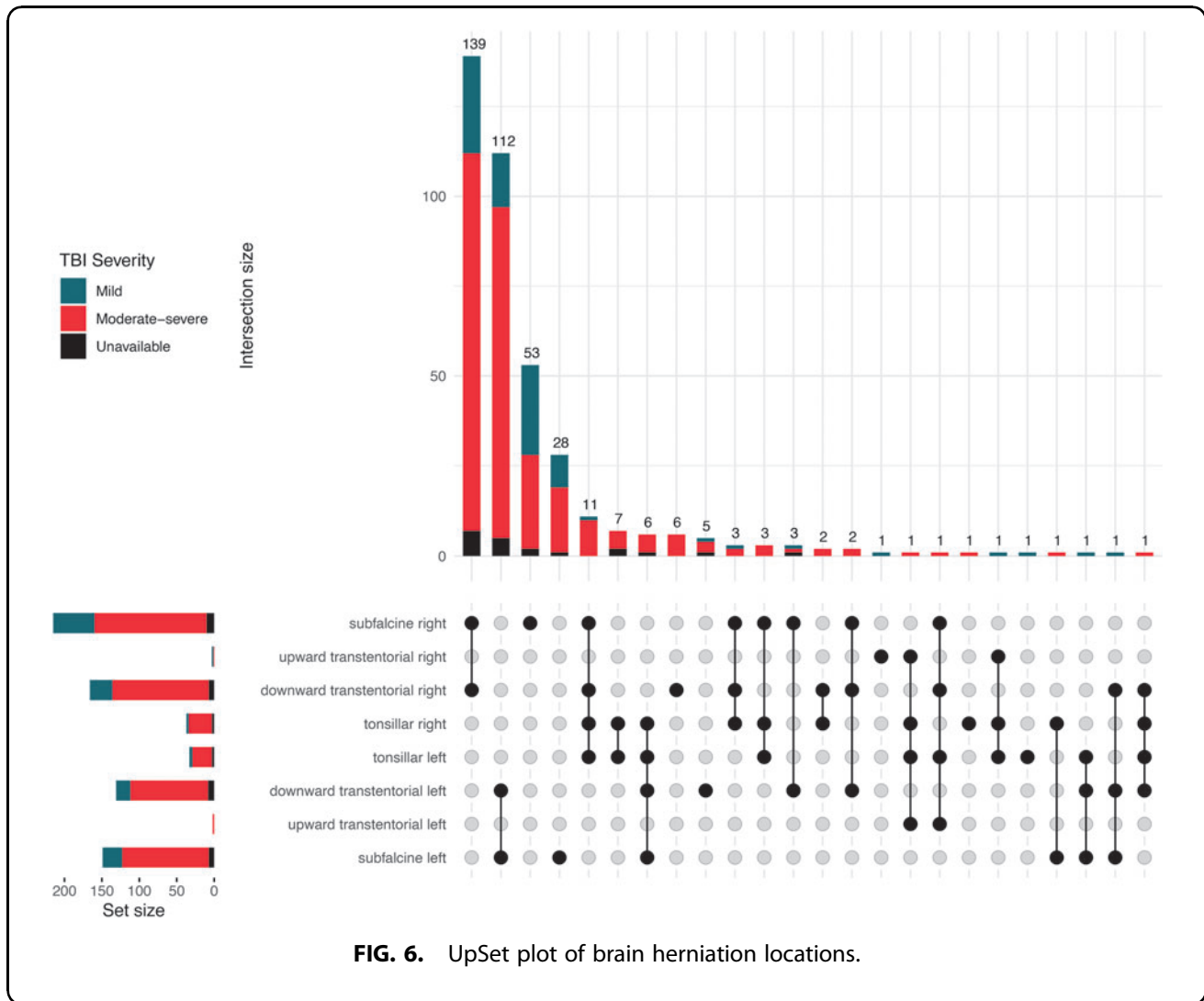
Upward transtentorial herniation is less common (1% of all patients with herniation in CENTER-TBI) and typically occurs in patients with sizable posterior fossa lesions (Fig. 2 Panel 1 G2). Parts of the midbrain are then pushed upwards through the tentorium cerebelli. In these cases, the fourth ventricle is often compressed or absent (Fig. 2 Panel 1 G2, arrow).

Tonsillar herniation is also uncommon and occurs when the tonsils of the cerebellum are pushed into the foramen magnum, compressing the medulla oblongata. This may lead, besides to further loss of consciousness, to breathing disturbances, and dysregulation of the arterial blood pressure. In the CENTER-TBI dataset, tonsillar herniation was infrequent (10% of all patients with herniation) and most times bilateral, in combination with subfalcine and/or uncal herniation.

Recommendation. Given the relatively high frequency of occurrence of radiological signs of cerebral herniation, and its relevance for medical management and surgical decision-making, we suggest considering including brain herniation in the CDEs. As format we suggest a structure similar to the other CDEs (Supplementary Text File).

Contusion

Background. Contusions (Fig. 2 Panel 2 I1-I5) are common primary injuries that usually occur near the brain's surface and can span both cortical and subcortical regions.^{12,13} Contusions are typically focal, mostly caused by energy transfer at the site of impact.³⁴ However, damage can also occur distant to the point of impact or in the contralateral hemisphere, due to the combination of forces exerted within the intracranial cavity and movement of the brain. Traumatic SAH is a common co-existing finding due to the strain on the cortico-pial vascular network.³⁴ On non-contrast CT scans, contusions are primarily encountered in the frontal and



temporal lobes (Fig. 2 Panel 2 I1-I5) and typically have a “speckled” appearance (i.e., a mixture of small hyperdense petechial hemorrhages with hypodense areas of perilesional edema or non-hemorrhagic contusion).^{12,13} On the admission CT scan, small contusions may not be directly visible.⁶ Delayed contusions can also occur after an initial negative scan, but are considered rare.⁵³

Core information: presence, multiplicity. Contusions were the third most common pathoanatomic lesion type on admission CT in the CENTER-TBI dataset (2623 contusions in 1280/4087 patients, 31%) and were encountered almost 3 times as often in patients with moderate-severe TBI compared with patients with mild TBI (1509 contusions in 677/1193 patients vs. 980 contusions in 540/2744 patients; 57% vs. 20%, respectively; $p < 0.001$). In contrast to other hemorrhagic lesion types (aSDHs, EDHs), solitary contusions are rarer than multiple simultaneous ones (55% of all patients with contusions had at least two con-

tusions). Up to 12 individual contusions on admission CT have been observed in our dataset. Multiple contusions were encountered in 60% and 46% of patients with contusions in the moderate-severe and mild TBI subgroups respectively.

Supplementary information: size. The majority of individual contusions on the admission CT in CENTER-TBI were small, below 5 cm³ (median volume 1.4 cm³, IQR 0.4-5.6). Contusions encountered in patients with moderate-severe TBI were on average more voluminous compared with those in patients with mild TBI (median volume 1.6 cm³, IQR 0.4-6.8 vs. 1.2, IQR 0.3-4.4, $p < 0.001$; Table 5). The majority of large contusions >20 cm³ were diagnosed in moderate-severe TBI (Fig. 4). A total of 146 patients (11% of patients with contusion) had a contusion volume greater than 25 cm³, thus qualifying as a mass lesion according to the Marshall CT Classification.³¹ Of these, 85 patients (58%) were treated surgically for the contusion mass lesion and/or other co-

Table 5. Characteristics of Contusions on Admission CT

	Contusions in all TBIs	Contusions in mild TBI	Contusions in moderate-severe TBI	p value*	Missing
	N = 2623	N = 980	N = 1509		
Number of contusions (%)				< 0.001	0.0
1	579 (22.1)	289 (29.5)	270 (17.9)		
2	728 (27.8)	300 (30.6)	378 (25.0)		
3-12	1316 (50.2)	391 (39.9)	861 (57.1)		
Supplementary CDEs: size					
Volume, cm ³ (median [IQR])	1.44 [0.36, 5.64]	1.20 [0.33, 4.36]	1.64 [0.39, 6.78]	< 0.001	0.1
Supplementary CDEs: location (Table S14)					
Emerging CDEs: characteristics					
Hemorrhagic (%)	2618 (99.8)	978 (99.8)	1506 (99.8)	1.000	0.0
Non-hemorrhagic (%)	1924 (73.4)	697 (71.1)	1130 (74.9)	0.042	0.0
Cortical (%)	2254 (85.9)	807 (82.3)	1332 (88.3)	< 0.001	0.0
Subcortical (%)	1354 (51.6)	481 (49.1)	803 (53.2)	0.048	0.0
Deep brain structures (%)	9 (0.3)	2 (0.2)	6 (0.4)	0.638	0.0
Probable brain laceration (%)	4 (0.2)	1 (0.1)	3 (0.2)	0.939	0.0
Extra CDE: intracerebral hemorrhage component					
Intracerebral hemorrhage component (%)	98 (3.7)	34 (3.5)	61 (4.0)	0.534	0.0

* p values derived from χ^2 statistics for categorical variables and Mann-Whitney U tests for continuous variables, comparing contusions encountered in patients with mild TBI vs. contusions in patients with moderate-severe TBI.

CDE, common data element; CT, computed tomography; IQR, interquartile range; TBI, traumatic brain injury.

existing lesions, including 12/34 (35%) patients with contusion mass lesion who were classified as having a mild TBI.

Supplementary information: location. Most contusions are small and confined to a single location (Supplementary Fig. S24). The most common locations where they were encountered were frontal (51%), followed by temporal (40%). Contusions in deeper brain structures like the internal capsule (anterior or posterior), thalamus, basal ganglia, but also contusions in the brainstem and cerebellum were rare (Supplementary Table S14). Lesions in the deeper regions are more common in the context of intracerebral hemorrhage (see next section). We also observed 158 bifrontal contusions (6% of all contusions), which were recorded as a single lesion (as opposed to two separate lesions, one right and the other left). Bifrontal contusions are a distinct traumatic phenotype that may cause the “talk and die” phenomenon.⁵⁴ Overall, the locations of contusions encountered in patients with moderate-severe and mild TBI were distributed similarly (Supplementary Table S14), except for left temporal location, which was observed significantly more often for contusions in patients with moderate-severe TBI compared with contusions in patients with mild TBI (22% vs. 18%, $p=0.01$).

Emerging information: characteristics. Contusions can also be further subdivided according to their nature (i.e., hemorrhagic, non-hemorrhagic) or by providing location details (i.e., cortical, subcortical, deep brain structures).^{12,13} In most cases, contusions contain both hemorrhagic and non-hemorrhagic components (73% of contusions in our dataset). Some contusions (4%) even contained a large hemorrhagic component that could be

classified as an intracerebral hematoma if not for surrounding admixture. Likewise, most contusions (52%) span both the cortical and subcortical regions. A probable brain laceration manifests as a linear pattern of hemorrhagic/non-hemorrhagic (penetrating) injury, typically associated with overlying skull fracture and was rare (0.2%) in our primarily adult population. Nevertheless, this type of laceration is not uncommon among children with transiently depressed skull sections. In our dataset, brain laceration occurred particularly in cases involving penetrating bullets or other foreign bodies.

Intracerebral hemorrhage

Background. Intracerebral hemorrhage (ICH) is differentiated from contusion because it predominantly consists of a collection of homogeneous blood (Fig. 2 Panel 2 J1-J5).^{12,13} ICHs typically do not have a speckled appearance. In most cases, the terms “intracerebral hemorrhage” and “intracerebral hematoma” are used interchangeably to refer to more extensive collections of blood (i.e., >5 mm) that are less superficial than contusions.^{6,12,13} Very small collections of intracerebral blood, that more often coexist with contusions or are scattered throughout the brain, may represent diffuse or traumatic axonal injury (DAI/TAI) or micro-hemorrhages. On follow-up scans, but also in the acute phase after injury, the distinction between contusion and ICH can be difficult, and some overlap between these two entities is common. Moreover, as mentioned in the Contusion section, some lesions may contain a large uniform hemorrhagic component (that in isolation could be classified as an ICH) surrounded by an admixture of hemorrhagic and non-hemorrhagic components. In CENTER-TBI we considered such lesions contusions and reserved the

ICH classification for lesions without admixture components. It is better to consider intraparenchymal bleedings as part of a spectrum. For example, multiple small hyperdense petechial hemorrhages within a contusion can merge and form a more homogeneous collection that is better classified as a hematoma. Or for instance, small, isolated bleedings classified as traumatic axonal injuries (TAIs) in the acute phase can progress into an ICH, thus altering the appearance and characterization of the injury (Fig. 2 Panel 2 J3-J5).

Core information: presence, multiplicity. ICHs were relatively rare on the admission CT in our cohort (151 ICHs in 126/4087 patients, 3%). In comparison, contusions occurred in approximately 10 times more patients. ICHs were encountered significantly more often in patients with moderate-severe TBI compared with patients with mild TBI (97 ICHs in 80/1193 patients vs. 46 ICHs in 39/2744 patients; 7% vs. 1% respectively, $p < 0.001$). While more than a half of patients with contusions had 2 or more contusions present at the same time, patients with ICH usually had a single ICH lesion (86% of cases solitary ICH). Contusion(s) co-occurred in 68/126 patients with ICH (54%).

Supplementary information: size. The TBI CDEs recommend measuring the size of the entire ICH and also separately the hemorrhagic component (not recorded in CENTER-TBI). In general, observed ICHs were larger than contusions (median ICH volume 9.1 cm^3 , IQR 1.6-26.8 vs. median contusion volume 1.4 cm^3 , IQR 0.4-5.6). Volumes were not significantly different between ICHs encountered in patients with moderate-severe TBI and those in patients with mild TBI (median volume 6.7 cm^3 , IQR 1.4-24.1 vs. 11.9 , IQR 2.1-31.9, $p = 0.33$; Supplementary Table S15). However, 15 large ICHs $> 20 \text{ cm}^3$ were diagnosed in mild TBI, with over half in the frontal lobe (Fig. 4). A total of 37 patients (29% of patients with ICH) had an ICH volume higher than 25 cm^3 , thus qualifying as a mass lesion according to the Marshall CT Classification.³¹ Of these, 16 patients (43%) were treated surgically for the ICH mass lesion and/or other co-existing lesions, including 4/14 (29%) patients with ICH mass lesion who were classified as having a mild TBI.

Supplementary information: location. Like contusions, ICHs were mostly confined to a single location (Supplementary Fig. S25) and the most common location where ICHs were encountered was frontal (53%), followed by temporal (29%). In 12% of ICHs, the location was in the internal capsule (anterior or posterior), thalamus or basal ganglia. No ICHs were reported in the brainstem, potentially because of the size and aspect of hemorrhagic lesions observed in this area, which were classified as contusions, traumatic axonal injury, cervico-

medullary/brainstem injury, or Duret hemorrhage. Overall, the locations of ICHs encountered in patients with moderate-severe and mild TBI were distributed similarly (Supplementary Table S15), except for right frontal location, which was observed significantly more rarely for ICHs of patients with moderate-severe TBI compared with ICHs of patients with mild TBI (19% vs. 42%, respectively; $p = 0.005$).

Emerging information: characteristics. ICHs can be layered, meaning they contain a fluid level, and a surrounding ring of non-hemorrhagic signal (i.e., perilesional edema) may be present (Fig. 2 Panel 2 J2, J5).^{12,13} Around 17% of ICHs in our dataset were layered and around a quarter had a surrounding ring. Both traits were more often noted in ICHs of patients with mild TBI (Supplementary Table S15).

Intraventricular hemorrhage

Background. Traumatic intraventricular hemorrhage (Fig. 2 Panel 2 K1-K5) is a primary injury that occurs when subependymal veins in the fornix, septum pellucidum, or choroid plexus are damaged, when an adjacent intracerebral hemorrhage breaches into the ventricles, or it can be a secondary injury because of reflux of tSAH into the ventricular system.⁵⁵ In the acute phase, IVH is hyperdense on non-contrast CT (Fig. 2 Panel 2 K1-K5). When the patient is supine, it typically presents as a horizontal sedimented blood-CSF level in the occipital horns of the lateral ventricles or fourth ventricle (Fig. 2 Panel 2 K1 [white arrow], K4, and K5 [right arrow]).⁵⁶ IVH can be easily missed on non-contrast CT if the bleeding is only mild, and it is best appreciated on magnetic resonance (MR) SWI.⁵⁷ IVH often co-occurs with other lesions and should raise the suspicion of DAI/TAI.⁵⁸ Several classification systems exist to grade the severity of IVH and predict clinical outcome.⁵⁹⁻⁶² These systems have shown a good prognostic classification performance.⁶³ However, they were based on relatively low numbers and mostly in the context of intracerebral hemorrhages, not specifically TBI.

Core information: presence. In CENTER-TBI, IVH was observed on the admission CT in 491/4087 patients (12%), significantly more often in patients with moderate-severe TBI than patients with mild TBI (347/1193 patients vs. 121/2744 patients; 29% vs. 4%, respectively; $p < 0.001$).

Supplementary information: location. IVH is typically classified based on location.^{12,13} It occurs most often in the lateral ventricles, which were affected in 94% of patients with IVH in CENTER-TBI. The most frequent presentation of IVH was hemorrhage in both lateral

ventricles (Fig. 2 Panel 2 K1-K3, K5), followed by isolated left ventricle and isolated right ventricle hemorrhage (Supplementary Fig. S26). In 41 patients in our dataset (8% of all IVH cases), IVH was present in all four ventricles simultaneously (Supplementary Fig. S26; Fig. 2 Panel 2 K3). IVH in the third and fourth ventricles is less common (15%, 23% of IVH cases, respectively; Table 6). These ventricles are more often affected in various combinations with each other or the lateral ventricles, than in isolation (Supplementary Fig. S26).

Emerging information: ventriculomegaly (acute hydrocephalus), hemorrhage volume. One of the effects of IVH can be acute or delayed hydrocephalus or ventriculomegaly, caused by clotted blood that obstructs the CSF drainage pathways or other mechanisms.⁶⁴ IVH volume was not recorded, as no consensus exists on the measurement of IVH volume, particularly when it spans multiple ventricles.

Diffuse axonal injury and traumatic axonal injury (DAI/TAI)

Background. Diffuse and traumatic axonal injury (Fig. 2 Panel 2 L1-L5) is a primary injury that typically consists of scattered, small hemorrhagic and/or non-hemorrhagic abnormalities that correlate with pathologic findings of relatively widespread injury to white matter axons.^{12,13} TAI consists of typically small, hemorrhagic and/or non-hemorrhagic lesions, in a more confined white matter distribution (Fig. 2 Panel 2 L1, L2, L5) than in DAI. DAI refers to more widespread lesions, in multiple white matter distributions, including the subcortical hemispheric white matter (Fig. 2 Panel 2 L3, L4), the corpus callosum, the brainstem, and/or cerebellar regions.^{12,13} For imaging reporting purposes, the distinction between DAI and TAI, according to the CDEs, is made based on the number of separate foci of signal abnormality: TAI includes 1-3 foci, DAI includes more than three.^{12,13}

DAI/TAI is associated with rotational acceleration/deceleration forces and can be observed weeks, months, and even years after the injury.⁶⁵ T2*-gradient echo (GRE) and/or SWI sequences are far more sensitive than non-contrast CT in the detection of cerebral microhemorrhages, also referred to as traumatic microbleeds

(TMBs), that are suggestive of DAI/TAI (Fig. 2 Panel 2 L4; Fig. 7B).³ SWI and T2* sequences detect DAI lesions in 20 to 30% of patients with a negative admission non-contrast CT scan.^{66,67} However, lesion volume on FLAIR sequences tends to be the predominant predictor of clinical outcome, compared with the number of lesions on SWI.^{68,69} TMBs may thus suggest DAI, but do not always show histologically associated damaged axons.⁷⁰ In the past, this has led to substantial confusion about the used terminology. Therefore, significant efforts are underway to shift away from characterizing small vascular injuries as DAI/TAI, as they can, but do not consistently, involve injured axons. A different term is required to more effectively underscore the point that axonal damage is not always present and it is believed that even with current imaging techniques, the true extent of axonal injury and how it affects patients clinically is still heavily underestimated. During the recent NIH-NINDS workshop on TBI classification and nomenclature, held in January 2024 in Bethesda (<https://www.ninds.nih.gov/news-events/events/ninds-tbi-classification-and-nomenclature-workshop>), the term Traumatic Axonal and/or Microvascular Injury (TAMVI) was proposed for consideration beyond DAI/TAI given this newer evidence from radiological-pathological studies.

Core information: presence. In the CENTER-TBI study, TAI was observed on the admission CT in 257/4087 patients (6%), significantly more often in patients with moderate-severe TBI than patients with mild TBI (151/1193 patients vs. 92/2744 patients; 13% vs. 3%, respectively; $p < 0.001$). DAI was observed less often than TAI, in only 79/4087 patients (2%), similarly more often in patients with moderate-severe TBI than in patients with mild TBI (65/1193 patients vs. 12/2744 patients; 5% vs. 0.4%, respectively; $p < 0.001$). We acknowledge that these data underestimate the true occurrence of TAI/DAI, as CT scanning is less sensitive at detecting these lesions compared with MRI.

Supplementary information: location, number of foci of signal abnormality. Most patients with TAI had a single lesion (61%), with 2-3 foci being more often encountered in patients with TAI who had moderate-severe TBI rather than mild TBI (47% vs. 26%,

Table 6. Locations of Intraventricular Hemorrhage on Admission CT

Ventricle	<i>Intraventricular hemorrhage in all TBIs</i>	<i>Intraventricular hemorrhage in mild TBI</i>	<i>Intraventricular hemorrhage in moderate-severe TBI</i>	χ^2 p value	Missing
	N = 491	N = 121	N = 347		
Lateral left (%)	361 (73.5)	84 (69.4)	262 (75.5)	0.233	0.0
Lateral right (%)	316 (64.4)	73 (60.3)	229 (66.0)	0.312	0.0
Third (%)	74 (15.1)	14 (11.6)	57 (16.4)	0.256	0.0
Fourth (%)	111 (22.6)	20 (16.5)	83 (23.9)	0.118	0.0

CT, computed tomography; TBI, traumatic brain injury.

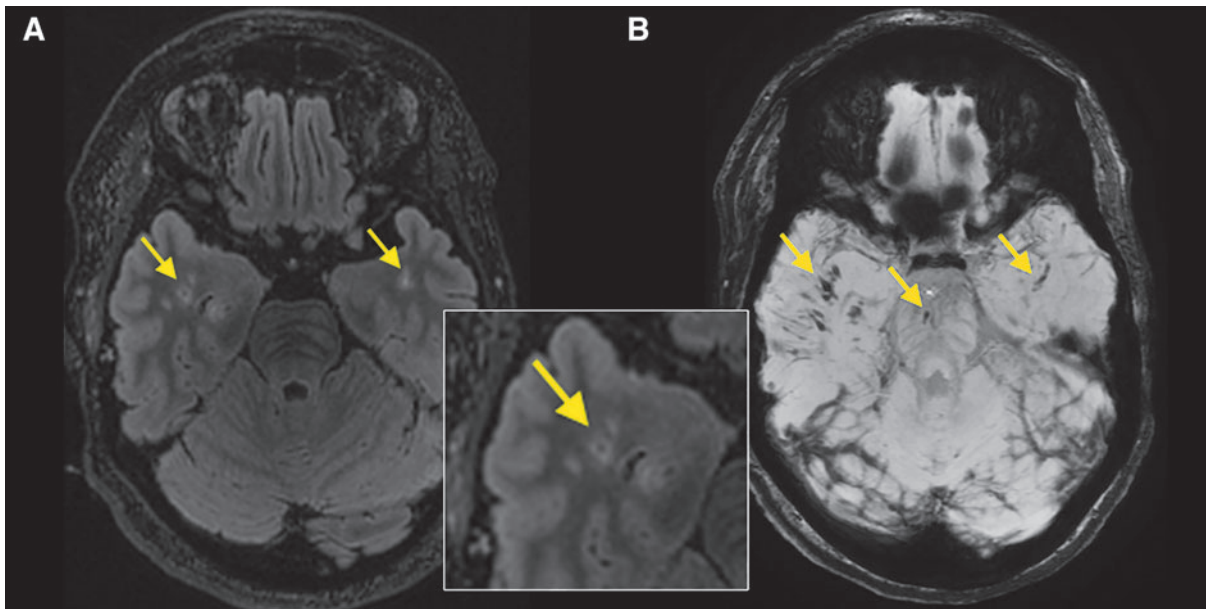


FIG. 7. Axial fluid-attenuated inversion recovery (FLAIR) (A) and susceptibility weighted imaging (SWI) (B) magnetic resonance (MR) sequences of a traumatic brain injury (TBI) patient with diffuse axonal injury (DAI). (A, B) illustrate typical shearing injuries (arrows) consistent with DAI in the bilateral temporal lobes and brainstem (lesion in brainstem only visible on SWI). MR is significantly more sensitive than non-contrast computed tomography in detecting these kinds of injuries and is therefore the preferred modality for investigating possible DAI/traumatic axonal injury (TAI).

$p=0.005$; Supplementary Table S16). The 1-3 lesion(s) of patients with TAI were mostly all confined to a single white matter territory (Supplementary Fig. S27). The locations where signal abnormalities were found most often were the frontal subcortical white matter (43% of TAI patients), the corpus callosum (25%) and brainstem (20%; Fig. 8A). The frontal region and the corpus callosum were also the regions most affected by multiple foci simultaneously (Fig. 8A).

In patients with DAI, the median number of observed foci was 5, IQR 4.0-9.5. Patients with DAI and moderate-severe TBI had significantly more lesions than those with mild TBI (median 6, IQR 5-10 vs. median 4, IQR 4-5.5, $p=0.01$; Supplementary Table S17). A quarter of patients with DAI had 10 or more foci of signal abnormality, with 41 being the maximum reported. In contrast to TAI, the lesions in DAI spanned multiple white matter territories simultaneously (Supplementary Fig. S28). Like TAI, the regions most often affected were frontal (78% of patients with DAI had at least one frontal lesion) and the corpus callosum (52%). The frontal region was also the only location where more than 10 simultaneous lesions were reported unilaterally (Fig. 8B). Moreover, whenever the right frontal region was affected in patients with DAI, it usually contained four or more foci on its own, apart from potential other foci in different locations.

Penetrating injuries

Background. Penetrating injuries (Supplementary Fig. S29), or open-head-injuries, are primary injuries caused by indriven fragments or foreign bodies, which penetrate any of the normal layers of the head, including the scalp, skull, dura mater, and brain.^{12,13} They are less common than closed-head injuries and are considered prognostically worse.⁷¹ Traumatic intracranial aneurysms are more common in penetrating brain injuries, and additional diagnostic procedures may be indicated in high-risk patients, for example when an intracranial hematoma is close to a major cerebral artery, or if the missile tract crosses one of these arteries.

Core information: presence. As opposed to other TBI datasets, penetrating injury was not an exclusion criterion for enrollment in the CENTER-TBI study. Even so, only 18 penetrating injuries were observed (0.4% of all patients), involving significantly more frequently patients with moderate-severe TBI than patients with mild TBI (12/1193 patients vs. 5/2744 patients; 1% vs. 0.2%, respectively; $p=0.001$).

Supplementary information: deepest extent penetrated (scalp, skull, dura, parenchyma). The extent of damage depends on the mechanism, modality, kinetic

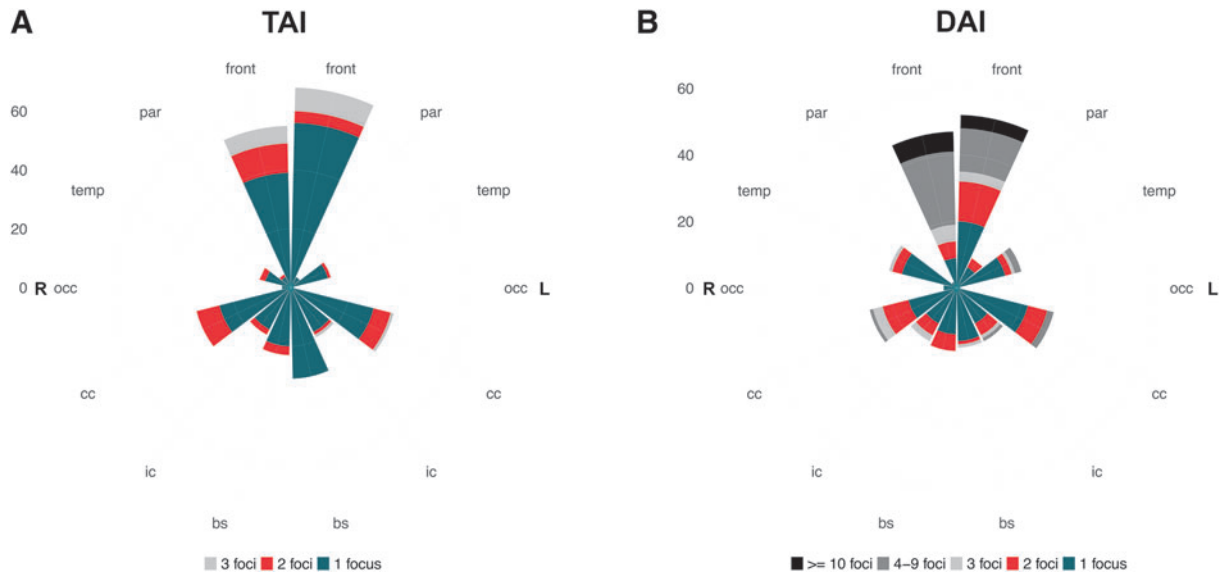


FIG. 8. Polar plots of diffuse axonal injury (DAI)/traumatic axonal injury (TAI) number of foci per location. bs, brainstem; cc, corpus callosum; front, frontal; ic, internal capsule; occ, occipital; par, parietal; temp, temporal.

energy, and location of impact (e.g., certain parts of the calvarium are thinner and thus more vulnerable). All penetrating injuries observed in our cohort reached the parenchyma, passing through bone (which was oftentimes indriven) and dura. The scalp was not always penetrated, as some injuries entered through the skull base.

Supplementary information: location. Penetrating injuries in the CENTER-TBI study were usually unilobar (11/18 injuries), often confined to the frontal lobe (4/11 injuries; Supplementary Fig. S30). In seven patients, multiple locations were simultaneously affected (multilobar), usually by cross-midline trajectory of gunshot wounds (e.g., entrance frontal left, exit parietal right).

Supplementary information: modality/mechanism (stab wound/gunshot wound/other foreign body). Penetrating injuries are often classified by mechanism (i.e., high-velocity, e.g., caused by projectiles, firearms, shockwaves, etc.; or low-velocity penetrations, e.g., caused by knives, glass, etc.).^{12,13} A third of penetrating injuries in our cohort were caused by high-velocity mechanisms like gunshot wounds (six patients, all with moderate-severe TBI).

Emerging information: indriven fragments, through and through trajectory, transventricular trajectory, crosses midline. The type (bone, foreign object) and trajectory of the penetrating fragment can also be specified. For example, a through-and-through (entrance and exit sites), also termed perforating injury, and/or trans-

ventricular trajectory (Supplementary Fig. S29C) can occur with penetrating bullets or other indriven fragments, such as bone fragments or foreign bodies. Transventricular trajectories have been associated with poor clinical outcome.⁷² The only penetrating injuries in our cohort with complex trajectories were those caused by gunshot wounds: 6/6 crossed the midline, 5/6 had a transventricular trajectory and 2/6 had a through-and-through trajectory.

Cervicomedullary junction/brainstem injury

Background. Cervicomedullary injuries and brainstem hemorrhages, in the context of trauma, can be primary (e.g., contusion, laceration, TAI, etc.) or secondary.^{12,13} They are most commonly focal. Secondary brainstem hemorrhages are not very common and are typically associated with raised ICP and rapidly evolving downward transtentorial herniation.⁷³ These secondary hemorrhages are often referred to as “Duret hemorrhages,” and are associated with poor prognosis.⁷³ Their pathophysiology is still under debate. The cause is likely multi-factorial, with stretching and laceration of pontine perforating branches of the basilar artery as the most probable explanation.⁷³

Core information: presence. In the CENTER-TBI study, cervicomedullary junction/brainstem injuries were observed on admission CT in only 5/4087 patients (0.1%), all with moderate-severe TBI. Duret hemorrhages were mentioned four times in the free-text box

of incidental findings, while they could also be classified under “brainstem injury.”

Supplementary information: location. These injuries are often classified based on their nature (primary vs. secondary) and location (midbrain, pons, medulla, cervical).^{12,13} In most cases, however, multiple anatomic areas are involved. Duret hemorrhages are commonly located in the ventral and paramedian regions of the mesencephalon and/or pons (Fig. 9).⁷³

Findings with pathophysiologic connotations

Cerebral edema

Background. Cerebral edema (Fig. 2 Panel 2 M1-M4) is a secondary injury and refers to an abnormal accumulation of water in the brain’s intracellular and/or extracellular spaces.^{12,13,74} It should be differentiated from cerebral swelling due to vascular engorgement (see the “Brain Swelling” section below).

Core information: presence. Cerebral edema was rarely reported on the admission CT in our cohort (56/4087 patients, 1.4%), almost exclusively in patients with moderate-severe TBI (49/1193 patients vs. 4/2744 patients with mild TBI; 4% vs. 0.1%, respectively; $p < 0.001$).

Supplementary information: extent. Cerebral edema may be classified as focal (involves less than half of one lobe), lobar (affects more than half of one lobe), multi-lobar (involves multiple lobes), hemispheric (involves an entire hemisphere; Fig. 2 Panel 2 M1), bihemispheric (involves both hemispheres; Fig. 2 Panel 2 M2-M4), in the posterior fossa (affects the cerebellum and/or brainstem) or global edema (affects the entire brain; Fig. 2 Panel 2 M3, M4). In our cohort, cerebral edema on the admission CT was mostly global (71%), followed by hemispheric (15%).

Emerging information: type, volume of edema. Cerebral edema can also be classified according to mechanism into vasogenic, cytotoxic, interstitial, or osmotic. All types of edema will appear hypodense on the admission CT, making it nearly impossible to differentiate edema types. Loss of grey-white matter differentiation may indicate cytotoxic processes instead of brain swelling by other causes.⁷⁵ In patients with TBI, vasogenic and cytotoxic edema are likely to overlap.⁷⁶ In two thirds of patients with cerebral edema in our cohort, the edema was labeled as vasogenic. Although rarely, fluid can also accumulate within the extracellular space of the periventricular white matter due to obstructive hydrocephalus, which is sometimes referred to as hydrocephalic

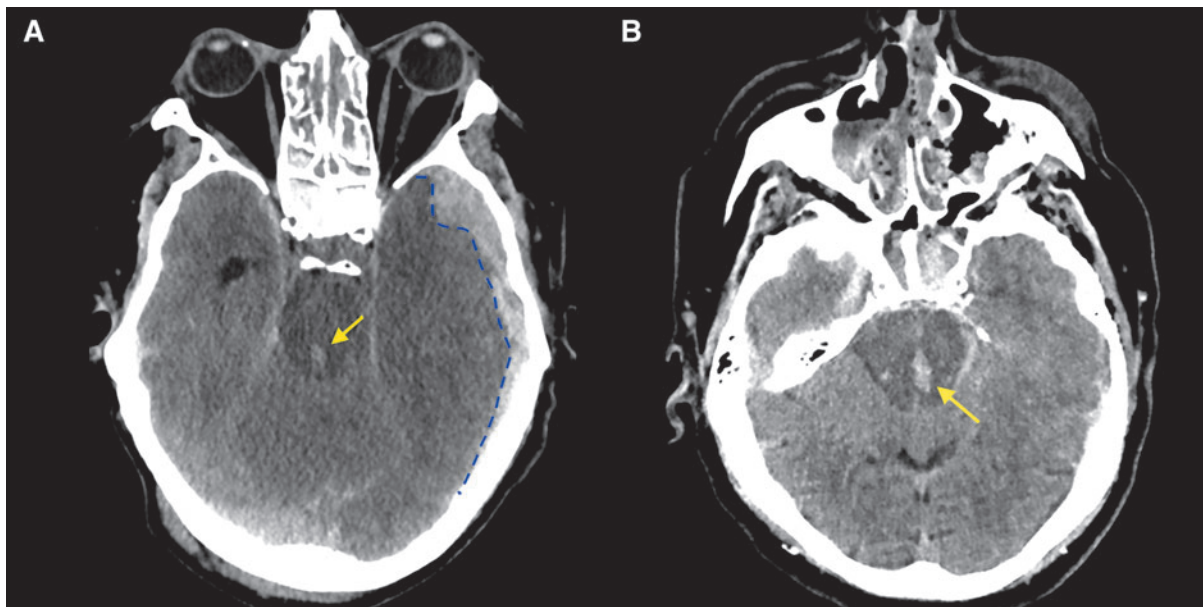


FIG. 9. Axial non-contrast computed tomography images with soft tissue window of two different traumatic brain injury (TBI) patients with secondary brainstem hemorrhage. **(A)** Shows focal injury in the brainstem at the level of the pontomesencephalic junction (arrow). There is a left acute temporal subdural hematoma (SDH; blue dashed line), causing downward transtentorial herniation and obliteration of the basal cisterns. **(B)** Shows multiple hemorrhages in the pons and midbrain (arrow) in a patient with bilateral SDH, subfalcine and downward transtentorial herniation, midline shift (MLS), cisternal and ventricular compression (not shown).

or “interstitial” edema.⁷⁷ Osmotic or ionic edema is another subtype that can occur in the proximity of bleedings, infarctions, or contusions due to high osmolality in the affected tissue compared with plasma, which can trigger a water influx.⁷⁷ Other increases in brain mass that do not fit these definitions, or are believed to have different underlying pathophysiology, are commonly referred to as “brain swelling.”^{12,13}

Brain swelling

Background. Brain swelling refers to a non-specific increase in brain tissue mass that can result from an increase in water content or intravascular blood volume (i.e., “hyperemia”). An increase in intravascular blood volume can be caused by venous outflow obstruction, cerebral dysautoregulation in the context of systemic hypertension, or in hypermetabolic states where there is a hyperperfusion of brain tissue.^{12,13} According to the CDEs, cerebral hyperemia can appear as focal or diffuse mass effect (i.e., sulcal/cisternal effacement) with preservation of the gray-white differentiation (GWD). In the CENTER-TBI study, the reviewers reported cerebral “hyperemia” only if findings were in accordance with this definition, and if the findings did not fit the definitions included under edema (e.g., Fig. 2 Panel 2 M5). Of note, it is very difficult to determine whether actual cerebral hyperemia is present from a non-contrast CT. Therefore, the term “hyperemia” in the CENTER-TBI study should always be considered “possible hyperemia”.

Core information: presence. Brain swelling was very rarely reported on the admission CT in our cohort (14/4087 patients, 0.3%), exclusively in patients with moderate-severe TBI (14/1193 patients, 1.2%). In eight of these 14 patients, the observed aspect was indicative of cerebral hyperemia (Fig. 2 Panel 2 M5) due to preserved GWD, with diffuse mass effect and sulcal/cisternal effacement.

Supplementary information: location, extent. Similar to cerebral edema, hyperemia may be classified based on which locations are affected and the extent.^{12,13} Often, in cases where the central review panel was in doubt between brain swelling caused by edema or hyperemia, there was local swelling of the temporal lobes, accompanied by compression of cisterns and cortical sulcal effacement, but some preservation of GWD (Fig. 2 Panel 2 M5).

Ischemia/infarction/hypoxic-ischemic injury

Background. Cerebral ischemia and other related terms (e.g., infarction, hypoxic-ischemic injury) refer to findings in tissue that reflect a deficit between oxygen

demand and delivery.^{12,13} Post-traumatic cerebral ischemia and infarction are secondary injuries typically hypodense on non-contrast CT (Supplementary Fig. S31, S32a-e) and hyperintense on FLAIR images (Supplementary Fig. S32f). Early detection and intervention (e.g., decompressive surgery, anticoagulation, or others) can minimize the damage to the brain tissue caused by these injuries and may reverse it in some cases.⁷⁸ However, post-traumatic ischemia is now considered more common than previously thought and an independent prognostic factor for poor clinical outcome.^{79,80}

Core information: presence. Ischemia was very rarely reported on the admission CT in our cohort (4/4087 patients, 0.1%), exclusively in patients with moderate-severe TBI (4/1193 patients, 0.3%).

Supplementary information: location, extent, acute versus subacute. Ischemia and infarction are often classified based on location and/or the extent of the deficit.^{12,13} The location of vascular territories can help to distinguish between infarction and non-hemorrhagic contusion.⁸¹ A distinction can also be made based on aspect in the acute versus subacute stage (i.e., hypodense, isodense, hyperdense or mixed).

Emerging information: pattern. Further classification can be made based on the pattern of injury, which is related to the cause. Watershed infarction occurs after prolonged systemic hypotension and typically affects the junctions of vascular territories, (i.e., territories supplied by the anterior cerebral artery, middle cerebral artery, and/or posterior cerebral artery).⁸² One of the most common causes of ischemia or infarction is the occlusion of a large artery due to subfalcine and/or transtentorial herniation, induced by a space-occupying extra- or intra-axial bleeding (e.g., EDH, SDH, ICH, or contusion)⁶ or brain swelling, and frequently involves the posterior cerebral artery. Lacunar infarctions are small infarctions caused by an occlusion of a single terminal branch of these large arteries.⁸³ Venous infarctions occur due to obstruction of one of the larger intracerebral veins by a thrombus or external compression (e.g., by a mass lesion).⁸⁴

Incidental findings (extra CDE recorded in CENTER-TBI)

Incidental findings were reported in 15.2% of patients, less frequently in patients with moderate-severe TBI (13%) compared with those with mild TBI (16.4%). The most frequent incidental findings were (abnormal) prominent ventricles (104/4087, 2.5% of all patients), old strokes (1.9%), various cysts (1.7%, mostly arachnoid cysts), various chronic subdural collections (1.1%) and past neurosurgical interventions (1.1%). Other types of incidental findings were reported in less than 1% of patients:

prior TBI, various anatomical variants (e.g., cavum septum pellucidum), tumoral formations, hydrocephalus, mega cisterna magna, acute strokes, and Duret hemorrhages not classified under cervicomedullary/brainstem injury.

Co-occurrence and clustering of pathoanatomic lesion types

Of the 4087 admission CTs we reviewed, 2567 (63%) showed traumatic abnormalities, with at least one of the NINDS TBI core CDEs present. In a fifth of these, only a single type of core CDE (a single pathoanatomic lesion type, solitary or not) was reported (539 scans, 21% of positive scans, 13% of all scans). In these patients, the most frequent isolated findings that were observed were tSAH (208 patients), skull fracture(s) (132 patients), aSDH(s) (87 patients) and contusion(s) (54 patients). In the remaining 2028 scans (79% of positive scans, 50% of all scans), various combinations of different pathoanatomic lesion types were observed, ranging from 2 to 12 simultaneous, distinct lesion types. Some of these lesion types were highly correlated (Fig. 10). Of patients with positive scans (1345 with mild TBI, 1112 with moderate-severe TBI), those with moderate-severe TBI had on average more simultaneous types of lesions than patients with mild TBI (median 5, IQR 3-7 distinct pathoanatomic lesion types vs. median 2, IQR 1-4, $p < 0.001$; Fig. 11)

Cluster analysis of lesion types on positive CTs in the two subgroups (Fig. 12), shows early clustering of markers of mass effect (MLS, cisternal and ventricular compression), indicating once again the high correlation between these characteristics. In patients with moderate-severe TBI, these markers of mass effect also cluster with aSDH. Cerebral edema was mostly encountered in patients with moderate-severe TBI and seemed to be an overarching feature of the aSDH cluster with mass effect markers, indicating a pattern of secondary injury caused by a large aSDH. As mentioned earlier and in line with previous research, other pathoanatomic lesion types also tend to cluster. For instance, in both subgroups we found evidence of early clustering of EDH with skull fracture and contusions with tSAH, with all four clustering in patients with moderate-severe TBI. Interestingly, IVH and DAI/TAI also tend to cluster together, which corroborates that the presence of IVH can in fact serve as a marker for DAI/TAI.⁵⁸ IVH and DAI/TAI also seemed clustered with intracerebral hemorrhage, indicating a pattern of injury affecting deeper cerebral vascular structures simultaneously.

CT classification scores. Multiple classification schemes or severity grading systems have been developed in the past for injury characterization and clinical outcome prediction, either on their own or in combination with demographic and clinical variables. These provide a summary score, which reflects the overall findings on a scan, based on

the presence or absence of selected non-contrast CT features (Table 7; Supplementary Table S18).^{31,39-41,85-87}

The most validated imaging-based descriptive scheme is the Marshall classification, which was originally developed for patient classification, not necessarily prognosis, but has been used for outcome prediction ever since.³¹ Although this classification is considered a very strong tool to predict 6-month mortality in TBI, it has several limitations, including the fact that the scale is not ordinal and that it does not consider the presence of tSAH, which is the most frequently observed CT abnormality with significant association with poorer outcome,⁸⁵ and also the most commonly encountered pathoanatomic lesion type in our dataset. The Rotterdam CT score was developed from a prognostic perspective, and overcomes these limitations by using individual features, including tSAH, and has been reported to have an equal or greater predictive value compared with the Marshall classification.⁸⁸ Other, more recent scales like the Helsinki and Stockholm scoring systems achieve similar discrimination performance and sometimes even outperform the Marshall and Rotterdam classifications.⁸⁹ Unfortunately, these scoring systems are also not accompanied by many visual examples, and since most scales are not CDE-based, certain terminology used in the scales may appear ambiguous. In Table 7, we list the features in the different scoring systems and refer to figures in which such features are illustrated.

The NeuroImaging Radiological Interpretation System (NIRIS) is a recently developed scoring system with CDE-based terminology that, in addition to predicting outcome, also suggests patient management actions based on imaging findings (Supplementary Table S18).^{89,90}

Prognostic tools are currently mostly used for research purposes and sometimes underperform in terms of outcome prediction accuracy. However, as the NIRIS intends, and if further validated and improved, these systems could play a role in clinical radiology routine, where the scores could be automatically extracted from structured and templated CDE reports and could inform patient management and communication.

As with all prognostic models, continuous validation of CT classification schemes and grading systems is necessary to ensure applicability to contemporary, diverse patient populations, across different clinical settings and geographic regions. Some of these scores were developed on samples of patients treated more than 30 years ago, meaning that predicted outcomes might not reflect the advances in treatment and rehabilitation that have occurred over time. As such, updating the predicted outcomes might be necessary. The use and evaluation of these imaging prognostic models or severity classifications should reflect clinical practice and integrate essential patient demographic, clinical, and laboratory data.

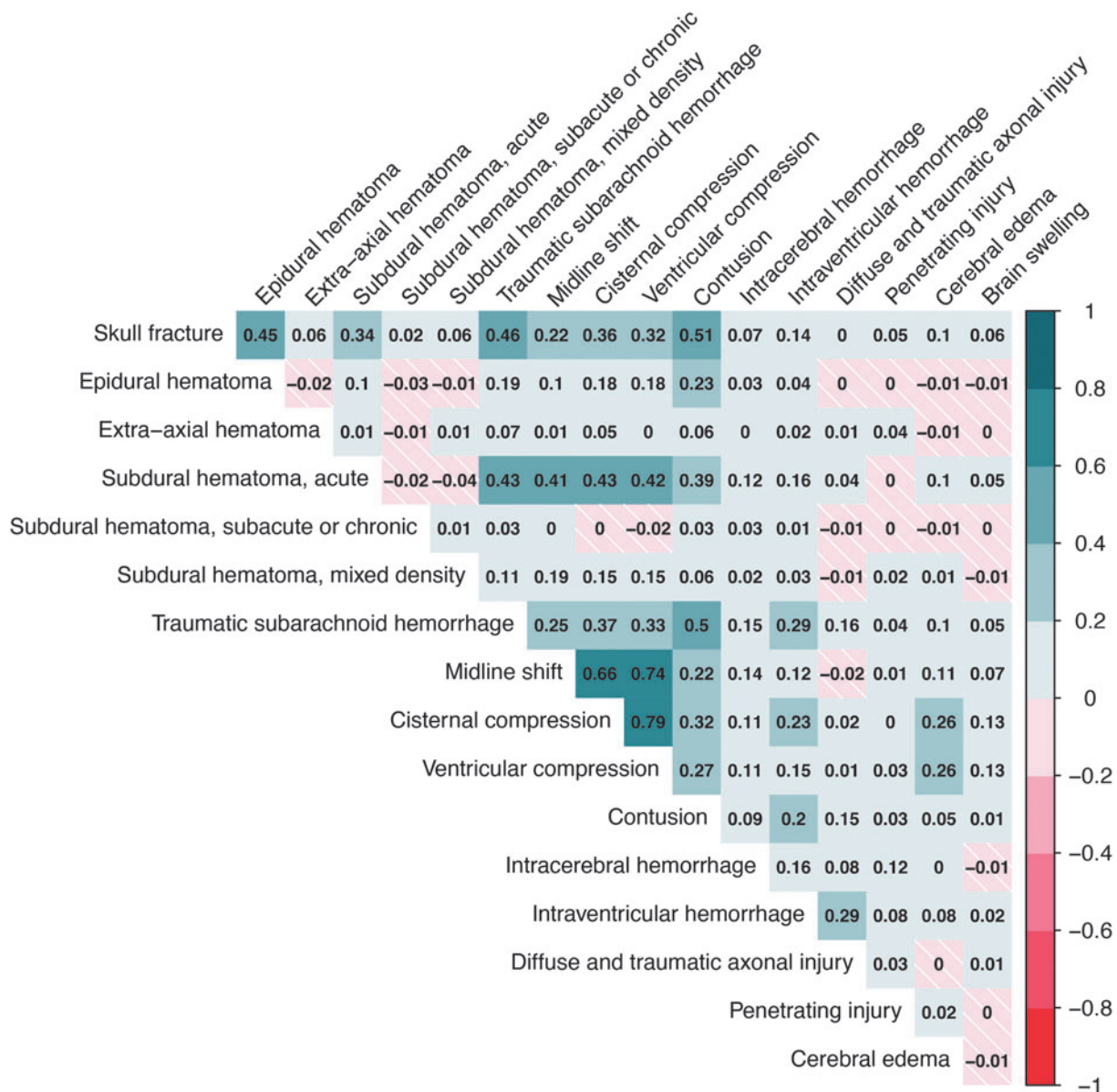


FIG. 10. Heatmap that shows the co-occurrence correlations of all possible pairs of National Institute of Neurological Disorders and Stroke (NINDS) core traumatic brain injury (TBI) common data elements (CDEs) in Collaborative European NeuroTrauma Effectiveness Research in Traumatic Brain Injury (CENTER-TBI). Lesion types with less than 10 observations in the entire sample are not shown. Some lesion types were highly correlated. In particular, the CDEs that indicate the presence of mass effect: midline shift (MLS), cisternal compression, and ventricular effacement were highly correlated with each other (range of phi correlation coefficients between pairs 0.66-0.79). These three CDEs were also correlated with the extra CDEs brain herniation and cortical sulcus effacement, with the highest correlation between any lesion types being that between MLS and brain herniation ($\phi=0.84$). Skull fractures were correlated with contusions ($\phi=0.51$), traumatic subarachnoid hemorrhage (tSAH; $\phi=0.46$), and epidural hematoma (EDH; $\phi=0.45$; of note, 98% of patients with EDHs had co-existing skull fractures). Contusions were also correlated with tSAH ($\phi=0.50$).

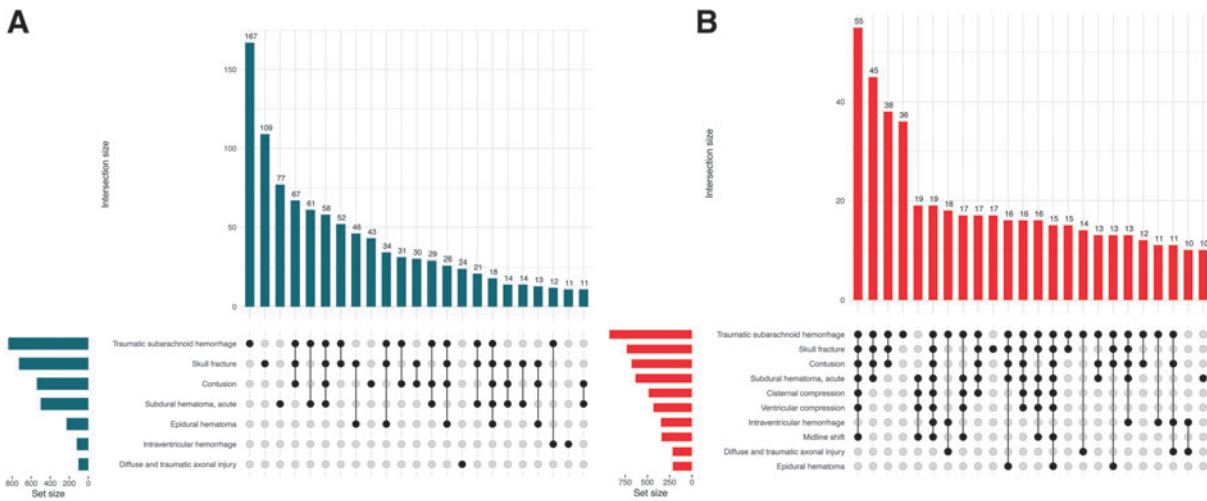


FIG. 11. UpSet plots of co-existing National Institute of Neurological Disorders and Stroke (NINDS) core traumatic brain injury (TBI) common data elements (CDEs) in mild **(A)** and moderate-severe **(B)** TBI patients. Core CDEs with less than 10 observations in the entire sample were not included in the analysis. Combinations with less than 10 occurrences in each subgroup and lesion types appearing exclusively in these less frequent combinations are not shown.

The distribution of the Marshall, Rotterdam, Helsinki, Fisher, Morris-Marshall, and Greene CT scores in CENTER-TBI is presented in Figure 13. Since subarachnoid blood is considered an important outcome predictor in TBI, the Fisher, Morris-Marshall and Greene CT score were also included. The Fisher CT score was originally

intended for scoring the quantity and distribution of subarachnoid hemorrhage following aneurysmal ruptures, with the purpose of predicting vasospasm, but has also been used in TBI. The Greene and Morris-Marshall classifications also include mass lesion, but none of these grading systems have been widely adopted. The

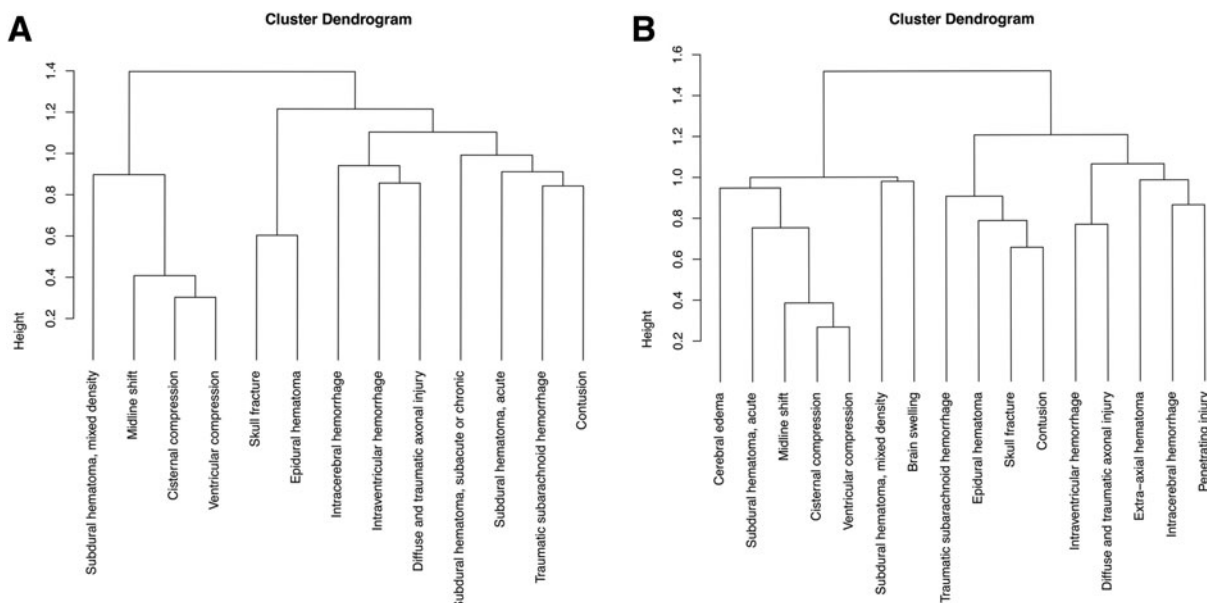


FIG. 12. Hierarchical clustering dendrograms of National Institute of Neurological Disorders and Stroke (NINDS) core traumatic brain injury (TBI) common data elements (CDEs) in **(A)** mild and **(B)** moderate-severe TBI patients. In each analysis, only lesions with 10 or more occurrences in that respective subgroup were included.

Table 7. Overview of CT Classification Systems

NCCT scoring system	Grade/characteristic	Radiologic imaging findings
Marshall	I	No visible intracranial pathology on NCCT
	II	Cisterns present with MLS <5 mm and/or lesion densities present <25 mL, may include bone fragments and foreign bodies
	III	Cisterns compressed or absent with MLS <5 mm, no high or mixed-density lesion >25 mL
	IV	MLS >5 mm, no high or mixed-density lesion >25 mL
	V + VI	High or mixed-density lesion >25 mL (e.g., Fig. 2 Panel 1 B1,B2,B4,B5; C4,C5; D1-D3; F1-F3; G1,G2 and Fig. 2 Panel 2 I1,I2,I4,I5; J1,J2; K5)
Rotterdam	Basal cisterns	0=normal (e.g., Supplementary Figure S19-20), 1=compressed (e.g., Fig. 2 Panel 2 H1-H3), 2=absent (e.g., Fig. 2 Panel 2 H4,H5)
	MLS	0=no shift or <=5 mm, 1=shift >5 mm (e.g., Fig. 2 Panel 1 C4; D2; F1-F3; G1)
	Epidural mass	0=present (e.g., Fig. 2 Panel 1 B1, B2, B4, B5), 1=absent (e.g. Fig. 2 Panel 1 B3 (< 25 mL))
	IVH/tSAH	0=absent, 1=present (Fig. 2 Panel 1 E1-E5; and Fig. 2 Panel 2 K1-K5)
	Score	Sum +1 (range=1 to 6)
Helsinki	Mass lesion type	SDH=2, ICH=2, EDH=-3
	Mass lesion size	Volume >25 mL=2 (see Marshall)
	IVH	0=absent, 3=present (see Rotterdam)
	Basal cisterns	0=normal, 1=compressed suprasellar cistern, 5=absent suprasellar cistern (e.g., Fig 2 Panel 2 H5)
	Score	Sum (range=-3 to 14)
Stockholm	tSAH	SAH in convexities (1: 1 to 5 mm, 2: > 5 mm) + SAH in basal cisterns (1: 1 to 5 mm, 2: > 5 mm) + IVH (2=present), Sum (range=0 to 6)
	Tally	MLS (mm)/10 + tSAH score/2 - 1 if EDH +1 if DAI (basal ganglia, splenium, or brainstem) +1 if dual-sided SDH +1

CT, computed tomography; DAI, diffuse axonal injury; ICH, intracerebral hemorrhage; MLS, midline shift; NCCT, non-contrast computed tomography; SDH, subdural hematoma; tSAH, traumatic subarachnoid hemorrhage; IVH, intraventricular hemorrhage.

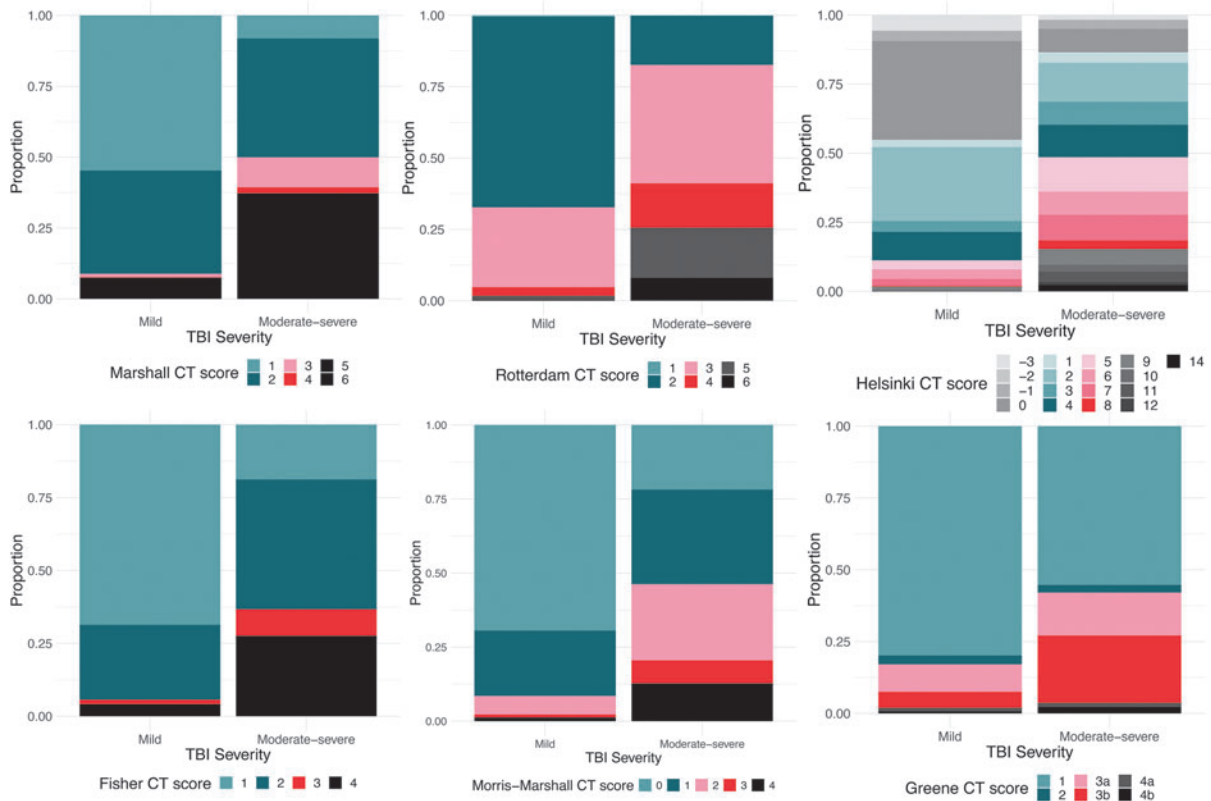


FIG. 13. Traumatic brain injury (TBI) classification and grading system scores in the Collaborative European NeuroTrauma Effectiveness Research in TBI (CENTER-TBI) study, based on admission non-contrast computed tomography (CT) findings. The distribution of scores on the 6 CT classification systems and their association with mortality and unfavorable outcome at 6 months in CENTER-TBI is presented in Supplementary Table S19. In CENTER-TBI, Marshall CT scores 5 and 6 were combined.

distribution of scores varied greatly between patients with moderate-severe TBI and those with mild TBI, for every classification system (p values <0.001 ; Supplementary Table S19). As expected, patients with moderate-severe TBI had more heterogeneous score distributions, and more often higher scores, associated with worse predicted outcomes, than patients with mild TBI. In general, for all classifications, higher scores were associated with worse outcomes (Fig. 14).

Discussion

This is the first comprehensive pictorial review of the NINDS TBI CDEs, based on over 4000 admission CT scans from the CENTER-TBI study, with descriptive information about core data elements and information

about supplemental and emerging elements, including locations and estimated volumes of lesions.

Our study shows that traumatic subarachnoid hemorrhage (45.3%), skull fractures (37.4%), contusions (31.3%), and acute subdural hematoma (28.9%) are the most frequently occurring non-contrast CT findings in acute TBI. The ranking of these lesions is the same in patients with moderate-severe TBI (baseline GCS score 3-12), compared with those with mild TBI (baseline GCS score 13-15). However, the frequency of occurrence is up to three times higher in moderate-severe TBI. Other lesion types also occur more often in patients with moderate-severe TBI and are often larger in volume (in the case of bleedings), and more diffuse (i.e., span multiple locations). In most TBI patients, there is a co-occurrence and clustering of pathoanatomic lesion

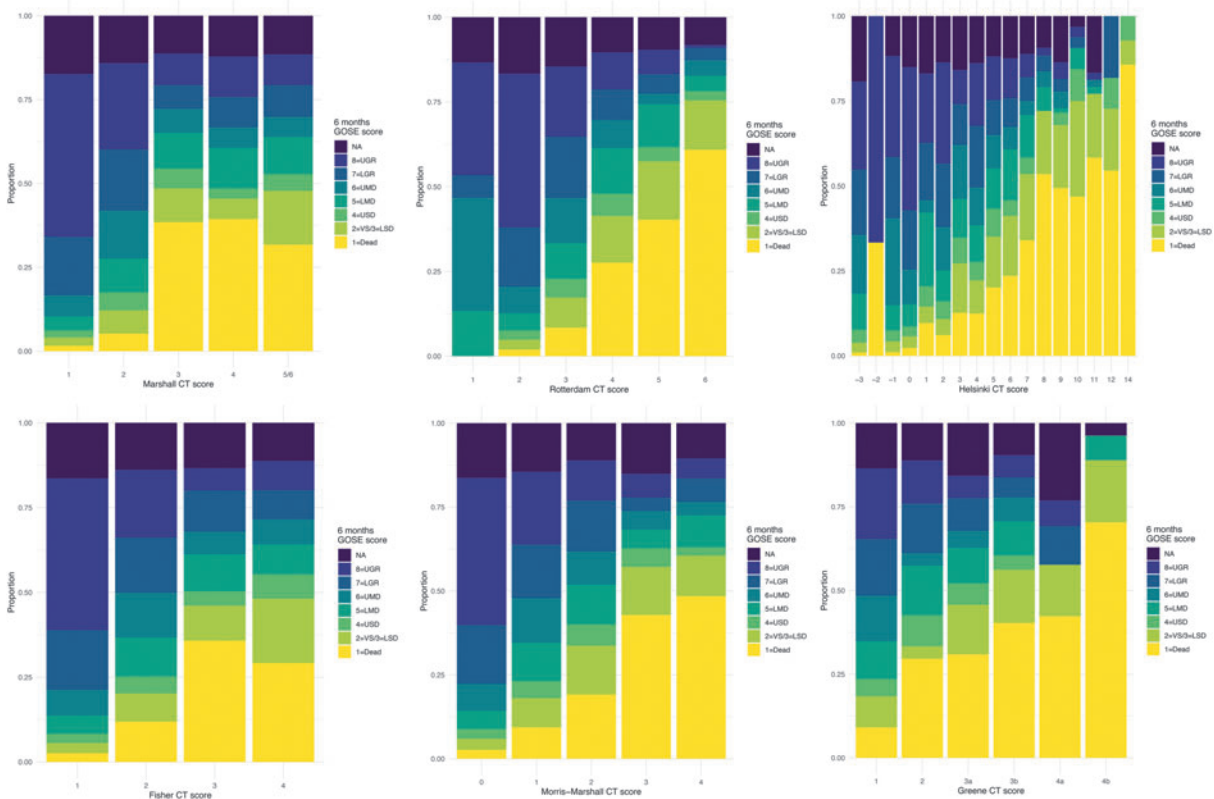


FIG. 14. Six-month GOSE scores within the categories of traumatic brain injury (TBI) classification and grading systems in Collaborative European NeuroTrauma Effectiveness Research in TBI (CENTER-TBI) based on admission non-contrast CT findings. We can observe that the proportion of worse outcomes generally increases with the CT score category, for all six classifications. Some categories (e.g., Helsinki CT score -2) have very few observations (Supplementary Table S19). GOSE scores were assessed by in-person/telephonic interviews or postal questionnaires, and as such a clear distinction between GOSE 2 (VS) and GOSE 3 (LSD) was not always possible. As a result of this, these two categories were combined, giving a seven-point ordinal scale. CT, computed tomography; GOSE, Glasgow Outcome Scale-Extended; LGR, lower good recovery; LMD, lower moderate disability; LSD, lower severe disability; NA, not available; UGR, upper good recovery; UMD, upper moderate disability; USD, upper severe disability; VS, vegetative state.

types, with significant differences between moderate-severe and mild TBI patients. The clustering in mild TBI patients is very similar to what Yuh et al described.⁹¹ For instance, aSDH, contusion, and tSAH typically cluster together and have been associated with linear acceleration and deceleration forces.⁹¹ In our study, and in line with Yuh et al and colleagues, IVH and DAI/TAI cluster together, however this time also with intracerebral hemorrhage. These injuries are probably caused by more rotational acceleration and deceleration forces.⁹² Epidural hematoma and skull fracture formed a separate cluster in our cohort of mild TBI patients. Often these patients have good outcomes.⁹¹ Interestingly, in moderate-severe TBI patients, contusions were added to this cluster, which also indicates a higher level and probably a combination of impact forces. In moderate-severe TBI patients, patterns were thus more complex, with more co-existing lesion types and more frequent signs of mass effect (i.e., edema, MLS, cisternal and ventricular compression). For instance, we found a specific aSDH cluster, with mass effect, including secondary injuries like edema, which is very different from the mild TBI patients. Secondary injuries related to mass effect were at least 7 to 8 times more frequent in moderate-severe TBI (e.g., edema, brain swelling).

Patients who were clinically classified based on the baseline GCS score as “mild TBI” sometimes displayed remarkable imaging findings, such as hemorrhagic mass lesions with volumes higher than 25 cm³, which were mostly located in the frontal lobes. Moreover, in over a hundred mild TBI patients (i.e., 117), imaging features and clusters of imaging features that are suggestive of serious underlying pathophysiology were present (MLS, all cisterns absent, 3rd or 4th ventricle obliteration, brain herniation). Further, since a large threshold was used to report MLS (> 5 mm), the true number of patients with a shift of the midline was probably underestimated. The median time from injury to scan in the 117 patients with mild TBI and markers of significant mass effect was 3.1 h (IQR 1.7-5.7 h) and the median age was 62 years (IQR 49-73). In 61/117 (52%) of these patients, clinical deterioration was recorded at some point during hospitalization, either before or after the scan, while others remained in an acceptable or good neurologic condition, despite their imaging findings, and were treated conservatively. Interestingly, the average age in this subgroup of 117 patients was significantly higher than that of the rest of our sample and that of the patients with mild TBI, but without signs of mass effect. Additionally, sporadic data-entry errors in recorded GCS scores cannot be excluded. These findings highlight the limitations of a unidimensional, static approach to severity classification by the GCS and illustrate how imaging characteristics can contribute to more refined characterization.

The need for improved characterization of TBI severity has been recognized by the NIH/NINDS, which

resulted in the implementation of a task force, consisting of six working groups, to develop a more refined and multi-dimensional approach to characterization of TBI. The working groups convened at a workshop on TBI classification and nomenclature in January 2024 (<https://www.ninds.nih.gov/news-events/events/ninds-tbi-classification-and-nomenclature-workshop>). The aim of the workshop was two-fold: 1) to highlight the working groups’ findings after reviewing data from previous and existing clinical studies and 2) to seek public input and feedback from the TBI community and stakeholders with the goal of informing the development of a more precise, and evidence-based classification system—beyond the terms that are currently used “mild, moderate, severe”. The inclusion of imaging and other markers (such as blood-based biomarkers) has been proposed as a more informative approach that could improve the characterization of these patients.

Multiple classification systems exist that group specific CT features with a main aim to predict clinical outcome. In our study, the distribution of scores on each of these classifications also varied greatly between patients with mild and moderate-severe TBI. As expected, patients with moderate-severe TBI had a more heterogeneous score distribution, and more often higher scores, predictive of worse clinical outcomes, compared with patients with mild TBI. Observed outcomes for the various CT score categories were generally worse for higher scores, but no formal model validation was performed in the present study. Acute trauma-induced vascular abnormalities like dissections, (pseudo-)aneurysms or venous sinus injuries were rarely encountered in our dataset. The low number of vascular lesions may be explained by the lack of contrast-enhanced imaging in the acute phase, and the fact that some lesions (e.g., pseudoaneurysms) may develop over time, and are not yet visible on admission CTs. Studies have shown that these abnormalities are quite rare in general, even in level I trauma centers.⁹³ However, incorporating CTA in targeted patients can be useful.⁹⁴ For a more comprehensive discussion on these specific lesion types, we refer to the supplementary materials (Supplementary Text File).

Certain lesions with pathophysiological connotations like brain swelling and ischemia, or subacute/chronic hematomas were also rare in the acute phase. Typically, these pathologies are encountered on serial follow-up imaging.

Critical appraisal of the NINDS CDEs and considerations for their improvement

The radiologic NINDS TBI CDEs were developed over 10 years ago and are subject to updates and improvements based on data and experience. Minor changes, mostly with respect to terminology of the classification of CDEs as basic, supplemental, or emerging, have been implemented over the past years. Multiple

studies have been published regarding the radiologic CDEs and have mostly focused on reliability and validation.^{15,16,90,95-97} In addition, a whole series of studies have already been published using mostly core imaging CDE data from the CENTER- and Transforming Research and Clinical Knowledge in TBI (TRACK-TBI) studies.^{91,98-107} The empirical experience of CENTER-TBI and other observational studies, such as TRACK-TBI, can provide a solid evidence base to inform updating of the CDEs. Overall, the CENTER-TBI experience in using the radiologic TBI CDEs is overwhelmingly positive as they provide a standardized and structured approach for radiologic assessment, thus facilitating validation and meta-analyses across studies. An example is the study by Yuh and coworkers described above, on CT features associated with adverse outcome after mild TBI.⁹¹ The radiologic TBI CDEs were primarily developed from a research perspective. They also have great potential for broad implementation into clinical practice. We found, however, that completion of the reading templates is time-consuming, up to sometimes more than an hour per patient, depending on the complexity of the pathology. An abbreviated version, for example restricted to core descriptions, would be needed for templated and structured clinical reporting. Expert consensus-based templates would also be needed, like the ones used in the reporting and data systems (RADS) by the American College of Radiology (<https://www.acr.org/Clinical-Resources/Reporting-and-Data-Systems>). Redundant information can be omitted and other elements can be adjusted based on the insights gained from the CENTER-TBI experience and analogous studies.

Redundancy and overlap

The current radiologic CDEs have many elements. Some CDEs, such as vascular dissection, traumatic aneurysm, venous sinus injury, cervicomedullary/brainstem injury, and ischemia were only rarely reported (≤ 5 times). Inclusion of CDEs should, however, not only depend on frequency of occurrence, but also on clinical relevance taking the timing of CT scanning into consideration. For example, vascular dissection and traumatic aneurysm have high clinical relevance, and may have been underreported in CENTER-TBI. Ischemia may not be relevant in the acute phase of an admission scan but becomes more important over time.

We found that “hydrocephalus” appears in three different elements (i.e., in the context of tSAH, ventricular effacement, and IVH), which could be grouped into one distinct CDE with different subtypes. Moreover, acute ventricular dilatation in our dataset was not reported in the context of tSAH or IVH but was mostly seen in patients with large subdural hematomas, where midline shift and ipsilateral compression of the ventricles leads to en-

largement of the contralateral ventricles. Brainstem compression is also an option that appears in three elements (i.e., ventricular effacement, cisternal compression, and cervicomedullary/brainstem injury). To avoid reporting redundancy, cisternal compression could be used as the single element to denote brainstem compression.

Additional elements

In the CENTER-TBI study, and in clinical routine, radiologists often describe the subtype of cerebral herniation (i.e., subfalcine, transtentorial, etc.). Although highly correlated with MLS, we show that herniation subtypes are also highly correlated with other features that are clinically relevant to report (e.g., transtentorial herniation and subsequent cisternal compression). It could therefore be useful to add this CDE in the next update, as the granularity of the subtype contains important clinical information. In CENTER-TBI, the reviewers experienced difficulties in differentiating between clear-cut edema, brain swelling and hyperemia, and felt more comfortable adding “cortical sulcus effacement” as an extra CDE in the acute phase. We suggest considering adding “cortical sulcus effacement” as new element, or at least to provide better guidance for scoring edema, brain swelling and hyperemia. As opposed to free-text reporting, the current reporting templates do not include an option to denote a level of confidence or add nuance to the reported observations. In CENTER-TBI, when readers wanted to elaborate on a certain lesion, or in complex cases where the reporting templates were lacking a certain option, the free-text box in the incidental findings was often used. This indicates a need for reporting some level of (un)certainty. Although we in general would discourage an option for free-text entries, in this case, inclusion of a “comment” box may be considered. The relatively high incidence of incidental findings in the CENTER-TBI population (15.2%) motivates inclusion of incidental findings as a separate CDE. Finally, we suggest including one or more of the CT classification systems as supplemental CDEs.

Ambiguity in definitions and measurements

Some issues exist with definitions that are still in flux (e.g., “DAI/TAI,” cerebral “hyperemia,” “gliding contusions”), which can be a source of systematic observer variation. For instance, in CENTER-TBI, cerebral hyperemia was only used as a subtype of brain swelling when it corresponded with the CDE definition but was rarely reported. Only in cases with mostly global edema and without large bleedings, and in cases where it was difficult to distinguish between edema or hyperemia, “brain swelling” was used, which is also the most common term used in clinical radiology settings in this context. A better description or collapsing of these entities

might be needed in an updated version of the CDEs. Although volumetric measurements appear objective, they depend on the imaging plane in which they are performed and can be time-consuming. Finally, some thresholds in the current version of the CDEs appear somewhat arbitrary (e.g., 2 mm for MLS, 1 cm thickness in the context of depressed fractures, 3 mm in the context of a diastatic skull fracture and “mass-like tSAH”). It would be useful if these thresholds were supported by evidence and guidelines established on how to take these measurements.

Dynamic changes

A challenging aspect in both the reporting and the analysis of neuroimaging findings is the evolution over time. Most individual pathoanatomic lesion types (except for skull fractures and incidental findings, for the most part) are dynamic in the acute and subacute period after TBI. Individual primary lesions may resolve or expand, separate, or coalesce, either spontaneously or because of directed therapies, and secondary injuries may appear or evolve accordingly. Such changes will be apparent in those patients with serial imaging. For instance, compared with a pre-operative SDH or EDH, the evacuated bleedings that remain post-operatively will often be labeled as EAH, or contusions that coalesce between locations can change into “intracerebral hemorrhages.” At present, no specific reporting recommendations to record such dynamic transitions of individual lesions exist. A technical solution would be to implement unique lesion identifiers in structured reporting templates, so that all observed individual lesions could be tracked longitudinally on serial imaging, along with changes in their core, supplemental and emerging information. Such lesion-level reporting would facilitate subsequent analysis for both mechanistic and prognostic purposes.

Limitations

We acknowledge several limitations to our study. The CENTER-TBI dataset consists of images from over 60 European recruiting centers with substantial inter-center differences in recruitment number (i.e., university hospitals and level I trauma centers recruited more patients). Also, CENTER-TBI only included patients with an indication for CT scanning, which created a bias towards patients with intracranial pathology.

Second, although the use of imaging CDEs minimizes observer variability, it remains a qualitative interpretation, even when a double reading paradigm is implemented. Such subjective interpretations can still be prone to observer and data entry errors.

Third, we did not report CDEs for atrophy/encephalomalacia, since we focused on acute non-contrast CT. Atrophic changes are longitudinal in nature

and are better captured with MRI algorithms like voxel-based morphometry (VBM).

Fourth, some mismatch between the times of GCS evaluation and imaging acquisition is unavoidable, as CT scanning is generally performed only after the baseline GCS is documented. In CENTER-TBI, missing post-stabilization GCS scores were imputed with the closest in-time available value, meaning that for some patients, hospital arrival or pre-hospital GCS scores were used. We recognize that both the imaging findings and the baseline GCS score represent a snapshot in time, whilst the disease course is dynamic. Particularly in patients in whom pre-hospital GCS assessments were used as baseline value, transitions between higher and lower GCS scores could translate to different classifications of TBI severity. For example, it is possible that an admission CT was only ordered for an initially mild TBI patient after they deteriorated to a lower GCS value (Table 2). Specifically in the elderly, a decline in GCS from 15 to 14 can already be associated with worse clinical outcome.¹⁰⁸ Additionally, we recognize that relying exclusively on an admission GCS score of 13 or higher, without subsequent reassessment or updates within the initial hours, does not represent the definitive benchmark for categorizing mild TBI. Divergent perspectives exist within the literature, with some authors defining the GCS 13-15 range as mild, while others designate only GCS 14 and/or 15 as such.¹⁰⁹ Moreover, there is an ongoing debate to revisit the classification of patients with a GCS score of 13 as “moderate” TBI due to notable differences in neuroimaging findings and the necessity for neurosurgical procedures compared with those with scores of 14-15.

Further, certain criteria, such as posttraumatic amnesia not exceeding 24 h, are incorporated by the World Health Organization (WHO) task force definition of mild TBI.¹¹⁰ It is thus likely that some cases identified as “mild” in our study may have exhibited prolonged posttraumatic amnesia, potentially warranting reclassification as “moderate” TBI.

In our investigation, we opted for a conventional differentiation between moderate-severe and mild TBI, a common practice. However, our findings indicate that this classification is constrained and one-dimensional. Our results also emphasize that the effectiveness of this distinction is contingent upon the method and timing of employing the GCS scoring. While acknowledging the limitation of potential mismatches between the times of GCS evaluation and imaging acquisition in our study, we highlight the possible importance of reporting imaging findings to enhance severity characterization.

Fifth, we acknowledge that the ABC/2 method used for volumetric calculations, may not always be a correct representation of the actual volume of lesions. Expert

segmentations remain the reference standard. Even so, it remains difficult to have a solid comparison of ABC/2 method with this reference standard, as no measures of pixel similarity or overlap like the Dice coefficient can be calculated. However, studies have shown that it can be a good estimation of the volume of lesions and was therefore considered in this study.¹¹¹⁻¹¹³ In the future, these measurements might be validated by comparing with actual manual volume segmentations.

Sixth, we recognize that the critical appraisal of the NINDS radiologic CDEs represents little more than expert opinion. However, it is based on the vast experience of the CT reviewers involved in CENTER-TBI and forms a solid evidence base to inform updating of the CDEs to version 3.0.

Seventh, we recognize the need to better represent children, especially the youngest, who are significantly affected by TBI and frequently admitted to hospitals. MRI use in the pediatric population is increasing, driven by concerns over radiation and the demand for higher resolution imaging.

Future perspective

Advanced computational methods like natural language processing (NLP) algorithms are available that can be used to extract core CDEs from free-text radiology reports with good accuracy.¹¹⁴ One problem with this method however, is that it faces linguistic challenges that are similar to those of humans, and that these algorithms have difficulties handling incomplete reports or reports with variable content.¹¹⁵ Moreover, it is not clear how well these methods perform on more granular supplemental and emerging levels of the CDEs.

In the future, speech-enabled structured reporting using CDE-based itemized templates integrated into the radiologist's workflow would likely be the preferred method. This approach, would allow radiologists to incrementally enhance report details in a structured way, and would not only promote standardized communication across the patient care pathway but could also produce machine-readable data capable of constructing research registries with detailed lesion information surpassing the scale of the CENTER and TRACK-TBI studies.

In upcoming iterations of the CDEs, tools that allow radiologists and investigators to selectively choose and expand only the elements pertinent to the specific needs of a clinical report or research study from a predetermined set of elements would be favorable. For instance, when addressing an acute non-contrast CT scan of an elderly patient, specific elements could pop up, or be selected, from a primary tree using a drop-down list. This functionality would also potentially minimize the redundancy and overlap we encountered in the current system.

Emerging information about abnormal imaging findings can also be drawn from computer-aided image analysis.^{12,13} In this study, we did not include computational measurements. However, currently, there are multiple algorithms that have been developed that already perform better than humans at detecting acute bleeding on non-contrast CT scans.^{116,117} Some of these algorithms are used to flag abnormal scans and move them up the radiologists' worklist.¹¹⁸

Tools were also developed using CENTER-TBI data that can automatically extract and quantify certain features or CDEs from non-contrast CT scans, especially those that are related to mass effect (e.g., MLS, compression of cisterns, and certain bleedings with segmented lesion volume).^{119,120} Other algorithms have been developed to track the progression of lesion volume, demonstrating potential applications for imaging-based precision medicine and patient follow-up.^{107,121}

Many of these methods typically stay within the realm of research, with only a limited number transitioning into clinical practice. Given the considerable heterogeneity of TBI pathology, even with robust abnormality detection, these models encounter significant hurdles in segmentation and classification. The challenges arise from the necessity for extensive manually annotated datasets for both training and testing.

External validation in independent datasets is also particularly problematic, due to variations in annotation or segmentation software used by different researchers. Cumbersome and time-consuming manual segmentation, especially for certain lesion types like tSAH, along with poor CT resolution, and a lack of clear definition of boundaries between coexisting lesion types (e.g., tSAH, contusion and SDH) has hindered progress of algorithm development. Additionally, the lack of harmonized lesion definitions results in substantial inter-observer differences among experts, making comparisons of methodologies difficult.

In addition to CT-based algorithms, MRI-based algorithms exist that can automatically detect microbleeds with great accuracy,^{122,123} and segment different types of lesions.¹²⁴ Other already well-established algorithms can objectively quantify longitudinal changes in gray or white matter (e.g., voxel-based morphometry),¹²⁵⁻¹²⁷ even in severely-injured patients with heavily distorted brains.¹²⁸ Advanced neuroimaging methods, like diffusion MRI (dMRI) in particular, could help detect structural injury to axons. This technique thus has the potential to improve the characterization of "DAI," which is now generally considered a misnomer and, as mentioned above, efforts are on the way to improve the characterization of this pathologic entity. In addition, resting-state fMRI is a promising method that could help quantify functional changes in different brain networks, otherwise not visible with conventional neuroimaging.

Even though many of the above-described methods still need to mature and there is no clear consensus yet on the interpretation of the findings,¹²⁹ and the gap between research and the clinic remains substantial, computational approaches show great promise to standardize and accelerate certain aspects of image analysis, and can reveal pathology that is otherwise not visible to the naked eye. In the absence of a universal ground truth validation dataset however, reliable benchmarking of algorithms that quantify visible macroscopic abnormalities remains impossible, and we see a great need to develop a “ground truth validation dataset” for this specific purpose.

As additional evidence on the CDEs continues to accumulate, it is anticipated that a hybrid approach to interpretation and reporting will develop in the future. In routine clinical practice, this approach would ideally manifest itself through the adoption of a speech-enabled structured radiological reporting template, with evidence-based core and supplemental CDEs as items. These reports can then be enhanced by incorporating objective and quantitative measures of lesion burden derived from emerging advanced and externally validated computational tools and other markers for a more comprehensive diagnosis and targeted treatment approach.¹³⁰

Conclusion

We developed a comprehensive pictorial overview of the NINDS radiological TBI CDEs, supported by data from one of the largest structured imaging databases in TBI to date. This overview, accompanied by detailed analysis, serves as a valuable tool for evaluating, characterizing, and reporting the vast spectrum of complex acute CT abnormalities and pathophysiologic findings in acute brain-injured patients. Our research offers insight into the neuroimaging case-mix of current TBI patients, focusing on adults in the European context. Further, we highlight the drawbacks of adopting a one-dimensional, static approach, advocating for a more nuanced characterization of TBI. The results presented, combined with a critical appraisal of the CDEs, represent an empirical evidence base to inform updating of the CDEs to version 3.0.

Transparency, Rigor, and Reproducibility Summary

The study was pre-registered on clinicaltrials.gov with the identifier NCT02210221. A total of 4509 patients participated in the CENTER-TBI study, and 4087 were included in the analysis with an interpretable CT scan. The final clinical outcome assessments and adjudications were conducted by team members who were unaware of the relevant characteristics of the participants. As this study is primarily descriptive and a pictorial review, there was no need for a formal sample size calculation, and no prognostic models were developed. The key inclusion crite-

ria and outcome evaluations adhere to established standards. De-identified data and the analytical code from this study can be made available upon approval of a submitted study proposal at <https://www.center-tbi.eu/data>. The analytical code used for the analyses presented in this study is not publicly available in a repository. This paper will be published under a Creative Commons Open Access license and will be freely accessible at <https://www.liebertpub.com/loi/neu> upon publication.

Acknowledgments

We thank Charlotte Timmermans and Ruben Houbrechts for their support during central review. We would also like to thank all the CENTER-TBI collaborators who participated in scanning and uploading the images to the imaging repository.

The CENTER-TBI Participants and Investigators

Cecilia Åkerlund, Department of Physiology and Pharmacology, Section of Perioperative Medicine and Intensive Care, Karolinska Institutet, Stockholm, Sweden; Krisztina Amrein, János Szentágothai Research Centre, University of Pécs, Pécs, Hungary; Nada Andelic, Division of Clinical Neuroscience, Department of Physical Medicine and Rehabilitation, Oslo University Hospital and University of Oslo, Oslo, Norway; Lasse Andreassen, Department of Neurosurgery, University Hospital Northern Norway, Tromsø, Norway; Audny Anke, Department of Physical Medicine and Rehabilitation, University Hospital Northern Norway, Tromsø, Norway; Anna Antoni, Trauma Surgery, Medical University Vienna, Vienna, Austria; Gérard Audibert, Department of Anesthesiology and Intensive Care, University Hospital Nancy, Nancy, France; Philippe Azouvi, Raymond Poincaré hospital, Assistance Publique–Hôpitaux de Paris, Paris, France; Maria Luisa Azzolini, Department of Anesthesiology and Intensive Care, S Raffaele University Hospital, Milan, Italy; Ronald Bartels, Department of Neurosurgery, Radboud University Medical Center, Nijmegen, the Netherlands; Pál Barzó, Department of Neurosurgery, University of Szeged, Szeged, Hungary; Romuald Beauvais, International Projects Management, ARTTIC, Munchen, Germany; Ronny Beer, Department of Neurology, Neurological Intensive Care Unit, Medical University of Innsbruck, Innsbruck, Austria; Bo-Michael Bellander, Department of Neurosurgery and Anesthesia and Intensive Care Medicine, Karolinska University Hospital, Stockholm, Sweden; Antonio Belli, NIHR Surgical Reconstruction and Microbiology Research Centre, Birmingham, U.K.; Habib Benali, Anesthésie-Réanimation, Assistance Publique–Hôpitaux de Paris, Paris, France; Maurizio Berardino, Department of Anesthesia and ICU, AOU Città della Salute e della Scienza di Torino-Orthopedic and Trauma Center, Torino, Italy; Luigi Beretta, Department of Anesthesiology and Intensive

Care, S Raffaele University Hospital, Milan, Italy; Morten Blaabjerg, Department of Neurology, Odense University Hospital, Odense, Denmark; Peter Bragge, BehaviourWorks Australia, Monash Sustainability Institute, Monash University, Victoria, Australia; Alexandra Brazinova, Department of Public Health, Faculty of Health Sciences and Social Work, Trnava University, Trnava, Slovakia; Vibeke Brinck, Quesgen Systems Inc., Burlingame, California, U.S.; Joanne Brooker, Australian and New Zealand Intensive Care Research Centre, Department of Epidemiology and Preventive Medicine, School of Public Health and Preventive Medicine, Monash University, Melbourne, Australia; Camilla Brorsson, Department of Surgery and Perioperative Science, Umeå University, Umeå, Sweden; Andras Buki, Department of Neurosurgery, Medical School, University of Pécs, Hungary and Neurotrauma Research Group, János Szentágothai Research Centre, University of Pécs, Hungary; Monika Bullinger, Department of Medical Psychology, Universitätsklinikum Hamburg-Eppendorf, Hamburg, Germany; Manuel Cabeleira, Brain Physics Lab, Division of Neurosurgery, Dept of Clinical Neurosciences, University of Cambridge, Addenbrooke's Hospital, Cambridge, UK; Alessio Caccioppola, Neuro ICU, Fondazione IRCCS Cà Granda Ospedale Maggiore Policlinico, Milan, Italy; Emiliana Calappi, Neuro ICU, Fondazione IRCCS Cà Granda Ospedale Maggiore Policlinico, Milan, Italy; Maria Rosa Calvi, Department of Anesthesiology and Intensive Care, S Raffaele University Hospital, Milan, Italy; Peter Cameron, ANZIC Research Centre, Monash University, Department of Epidemiology and Preventive Medicine, Melbourne, Victoria, Australia; Guillermo Carbayo Lozano, Department of Neurosurgery, Hospital of Cruces, Bilbao, Spain; Marco Carbonara, Neuro ICU, Fondazione IRCCS Cà Granda Ospedale Maggiore Policlinico, Milan, Italy; Simona Cavallo, Department of Anesthesia and ICU, AOU Città della Salute e della Scienza di Torino-Orthopedic and Trauma Center, Torino, Italy; Giorgio Chevillard, NeuroIntensive Care, Niguarda Hospital, Milan, Italy; Arturo Chieragato, NeuroIntensive Care, Niguarda Hospital, Milan, Italy; Giuseppe Citerio, School of Medicine and Surgery, Università Milano Bicocca, Milano, Italy, and NeuroIntensive Care Unit, Department Neuroscience, IRCCS Fondazione San Gerardo dei Tintori, Monza, Italy; Hans Clusmann, Department of Neurosurgery, Medical Faculty RWTH Aachen University, Aachen, Germany; Mark Coburn, Department of Anesthesiology and Intensive Care Medicine, University Hospital Bonn, Bonn, Germany; Jonathan Coles, Department of Anesthesia and Neurointensive Care, Cambridge University Hospital NHS Foundation Trust, Cambridge, U.K.; Jamie D. Cooper, School of Public Health and PM, Monash University and The Alfred Hospital, Melbourne, Victoria, Australia; Marta Correia, Radiology/MRI Department, MRC Cognition and Brain Sciences Unit, Cambridge, U.K.; Amra Čović, Institute of Medical Psychology and Medical Sociology, Universitätsmedizin Göttingen, Göttingen, Germany; Nicola Curry, Oxford University Hospitals NHS Trust, Oxford, U.K.; Endre Czeiter, Department of Neurosurgery, Medical School, University of Pécs, Hungary, and Neurotrauma Research Group, János Szentágothai Research Centre, University of Pécs, Hungary; Marek Czosnyka, Brain Physics Lab, Division of Neurosurgery, Dept of Clinical Neurosciences, University of Cambridge, Addenbrooke's Hospital, Cambridge, U.K.; Claire Dahyot Fizelier, Intensive Care Unit, CHU Poitiers, Poitiers, France; Paul Dark, University of Manchester NIHR Biomedical Research Centre, Critical Care Directorate, Salford Royal Hospital NHS Foundation Trust, Salford, U.K.; Helen Dawes, Movement Science Group, Faculty of Health and Life Sciences, Oxford Brookes University, Oxford, U.K.; Véronique De Keyser, Department of Neurosurgery, Antwerp University Hospital, Edegem, Belgium; Vincent Degos, Anesthésie-Réanimation, Assistance Publique-Hopitaux de Paris, Paris, France; Francesco Della Corte, Department of Anesthesia and Intensive Care, Maggiore Della Carità Hospital, Novara, Italy; Hugo den Boogert, Department of Neurosurgery, Radboud University Medical Center, Nijmegen, the Netherlands; Bart Depreitere, Department of Neurosurgery, University Hospitals Leuven, Leuven, Belgium; Đula Đilvesi, Department of Neurosurgery, Clinical Centre of Vojvodina, Faculty of Medicine, University of Novi Sad, Novi Sad, Serbia; Abhishek Dixit, Division of Anaesthesia, University of Cambridge, Addenbrooke's Hospital, Cambridge, U.K.; Emma Donoghue, Australian and New Zealand Intensive Care Research Centre, Department of Epidemiology and Preventive Medicine, School of Public Health and Preventive Medicine, Monash University, Melbourne, Australia; Jens Dreier, Center for Stroke Research Berlin, Charité-Universitätsmedizin Berlin, Corporate Member of Freie Universität Berlin, Humboldt-Universität zu Berlin, and Berlin Institute of Health, Berlin, Germany; Guy Loup Dulière, Intensive Care Unit, CHR Citadelle, Liège, Belgium; Ari Ercole, Division of Anaesthesia, University of Cambridge, Addenbrooke's Hospital, Cambridge, U.K.; Patrick Esser, Movement Science Group, Faculty of Health and Life Sciences, Oxford Brookes University, Oxford, U.K.; Erzsébet Ezer, Department of Anaesthesiology and Intensive Therapy, University of Pécs, Pécs, Hungary; Martin Fabricius, Departments of Neurology, Clinical Neurophysiology, and Neuroanesthesiology, Region Hovedstaden Rigshospitalet, Copenhagen, Denmark; Valery L. Feigin, National Institute for Stroke and Applied Neurosciences, Faculty of Health and Environmental Studies, Auckland University of Technology, Auckland, New Zealand; Kelly Foks,

Department of Neurology, Erasmus MC, Rotterdam, the Netherlands; Shirin Frisvold, Department of Anesthesiology and Intensive care, University Hospital Northern Norway, Tromsø, Norway; Alex Furmanov, Department of Neurosurgery, Hadassah-Hebrew University Medical Center, Jerusalem, Israel; Pablo Gagliardo, Fundación Instituto Valenciano de Neurorehabilitación (FIVAN), Valencia, Spain; Damien Galanaud, Anesthésie-Réanimation, Assistance Publique-Hôpitaux de Paris, Paris, France; Dashiell Gantner, ANZIC Research Centre, Monash University, Department of Epidemiology and Preventive Medicine, Melbourne, Victoria, Australia; Guoyi Gao, Department of Neurosurgery, Shanghai Renji Hospital, Shanghai Jiaotong University/School of Medicine, Shanghai, China; Pradeep George, Karolinska Institutet, INCF International Neuroinformatics Coordinating Facility, Stockholm, Sweden; Alexandre Ghuysen, Emergency Department, CHU, Liège, Belgium; Lelde Giga, Neurosurgery Clinic, Pauls Stradins Clinical University Hospital, Riga, Latvia; Ben Glocker, Department of Computing, Imperial College London, London, U.K.; Jagoš Golubovic, Department of Neurosurgery, Clinical Centre of Vojvodina, Faculty of Medicine, University of Novi Sad, Novi Sad, Serbia; Pedro A. Gomez, Department of Neurosurgery, Hospital Universitario 12 de Octubre, Madrid, Spain; Johannes Gratz, Department of Anesthesia, Critical Care and Pain Medicine, Medical University of Vienna, Austria; Benjamin Gravesteijn, Department of Public Health, Erasmus Medical Center-University Medical Center, Rotterdam, the Netherlands; Francesca Grossi, Department of Anesthesia & Intensive Care, Maggiore Della Carità Hospital, Novara, Italy; Russell L. Gruen, College of Health and Medicine, Australian National University, Canberra, Australia; Deepak Gupta, Department of Neurosurgery, Neurosciences Centre and JPN Apex trauma centre, All India Institute of Medical Sciences, New Delhi-110029, India; Juanita A. Haagsma, Department of Public Health, Erasmus Medical Center-University Medical Center, Rotterdam, the Netherlands; Iain Haitsma, Department of Neurosurgery, Erasmus MC, Rotterdam, the Netherlands; Raimund Helbok, Department of Neurology, Neurological Intensive Care Unit, Medical University of Innsbruck, Innsbruck, Austria; Eirik Helseth, Department of Neurosurgery, Oslo University Hospital, Oslo, Norway; Lindsay Horton, Division of Psychology, University of Stirling, Stirling, U.K.; Jilske Huijben, Department of Public Health, Erasmus Medical Center-University Medical Center, Rotterdam, the Netherlands; Peter J. Hutchinson, Division of Neurosurgery, Department of Clinical Neurosciences, Addenbrooke's Hospital and University of Cambridge, Cambridge, U.K.; Bram Jacobs, Department of Neurology, University of Groningen, University Medical Center Groningen, Groningen, the Netherlands; Stefan Jankowski, Neurointensive Care, Sheffield Teaching Hospitals NHS Foundation Trust, Sheffield, U.K.; Mike Jarrett, Quesgen Systems Inc., Burlingame, California, U.S.; Ji yao Jiang, Karolinska Institutet, INCF International Neuroinformatics Coordinating Facility, Stockholm, Sweden; Faye Johnson, Salford Royal Hospital NHS Foundation Trust Acute Research Delivery Team, Salford, U.K.; Kelly Jones, National Institute for Stroke and Applied Neurosciences, Faculty of Health and Environmental Studies, Auckland University of Technology, Auckland, New Zealand; Mladen Karan, Department of Neurosurgery, Clinical Centre of Vojvodina, Faculty of Medicine, University of Novi Sad, Novi Sad, Serbia; Angelos G. Koliass, Division of Neurosurgery, Department of Clinical Neurosciences, Addenbrooke's Hospital and University of Cambridge, Cambridge, U.K.; Erwin Kompanje, Department of Intensive Care and Department of Ethics and Philosophy of Medicine, Erasmus Medical Center, Rotterdam, the Netherlands; Daniel Kondziella, Departments of Neurology, Clinical Neurophysiology and Neuroanesthesiology, Region Hovedstaden Rigshospitalet, Copenhagen, Denmark; Evgenios Kornaropoulos, Division of Anaesthesia, University of Cambridge, Addenbrooke's Hospital, Cambridge, U.K.; Lars Owe Koskinen, Department of Clinical Neuroscience, Neurosurgery, Umeå University, Umeå, Sweden; Noémi Kovács, Hungarian Brain Research Program-Grant No. KTIA_13_NAP-A-II/8, University of Pécs, Pécs, Hungary; Ana Kowark, Department of Anaesthesiology, University Hospital of Aachen, Aachen, Germany; Alfonso Lagares, Department of Neurosurgery, Hospital Universitario 12 de Octubre, Madrid, Spain; Linda Lanyon, Karolinska Institutet, INCF International Neuroinformatics Coordinating Facility, Stockholm, Sweden; Steven Laureys, Cyclotron Research Center, University of Liège, Liège, Belgium; Fiona Lecky, Centre for Urgent and Emergency Care Research (CURE), Health Services Research Section, School of Health and Related Research (ScHARR), University of Sheffield, Sheffield, U.K. and Emergency Department, Salford Royal Hospital, Salford U.K.; Didier Ledoux, Cyclotron Research Center, University of Liège, Liège, Belgium; Rolf Lefering, Institute of Research in Operative Medicine (IFOM), Witten/Herdecke University, Cologne, Germany; Valerie Legrand, VP Global Project Management CNS, ICON, Paris, France; Aurelie Lejeune, Department of Anesthesiology-Intensive Care, Lille University Hospital, Lille, France; Leon Levi, Department of Neurosurgery, Rambam Medical Center, Haifa, Israel; Roger Lightfoot, Department of Anesthesiology and Intensive Care, University Hospitals Southampton NHS Trust, Southampton, U.K.; Hester Lingsma, Department of Public Health, Erasmus Medical Center-University Medical Center, Rotterdam, the Netherlands; Andrew I.R. Maas, Department of Neurosurgery, Antwerp University Hospital, Edegem, Belgium, and

Department of Translational Neuroscience, Faculty of Medicine and Health Science, University of Antwerp, Antwerp, Belgium; Ana M. Castaño León, Department of Neurosurgery, Hospital Universitario 12 de Octubre, Madrid, Spain; Marc Maegele, Cologne-Merheim Medical Center (CMMC), Department of Traumatology, Orthopedic Surgery and Sportmedicine, Witten/Herdecke University, Cologne, Germany; Marek Majdan, Department of Public Health, Faculty of Health Sciences and Social Work, Trnava University, Trnava, Slovakia; Alex Manara, Intensive Care Unit, Southmead Hospital, Bristol, Bristol, U.K.; Geoffrey Manley, Department of Neurological Surgery, University of California, San Francisco, California, U.S.; Costanza Martino, Department of Anesthesia and Intensive Care, M. Bufalini Hospital, Cesena, Italy; Hugues Maréchal, Intensive Care Unit, CHR Citadelle, Liège, Belgium; Julia Mattern, Department of Neurosurgery, University Hospital Heidelberg, Heidelberg, Germany; Catherine McMahon, Department of Neurosurgery, The Walton Centre NHS Foundation Trust, Liverpool, U.K.; Béla Melegh, Department of Medical Genetics, University of Pécs, Pécs, Hungary; David Menon, Division of Anaesthesia, University of Cambridge, Addenbrooke's Hospital, Cambridge, U.K.; Tomas Menovsky, Department of Neurosurgery, Antwerp University Hospital, Edegem, Belgium, and Department of Translational Neuroscience, Faculty of Medicine and Health Science, University of Antwerp, Antwerp, Belgium; Ana Mikolic, Department of Public Health, Erasmus Medical Center-University Medical Center, Rotterdam, the Netherlands; Benoit Misset, Cyclotron Research Center, University of Liège, Liège, Belgium; Visakh Muraleedharan, Karolinska Institutet, INCF International Neuroinformatics Coordinating Facility, Stockholm, Sweden; Lynnette Murray, ANZIC Research Centre, Monash University, Department of Epidemiology and Preventive Medicine, Melbourne, Victoria, Australia; Ancuta Negru, Department of Neurosurgery, Emergency County Hospital Timisoara, Timisoara, Romania; David Nelson, Department of Physiology and Pharmacology, Section of Perioperative Medicine and Intensive Care, Karolinska Institutet, Stockholm, Sweden; Virginia Newcombe, Division of Anaesthesia, University of Cambridge, Addenbrooke's Hospital, Cambridge, U.K.; Daan Nieboer, Department of Public Health, Erasmus Medical Center-University Medical Center, Rotterdam, the Netherlands; József Nyírádi, János Szentágothai Research Centre, University of Pécs, Pécs, Hungary; Otesile Olubukola, Centre for Urgent and Emergency Care Research (CURE), Health Services Research Section, School of Health and Related Research (ScHARR), University of Sheffield, Sheffield, U.K.; Matej Oresic, School of Medical Sciences, Örebro University, Örebro, Sweden; Fabrizio Ortolano, Neuro ICU, Fondazione IRCCS Cà Granda Ospedale Maggiore Policlinico, Milan, Italy; Aarno Palotie, Institute for Molecular Medicine Finland, University of Helsinki, Helsinki, Finland, Analytic and Translational Genetics Unit, Department of Medicine; Psychiatric and Neurodevelopmental Genetics Unit, Department of Psychiatry, Department of Neurology, Massachusetts General Hospital, Boston, MA, U.S., and Program in Medical and Population Genetics, The Stanley Center for Psychiatric Research, The Broad Institute of MIT and Harvard, Cambridge, MA, U.S.; Paul M. Parizel, Department of Radiology, University of Antwerp, Edegem, Belgium; Jean François Payen, Department of Anesthesiology and Intensive Care, University Hospital of Grenoble, Grenoble, France; Natascha Perera, International Projects Management, ARTTIC, Munchen, Germany; Vincent Perlbarg, Anesthésie-Réanimation, Assistance Publique-Hopitaux de Paris, Paris, France; Paolo Persona, Department of Anesthesia and Intensive Care, Azienda Ospedaliera Università di Padova, Padova, Italy; Wilco Peul, Department of Neurosurgery, Leiden University Medical Center, Leiden, the Netherlands and Department of Neurosurgery, Medical Center Haaglanden, the Hague, the Netherlands; Anna Piippo-Karjalainen, Department of Neurosurgery, Helsinki University Central Hospital, Finland; Matti Pirinen, Institute for Molecular Medicine Finland, University of Helsinki, Helsinki, Finland; Dana Pisica, Department of Public Health, Erasmus Medical Center-University Medical Center, Rotterdam, the Netherlands; Horia Ples, Department of Neurosurgery, Emergency County Hospital Timisoara, Timisoara, Romania; Suzanne Polinder, Department of Public Health, Erasmus Medical Center-University Medical Center, Rotterdam, the Netherlands; Inigo Pomposo, Department of Neurosurgery, Hospital of Cruces, Bilbao, Spain; Jussi P. Posti, Division of Clinical Neurosciences, Department of Neurosurgery and Turku Brain Injury Centre, Turku University Hospital and University of Turku, Turku, Finland; Louis Puybasset, Department of Anesthesiology and Critical Care, Pitié -Salpêtrière Teaching Hospital, Assistance Publique, Hôpitaux de Paris and University Pierre et Marie Curie, Paris, France; Andreea Radoi, Neurotraumatology and Neurosurgery Research Unit (UNINN), Vall d'Hebron Research Institute, Barcelona, Spain; Arminas Ragauskas, Department of Neurosurgery, Kaunas University of Technology and Vilnius University, Vilnius, Lithuania; Rahul Raj, Department of Neurosurgery, Helsinki University Central Hospital, Finland; Malinka Rambadagalla, Department of Neurosurgery, Rezekne Hospital, Latvia; Isabel Retel Helmrich, Department of Public Health, Erasmus Medical Center-University Medical Center, Rotterdam, the Netherlands; Jonathan Rhodes, Department of Anaesthesia, Critical Care and Pain Medicine NHS Lothian and University of Edinburgh, Edinburgh, U.K.; Sylvia Richardson, Director, MRC Biostatistics Unit,

Cambridge Institute of Public Health, Cambridge, U.K.; Sophie Richter, Division of Anaesthesia, University of Cambridge, Addenbrooke's Hospital, Cambridge, U.K.; Samuli Ripatti, Institute for Molecular Medicine Finland, University of Helsinki, Helsinki, Finland; Saulius Rocka, Department of Neurosurgery, Kaunas University of Technology and Vilnius University, Vilnius, Lithuania; Cecilie Roe, Department of Physical Medicine and Rehabilitation, Oslo University Hospital/University of Oslo, Oslo, Norway; Olav Roise, Division of Orthopedics, Oslo University Hospital, Oslo, Norway, and Institute of Clinical Medicine, Faculty of Medicine, University of Oslo, Oslo, Norway; Jonathan Rosand, Broad Institute, Cambridge MA Harvard Medical School, Boston MA, Massachusetts General Hospital, Boston MA, U.S.; Jeffrey V. Rosenfeld, National Trauma Research Institute, The Alfred Hospital, Monash University, Melbourne, Victoria, Australia; Christina Rosenlund, Department of Neurosurgery, Odense University Hospital, Odense, Denmark; Guy Rosenthal, Department of Neurosurgery, Hadassah-Hebrew University Medical Center, Jerusalem, Israel; Rolf Rossaint, Department of Anaesthesiology, University Hospital of Aachen, Aachen, Germany; Sandra Rossi, Department of Anesthesia and Intensive Care, Azienda Ospedaliera Università di Padova, Padova, Italy; Daniel Rueckert, Department of Computing, Imperial College London, London, U.K.; Martin Rusnák, International Neurotrauma Research Organisation, Vienna, Austria; Juan Sahuquillo, Neurotraumatology and Neurosurgery Research Unit (UNINN), Vall d'Hebron Research Institute, Barcelona, Spain; Oliver Sakowitz, Department of Neurosurgery, University Hospital Heidelberg, Heidelberg, Germany, and Klinik für Neurochirurgie, Klinikum Ludwigsburg, Ludwigsburg, Germany; Renan Sanchez Porras, Klinik für Neurochirurgie, Klinikum Ludwigsburg, Ludwigsburg, Germany; Janos Sandor, Division of Biostatistics and Epidemiology, Department of Preventive Medicine, University of Debrecen, Debrecen, Hungary; Nadine Schäfer, Institute of Research in Operative Medicine (IFOM), Witten/Herdecke University, Cologne, Germany; Silke Schmidt, Department Health and Prevention, University Greifswald, Greifswald, Germany; Herbert Schoechl, Department of Anaesthesiology and Intensive Care, AUVA Trauma Hospital, Salzburg, Austria; Guus Schoonman, Department of Neurology, Elisabeth-TweeSteden Ziekenhuis, Tilburg, the Netherlands; Rico Frederik Schou, Department of Neuroanesthesia and Neurointensive Care, Odense University Hospital, Odense, Denmark; Elisabeth Schwendenwein, Trauma Surgery, Medical University Vienna, Vienna, Austria; Charlie Sewalt, Department of Public Health, Erasmus Medical Center-University Medical Center, Rotterdam, the Netherlands; Ranjit D. Singh, Department of Neurosurgery, Leiden University Medical Center, Leiden, the Netherlands and Department of Neurosurgery, Medical Center Haaglanden, the Hague, the Netherlands; Toril Skandsen, Department of Neuromedicine and Movement Science, Norwegian University of Science and Technology, NTNU, Trondheim, Norway; Department of Physical Medicine and Rehabilitation, St. Olavs Hospital, Trondheim University Hospital, Trondheim, Norway; Peter Smielewski, Brain Physics Lab, Division of Neurosurgery, Dept of Clinical Neurosciences, University of Cambridge, Addenbrooke's Hospital, Cambridge, U.K.; Abayomi Sorinola, Department of Neurosurgery, University of Pécs, Pécs, Hungary; Emmanuel Stamatakis, Division of Anaesthesia, University of Cambridge, Addenbrooke's Hospital, Cambridge, U.K.; Simon Stanwort, Oxford University Hospitals NHS Trust, Oxford, U.K.; Robert Stevens, Division of Neuroscience Critical Care, John Hopkins University School of Medicine, Baltimore, U.S.; William Stewart, Department of Neuropathology, Queen Elizabeth University Hospital and University of Glasgow, Glasgow, U.K.; Ewout W. Steyerberg, Department of Public Health, Erasmus Medical Center-University Medical Center, Rotterdam, the Netherlands, and Department of Biomedical Data Sciences, Leiden University Medical Center, Leiden, the Netherlands; Nino Stocchetti, Department of Pathophysiology and Transplantation, Milan University, and Neuroscience ICU, Fondazione IRCCS Cà Granda Ospedale Maggiore Policlinico, Milano, Italy; Nina Sundström, Department of Radiation Sciences, Biomedical Engineering, Umeå University, Umeå, Sweden; Riikka Takala, Perioperative Services, Intensive Care Medicine and Pain Management, Turku University Hospital and University of Turku, Turku, Finland; Viktória Tamás, Department of Neurosurgery, University of Pécs, Pécs, Hungary; Tomas Tamosuitis, Department of Neurosurgery, Kaunas University of Health Sciences, Kaunas, Lithuania; Mark Steven Taylor, Department of Public Health, Faculty of Health Sciences and Social Work, Trnava University, Trnava, Slovakia; Aurore Thibaut, Cyclotron Research Center, University of Liège, Liège, Belgium; Braden Te Ao, National Institute for Stroke and Applied Neurosciences, Faculty of Health and Environmental Studies, Auckland University of Technology, Auckland, New Zealand; Olli Tenovuo, Division of Clinical Neurosciences, Department of Neurosurgery and Turku Brain Injury Centre, Turku University Hospital and University of Turku, Turku, Finland; Alice Theadom, National Institute for Stroke and Applied Neurosciences, Faculty of Health and Environmental Studies, Auckland University of Technology, Auckland, New Zealand; Matt Thomas, Intensive Care Unit, Southmead Hospital, Bristol, Bristol, U.K.; Dick Tibboel, Intensive Care and Department of Pediatric Surgery, Erasmus Medical Center, Sophia Children's Hospital, Rotterdam, the Netherlands; Marjolein Timmers, Department of Intensive Care and

Department of Ethics and Philosophy of Medicine, Erasmus Medical Center, Rotterdam, the Netherlands; Christos Toliaas, Department of Neurosurgery, Kings College London, London, U.K.; Tony Trapani, ANZIC Research Centre, Monash University, Department of Epidemiology and Preventive Medicine, Melbourne, Victoria, Australia; Cristina Maria Tudora, Department of Neurosurgery, Emergency County Hospital Timisoara, Timisoara, Romania; Andreas Unterberg, Department of Neurosurgery, University Hospital Heidelberg, Heidelberg, Germany; Peter Vajkoczy, Neurologie, Neurochirurgie und Psychiatrie, Charité–Universitätsmedizin Berlin, Berlin, Germany; Shirley Vallance, ANZIC Research Centre, Monash University, Department of Epidemiology and Preventive Medicine, Melbourne, Victoria, Australia; Egils Valeinis, Neurosurgery Clinic, Pauls Stradins Clinical University Hospital, Riga, Latvia; Zoltán Vámos, Department of Anaesthesiology and Intensive Therapy, University of Pécs, Pécs, Hungary; Mathieu van der Jagt, Department of Intensive Care Adults, Erasmus MC–University Medical Center Rotterdam, Rotterdam, the Netherlands; Gregory Van der Steen, Department of Neurosurgery, Antwerp University Hospital, Edegem, Belgium; Joukje van der Naalt, Department of Neurology, University of Groningen, University Medical Center Groningen, Groningen, the Netherlands; Jeroen T.J.M. van Dijk, Department of Neurosurgery, Leiden University Medical Center, Leiden, the Netherlands and Department of Neurosurgery, Medical Center Haaglanden, the Hague, the Netherlands; Inge A. M. van Erp, Department of Neurosurgery, Leiden University Medical Center, Leiden, the Netherlands and Department of Neurosurgery, Medical Center Haaglanden, the Hague, the Netherlands; Thomas A. van Essen, Department of Neurosurgery, Leiden University Medical Center, Leiden, the Netherlands and Department of Neurosurgery, Medical Center Haaglanden, the Hague, the Netherlands; Wim Van Hecke, icoMetrix NV, Leuven, Belgium; Caroline van Heugten, Movement Science Group, Faculty of Health and Life Sciences, Oxford Brookes University, Oxford, U.K.; Ernest van Veen, Department of Public Health, Erasmus Medical Center–University Medical Center, Rotterdam, the Netherlands; Thijs Vande Vyvere, Radiology Department, Antwerp University Hospital, Edegem, Belgium; Roel P. J. van Wijk, Department of Neurosurgery, Leiden University Medical Center, Leiden, The Netherlands and Dept. of Neurosurgery, Medical Center Haaglanden, the Hague, The Netherlands Alessia Vargiolu, NeuroIntensive Care Unit, Department Neuroscience, IRCCS Fondazione San Gerardo dei Tintori, Monza, Italy; Emmanuel Vega, Department of Anesthesiology-Intensive Care, Lille University Hospital, Lille, France; Kimberley Velt, Department of Public Health, Erasmus Medical Center–University Medical Center, Rotterdam, the Netherlands;

Jan Verheyden, icoMetrix NV, Leuven, Belgium; Paul M. Vespa, Director of Neurocritical Care, University of California, Los Angeles, U.S.; Anne Vik, Department of Neuromedicine and Movement Science, Norwegian University of Science and Technology, NTNU, Trondheim, Norway, Department of Neurosurgery, St.Olavs Hospital, Trondheim University Hospital, Trondheim, Norway; Rimantas Vilcinis, Department of Neurosurgery, Kaunas University of Health Sciences, Kaunas, Lithuania; Victor Volovici, Department of Neurosurgery, Erasmus MC, Rotterdam, the Netherlands; Nicole von Steinbüchel, Institute of Medical Psychology and Medical Sociology, Universitätsmedizin Göttingen, Göttingen, Germany; Daphne Voormolen, Department of Public Health, Erasmus Medical Center–University Medical Center, Rotterdam, the Netherlands; Petar Vulekovic, Department of Neurosurgery, Clinical Centre of Vojvodina, Faculty of Medicine, University of Novi Sad, Novi Sad, Serbia; Kevin K.W. Wang, Department of Emergency Medicine, University of Florida, Gainesville, Florida, U.S.; Daniel Whitehouse, Division of Anaesthesia, University of Cambridge, Addenbrooke’s Hospital, Cambridge, U.K.; Eveline Wiegers, Department of Public Health, Erasmus Medical Center–University Medical Center, Rotterdam, the Netherlands; Guy Williams, Division of Anaesthesia, University of Cambridge, Addenbrooke’s Hospital, Cambridge, U.K.; Lindsay Wilson, Division of Psychology, University of Stirling, Stirling, U.K.; Stefan Winzeck, Division of Anaesthesia, University of Cambridge, Addenbrooke’s Hospital, Cambridge, U.K.; Stefan Wolf, Department of Neurosurgery, Charité–Universitätsmedizin Berlin, Corporate Member of Freie Universität Berlin, Humboldt-Universität zu Berlin, and Berlin Institute of Health, Berlin, Germany; Zhihui Yang, Broad Institute, Cambridge MA Harvard Medical School, Boston MA, Massachusetts General Hospital, Boston MA, U.S.; Peter Ylén, VTT Technical Research Centre, Tampere, Finland; Alexander Younsi, Department of Neurosurgery, University Hospital Heidelberg, Heidelberg, Germany; Frederick A. Zeiler, Division of Anaesthesia, University of Cambridge, Addenbrooke’s Hospital, Cambridge, U.K., and Section of Neurosurgery, Department of Surgery, Rady Faculty of Health Sciences, University of Manitoba, Winnipeg, MB, Canada; Veronika Zelinkova, Department of Public Health, Faculty of Health Sciences and Social Work, Trnava University, Trnava, Slovakia; Agate Ziverte, Neurosurgery Clinic, Pauls Stradins Clinical University Hospital, Riga, Latvia; Tommaso Zoerle, Neuro ICU, Fondazione IRCCS Cà Granda Ospedale Maggiore Policlinico, Milan, Italy.

Ethical Approval

The CENTER-TBI study (EC grant 602150) has been conducted in accordance with all relevant laws of the EU if directly applicable or of direct effect and all

relevant laws of the country where the Recruiting sites were located, including but not limited to, the relevant privacy and data protection laws and regulations (the “Privacy Law”), the relevant laws and regulations on the use of human materials, and all relevant guidance relating to clinical studies from time to time in force including, but not limited to, the ICH Harmonised Tripartite Guideline for Good Clinical Practice (CPMP/ICH/135/95) (“ICH GCP”) and the World Medical Association Declaration of Helsinki entitled “Ethical Principles for Medical Research Involving Human Subjects.” Ethical approval was obtained for each recruiting site. The list of sites, Ethical Committees, approval numbers and approval dates can be found on the website: <https://www.center-tbi.eu/project/ethical-approval>

Consent for Publication

Informed Consent by the patients and/or the legal representative/next of kin was obtained, accordingly to the local legislations, for all patients recruited in the Core Dataset of CENTER-TBI and documented in the e-CRF.

Availability of Data and Materials

Data for the CENTER-TBI study has been collected through the Quesgen e-CRF (Quesgen Systems Inc, USA), hosted on the INCF platform and extracted via the INCF Neurobot tool (INCF, Sweden). For the Imaging repository, image data collection has been facilitated and hosted on the icometrix platform (icometrix, Leuven). The CENTER-TBI database is currently accessible through Mica/Opal. Access will be granted only after approval of a study plan proposal, submitted through the online system (<https://www.center-tbi.eu/data/study>).

Authors’ Contributions

Thijs Vande Vyvere: Conceptualization, methodology, investigation, data curation, project administration, writing—original draft, writing—review and editing; Dana Pisciă: Investigation, data curation, methodology, formal analysis, visualization, writing—review and editing; Guido Wilms: Conceptualization, supervision, investigation, writing—review and editing; Lene Claes: Writing—review and editing; Max Wintermark: Methodology, writing—review and editing; Pieter Van Dyck: Methodology, writing—review and editing; Annemiek Snoeckx: Methodology, resources, writing—review and editing; Sven Dekeyzer: Methodology, writing—review and editing; Luc van den Hauwe: Supervision, writing—review and editing; Pim Pullens: Supervision, writing—review and editing; Jan Verheyden: Resources, writing—review and editing; Christine Mac Donald: Writing—review and editing; Andrew Maas: Conceptualization, supervision, methodology, writing—review and editing, funding acquisition;

Paul M. Parizel: Conceptualization, supervision, methodology, resources, writing—review and editing, funding acquisition.

Funding Information

Data used in preparation of this manuscript were obtained in the context of CENTER-TBI, a large collaborative project with the support of the European Union 7th Framework program (EC grant 602150). Additional funding was obtained from the Hannelore Kohl Stiftung (Germany), from OneMind (USA), from Integra LifeSciences Corporation (USA, and from NeuroTrauma Sciences (USA)).

Author Disclosure Statement

Jan Verheyden is an employee of icometrix, a for-profit imaging biomarker company.

For the other authors, no competing financial interests exist.

Supplementary Material

Supplementary Table S1
 Supplementary Table S2
 Supplementary Table S3
 Supplementary Table S4
 Supplementary Table S5
 Supplementary Table S6
 Supplementary Table S7
 Supplementary Table S8
 Supplementary Table S9
 Supplementary Table S10
 Supplementary Table S11
 Supplementary Table S12
 Supplementary Table S13
 Supplementary Table S14
 Supplementary Table S15
 Supplementary Table S16
 Supplementary Table S17
 Supplementary Table S18
 Supplementary Table S19
 Supplementary Figure S1
 Supplementary Figure S2
 Supplementary Figure S3
 Supplementary Figure S4
 Supplementary Figure S5
 Supplementary Figure S6
 Supplementary Figure S7
 Supplementary Figure S8
 Supplementary Figure S9
 Supplementary Figure S10
 Supplementary Figure S11
 Supplementary Figure S12
 Supplementary Figure S13
 Supplementary Figure S14
 Supplementary Figure S15
 Supplementary Figure S16
 Supplementary Figure S17
 Supplementary Figure S18
 Supplementary Figure S19
 Supplementary Figure S20
 Supplementary Figure S21
 Supplementary Figure S22
 Supplementary Figure S23
 Supplementary Figure S24
 Supplementary Figure S25
 Supplementary Figure S26
 Supplementary Figure S27
 Supplementary Figure S28

Supplementary Figure S29
 Supplementary Figure S30
 Supplementary Figure S31
 Supplementary Figure S32
 Supplementary Text File

References

- Teasdale G, Jennett B. Assessment of coma and impaired consciousness. A practical scale. *Lancet* 1974;2(7872):81–84; doi: 10.1016/s0140-6736(74)91639-0
- Teasdale G, Maas A, Lecky F, et al. The Glasgow Coma Scale at 40 years: standing the test of time. *Lancet Neurol* 2014;13(8):844–854; doi: 10.1016/s1474-4422(14)70120-6
- Wintermark M, Sanelli PC, Anzai Y, et al. Imaging evidence and recommendations for traumatic brain injury: conventional neuroimaging techniques. *J Am Coll Radiol* 2015;12(2):e1–e14; doi: 10.1016/j.jacr.2014.10.014
- Aiken AH, Gean AD. Imaging of head trauma. *Semin Roentgenol* 2010;45(2):63–79; doi: 10.1053/j.ro.2009.09.007
- Kim JJ, Gean AD. Imaging for the diagnosis and management of traumatic brain injury. *Neurotherapeutics* 2011;8(1):39–53; doi: 10.1007/s13311-010-0003-3
- Parizel PM, Van Goethem JW, Ozsarlak O, et al. New developments in the neuroradiological diagnosis of craniocerebral trauma. *Eur Radiol* 2005;15(3):569–581; doi: 10.1007/s00330-004-2558-z
- Wintermark M, Sanelli PC, Anzai Y, et al. Imaging evidence and recommendations for traumatic brain injury: advanced neuro- and neurovascular imaging techniques. *AJNR Am J Neuroradiol* 2015;36(2):E1–E11; doi: 10.3174/ajnr.A4181
- Saatman KE, Duhaime AC, Bullock R, et al. Classification of traumatic brain injury for targeted therapies. *J Neurotrauma* 2008;25(7):719–738; doi: 10.1089/neu.2008.0586
- Mutch CA, Talbott JF, Gean A. Imaging evaluation of acute traumatic brain injury. *Neurosurg Clin N Am* 2016;27(4):409–439; doi: 10.1016/j.nec.2016.05.011
- Huff JS, Jahar S. Differences in interpretation of cranial computed tomography in ED traumatic brain injury patients by expert neuroradiologists. *Am J Emerg Med* 2014;32(6):606–608; doi: 10.1016/j.ajem.2014.03.010
- Laalo JP, Kurki TJ, Sonninen PH, et al. Reliability of diagnosis of traumatic brain injury by computed tomography in the acute phase. *J Neurotrauma* 2009;26(12):2169–2178; doi: 10.1089/neu.2009.1011
- Haacke EM, Duhaime AC, Gean AD, et al. Common data elements in radiologic imaging of traumatic brain injury. *J Magn Reson Imaging* 2010;32(3):516–543; doi: 10.1002/jmri.22259
- Duhaime A-C, Gean AD, Haacke EM, et al. Common data elements in radiologic imaging of traumatic brain injury. *Arch Phys Med Rehabil* 2010;91(11):1661–1666; doi: 10.1016/j.apmr.2010.07.238
- Hicks R, Giacino J, Harrison-Felix C, et al. Progress in developing common data elements for traumatic brain injury research: version two—the end of the beginning. *J Neurotrauma* 2013;30(22):1852–1861; doi: 10.1089/neu.2013.2938
- Rincon SP, Mukherjee P, Levin HS, et al. Interrater reliability of National Institutes of Health traumatic brain injury imaging common data elements for brain magnetic resonance imaging in mild traumatic brain injury. *J Neurotrauma* 2021;38(20):2831–2840; doi: 10.1089/neu.2021.0138
- Vande Vyvere T, Wilms G, Claes L, et al. Central versus local radiological reading of acute computed tomography characteristics in multi-center traumatic brain injury research. *J Neurotrauma* 2019;36(7):1080–1092; doi: 10.1089/neu.2018.6061
- Purysko AS, Rosenkrantz AB, Barentsz JO, et al. PI-RADS Version 2: a pictorial update. *RadioGraphics* 2016;36(5):1354–1372; doi: 10.1148/rg.2016150234
- Donegan T, Mueller L, Prabhakar H. LI-RADS: pictorial review of the new standardized reporting system of liver findings in patients with ESLD. *J Vasc Interv Radiol* 2014;25(3):S191–S192; doi: 10.1016/j.jvir.2013.12.516
- Rao B, Ikuta I, Mahajan A, et al. Brain tumor reporting and data system: a pictorial review. *Neurographics* 2021; 11(3):175–185; <https://doi.org/10.3174/ng.2000069>
- Rao AA, Feneis J, Lalonde C, et al. A pictorial review of changes in the BI-RADS fifth edition. *RadioGraphics* 2016;36(3):623–639; doi: 10.1148/rg.2016150178
- Maas AI, Menon DK, Steyerberg EW, et al. Collaborative European NeuroTrauma Effectiveness Research in Traumatic Brain Injury (CENTER-TBI): a prospective longitudinal observational study. *Neurosurgery* 2015;76(1):67–80; doi: 10.1227/neu.0000000000000575
- Wilson JT, Pettigrew LE, Teasdale GM. Structured interviews for the Glasgow Outcome Scale and the extended Glasgow Outcome Scale: guidelines for their use. *J Neurotrauma* 1998;15(8):573–585.
- Chavent M, Kuentz-Simonet V, Liquet B, et al. ClustOfVar: An R package for the clustering of variables. *J Stat Softw* 2012;50(13):1–16; doi: 10.18637/jss.v050.i13
- York G, Barboriak D, Petrella J, et al. Association of internal carotid artery injury with carotid canal fractures in patients with head trauma. *Am J Roentgenol* 2005;184(5):1672–1678; doi: 10.2214/ajr.184.5.01841672
- Prosser JD, Vender JR, Solares CA. Traumatic cerebrospinal fluid leaks. *Otolaryngol Clin North Am* 2011;44(4):857–873, vii; doi: 10.1016/j.otc.2011.06.007
- Bullock MR, Chesnut R, Ghajar J, et al. Surgical management of depressed cranial fractures. *Neurosurgery* 2006;58(3 Suppl):S56–S60; doi: 10.1227/01.Neu.0000210367.14043.0e
- Cunqueiro A, Scheinfeld MH. Causes of pneumocephalus and when to be concerned about it. *Emerg Radiol* 2018;25(4):331–340; doi: 10.1007/s10140-018-1595-x
- Zimmerman RA, Bilaniuk LT. Computed tomographic staging of traumatic epidural bleeding. *Radiology* 1982;144(4):809–812; doi: 10.1148/radiology.144.4.7111729
- Gupta VK, Seth A. “Swirl sign” in extradural hematoma. *World Neurosurg* 2019;121:95–96; doi: <https://doi.org/10.1016/j.wneu.2018.10.010>
- Pruthi N, Balasubramaniam A, Chandramouli BA, et al. Mixed-density extradural hematomas on computed tomography-prognostic significance. *Surg Neurol* 2009;71(2):202–206; doi: 10.1016/j.surneu.2007.10.032
- Marshall LF, Marshall SB, Klauber MR, et al. The diagnosis of head injury requires a classification based on computed axial tomography. *J Neurotrauma* 1992;9 Suppl 1:S287–S292
- Parker SL, Kabani AA, Conner CR, et al. Management of venous sinus-related epidural hematomas. *World Neurosurg* 2020;138:e241–e250; doi: 10.1016/j.wneu.2020.02.089
- Holbourn AS. Mechanics of head injuries. *Lancet* 1943;2:438.
- Meaney D, Olvey SE, Gennarelli TA. Biomechanical basis of traumatic brain injury. 2011; doi: 10.1016/B978-1-4160-5316-3.00328-2
- Lee MC, Haut RC. Insensitivity of tensile failure properties of human bridging veins to strain rate: implications in biomechanics of subdural hematoma. *J Biomech* 1989;22(6-7):537–542; doi: 10.1016/0021-9290(89)90005-5
- Yamashita T, Friede RL. Why do bridging veins rupture into the virtual subdural space? *J Neurol Neurosurg Psychiatry* 1984;47(2):121–127; doi: 10.1136/jnnp.47.2.121
- Wilms G, Marchal G, Geusens E, et al. Isodense subdural haematomas on CT: MRI findings. *Neuroradiology* 1992;34(6):497–499; doi: 10.1007/bf00598959
- Verma RK, Kottke R, Anderegg L, et al. Detecting subarachnoid hemorrhage: comparison of combined FLAIR/SWI versus CT. *Eur J Radiol* 2013;82(9):1539–1545; doi: 10.1016/j.ejrad.2013.03.021
- Fisher CM, Kistler JP, Davis JM. Relation of cerebral vasospasm to subarachnoid hemorrhage visualized by computerized tomographic scanning. *Neurosurgery* 1980;6(1):1–9; doi: 10.1227/00006123-198001000-00001
- Morris GF, Marshall LF. O-5-64 A new, practical classification of traumatic subarachnoid hemorrhage. *Clin Neurol Neurosurg* 1997;99; doi: 10.1016/S0303-8467(97)81312-1
- Greene KA, Marciano FF, Johnson BA, et al. Impact of traumatic subarachnoid hemorrhage on outcome in nonpenetrating head injury. Part I: a proposed computerized tomography grading scale. *J Neurosurg* 1995;83(3):445–452; doi: 10.3171/jns.1995.83.3.0445
- Thelin EP, Nelson DW, Vehviläinen J, et al. Evaluation of novel computerized tomography scoring systems in human traumatic brain injury: an observational, multicenter study. *PLoS Med* 2017;14(8):e1002368; doi: 10.1371/journal.pmed.1002368
- Maas AI, Stocchetti N, Bullock R. Moderate and severe traumatic brain injury in adults. *Lancet Neurol* 2008;7(8):728–741; doi: 10.1016/s1474-4422(08)70164-9
- Valadka AB, Gopinath SP, Robertson CS. Midline shift after severe head injury: pathophysiologic implications. *J Trauma Acute Care Surg* 2000;49(1):1–10; doi: 10.1097/00005373-200007000-00001

45. Bullock MR, Chesnut R, Ghajar J, et al. Guidelines for the Surgical Management of Traumatic Brain Injury Author Group: Acknowledgments. *Neurosurgery* 2006;58(suppl_3):S2-vi–S2-vi; doi: 10.1093/neurosurgery/58.suppl_3.S2-vi
46. McCafferty RR, Neal CJ, Marshall SA, et al. Neurosurgery and medical management of severe head injury. *Mil Med* 2018;183(suppl_2):67–72; doi: 10.1093/milmed/usy071
47. Ropper AH. Lateral displacement of the brain and level of consciousness in patients with an acute hemispherical mass. *N Engl J Med* 1986; 314(15):953–958; doi: 10.1056/NEJM198604103141504
48. Altafulla J, Bordes S, Jenkins S, et al. The basal subarachnoid cisterns: surgical and anatomical considerations. *World Neurosurg* 2019;129: 190–199; doi: <https://doi.org/10.1016/j.wneu.2019.05.087>
49. Zhu GW, Wang F, Liu WG. Classification and prediction of outcome in traumatic brain injury based on computed tomographic imaging. *J Int Med Res* 2009;37(4):983–995; doi: 10.1177/147323000903700402
50. Colquhoun IR, Burrows EH. The prognostic significance of the third ventricle and basal cisterns in severe closed head injury. *Clin Radiol* 1989;40(1):13–16; doi: 10.1016/s0009-9260(89)80006-6
51. Riveros Gilardi B, Muñoz López JI, Hernández Villegas AC, et al. Types of cerebral herniation and their imaging features. *RadioGraphics* 2019; 39(6):1598–1610; doi: 10.1148/rg.2019190018
52. Koenig MA, Bryan M, Lewin JL, 3rd, et al. Reversal of transtentorial herniation with hypertonic saline. *Neurology* 2008;70(13):1023–1039; doi: 10.1212/01.wnl.0000304042.05557.60
53. Chenoweth JA, Gaona SD, Faul M, et al. Incidence of delayed intracranial hemorrhage in older patients after blunt head trauma. *JAMA Surg* 2018;153(6):570–575; doi: 10.1001/jamasurg.2017.6159
54. Peterson EC, Chesnut RM. Talk and die revisited: bifrontal contusions and late deterioration. *J Trauma* 2011;71(6):1588–1592; doi: 10.1097/TA.0b013e31822b791d
55. Hashimoto T, Nakamura N, Ke R, Ra F. Traumatic intraventricular hemorrhage in severe head injury. *No Shinkei Geka: Neurol Surg* 1992; 20(3):209–215.
56. Parizel PM, Makkat S, Van Miert E, et al. Intracranial hemorrhage: principles of CT and MRI interpretation. *Eur Radiol* 2001;11(9):1770–1783; doi: 10.1007/s003300000800
57. Dekeyser S, van den Hauwe L, Vande Vyvere T, et al. Traumatic brain injury: imaging strategy. In: *Clinical Neuroradiology: The ESNR Textbook*. (Barkhof F, Jager R, Thurnher M, et al. eds.) Springer International Publishing: Cham; 2019; pp. 1–45.
58. Mata-Mbemba D, Mugikura S, Nakagawa A, et al. Intraventricular hemorrhage on initial computed tomography as marker of diffuse axonal injury after traumatic brain injury. *J Neurotrauma* 2015;32(5):359–365; doi: 10.1089/neu.2014.3453
59. Halleivi H, Dar N, Barreto A, et al. The IVH score: a novel tool for estimating intraventricular hemorrhage volume: clinical and research implications. *Crit Care Med* 2009;37:969–974; doi: 10.1097/CCM.0b013e318198683a
60. Graeb D, Robertson W, Lapointe J, et al. Computed tomographic diagnosis of intraventricular hemorrhage. Etiology and prognosis. *Radiology* 1982;143:91–96; doi: 10.1148/radiology.143.1.6977795
61. LeRoux P, Haglund M, Newell D, et al. Intraventricular hemorrhage in blunt head trauma: an analysis of 43 cases. *Neurosurgery* 1992;31: 678–685; doi: 10.1227/00006123-199210000-00010
62. Li R, Yang W-S, Wei X, et al. The slice score: a novel scale measuring intraventricular hemorrhage severity and predicting poor outcome following intracerebral hemorrhage. *Clin Neurol Neurosurg* 2020;195:105898; doi: <https://doi.org/10.1016/j.clineuro.2020.105898>
63. Hwang BY, Bruce SS, Appelboom G, et al. Evaluation of intraventricular hemorrhage assessment methods for predicting outcome following intracerebral hemorrhage. *J Neurosurg* 2012;116(1):185–192; doi: 10.3171/2011.9.Jns10850
64. Bu Y, Chen M, Gao T, et al. Mechanisms of hydrocephalus after intraventricular haemorrhage in adults. *Stroke Vasc Neurol* 2016;1(1):23–27; doi: 10.1136/svn-2015-000003
65. Blumberg PC, Jones NR, North JB. Diffuse axonal injury in head trauma. *J Neurol Neurosurg Psychiatry* 1989;52(7):838–841; doi: 10.1136/jnnp.52.7.838
66. Beauchamp MH, Ditchfield M, Babl FE, et al. Detecting traumatic brain lesions in children: CT versus MRI versus susceptibility weighted imaging (SWI). *J Neurotrauma* 2011;28(6):915–927; doi: 10.1089/neu.2010.1712
67. Mittl RL, Grossman RI, Hiehle JF, et al. Prevalence of MR evidence of diffuse axonal injury in patients with mild head injury and normal head CT findings. *AJNR Am J Neuroradiol* 1994;15(8):1583–1589.
68. Moe HK, Follstad T, Andelic N, et al. Traumatic axonal injury on clinical MRI: association with the Glasgow Coma Scale score at scene of injury or at admission and prolonged posttraumatic amnesia. *J Neurosurg* 2020;1–12; doi: 10.3171/2020.6.Jns20112
69. Moen KG, Brezova V, Skandsen T, et al. Traumatic axonal injury: the prognostic value of lesion load in corpus callosum, brain stem, and thalamus in different magnetic resonance imaging sequences. *J Neurotrauma* 2014;31(17):1486–1496; doi: 10.1089/neu.2013.3258
70. Griffin AD, Turtzo LC, Parikh GY, et al. Traumatic microbleeds suggest vascular injury and predict disability in traumatic brain injury. *Brain* 2019;142(11):3550–3564; doi: 10.1093/brain/awz290
71. Vakil MT, Singh AK. A review of penetrating brain trauma: epidemiology, pathophysiology, imaging assessment, complications, and treatment. *Emerg Radiol* 2017;24(3):301–309; doi: 10.1007/s10140-016-1477-z
72. Part 2: Prognosis in penetrating brain injury. *J Trauma* 2001; 51(2 Suppl):S44–S86
73. Parizel PM, Makkat S, Jorens PG, et al. Brainstem hemorrhage in descending transtentorial herniation (Duret hemorrhage). *Intensive Care Med* 2002;28(1):85–88; doi: 10.1007/s00134-001-1160-y
74. Iencean SM. Brain edema—a new classification. *Med Hypotheses* 2003;61(1):106–109; doi: [https://doi.org/10.1016/S0306-9877\(03\)00127-0](https://doi.org/10.1016/S0306-9877(03)00127-0)
75. Ho M-L, Rojas R, Eisenberg RL. Cerebral edema. *Am J Roentgenol* 2012;199(3):W258–W273; doi: 10.2214/AJR.11.8081
76. Unterberg AW, Stover J, Kress B, et al. Edema and brain trauma. *Neuroscience* 2004;129(4):1021–1029; doi: 10.1016/j.neuroscience.2004.06.046
77. Boulard G, Marguinaud E, Sesay M. [Osmotic cerebral oedema: the role of plasma osmolarity and blood brain barrier]. *Ann Fr Anesth Reanim* 2003;22(3):215–219; doi: 10.1016/s0750-7658(03)00009-1
78. Reinink H, Jüttler E, Hacke W, et al. Surgical decompression for space-occupying hemispheric infarction: a systematic review and individual patient meta-analysis of randomized clinical trials. *JAMA Neurol* 2021;78(2):208–216; doi: 10.1001/jamaneurol.2020.3745
79. Launey Y, Fryer TD, Hong YT, et al. Spatial and temporal pattern of ischemia and abnormal vascular function following traumatic brain injury. *JAMA Neurol* 2020;77(3):339–349; doi: 10.1001/jamaneurol.2019.3854
80. Latronico N, Piva S, Fagoni N, et al. Impact of a posttraumatic cerebral infarction on outcome in patients with TBI: the Italian multicenter cohort INCEPT study. *Crit Care* 2020;24(1):33; doi: 10.1186/s13054-020-2746-5
81. Choi PMC, Ly JV, Srikanth V, et al. Differentiating between hemorrhagic infarct and parenchymal intracerebral hemorrhage. *Radiol Res Pract* 2012;2012:475497–475497; doi: 10.1155/2012/475497
82. Bladin CF, Chambers BR. Clinical features, pathogenesis, and computed tomographic characteristics of internal watershed infarction. *Stroke* 1993;24(12):1925–1932; doi: 10.1161/01.str.24.12.1925
83. Yaghi S, Raz E, Yang D, et al. Lacunar stroke: mechanisms and therapeutic implications. *J Neurol Neurosurg Psychiatry* 2021; doi: 10.1136/jnnp-2021-326308
84. Lu A, Shen PY, Dahlin BC, et al. Cerebral venous thrombosis and infarct: review of imaging manifestations. *Applied Radiology* 2016;45(3):9–17
85. Maas AI, Hukkelhoven CW, Marshall LF, et al. Prediction of outcome in traumatic brain injury with computed tomographic characteristics: a comparison between the computed tomographic classification and combinations of computed tomographic predictors. *Neurosurgery* 2005;57(6):1173–1182; doi: 10.1227/01.neu.0000186013.63046.6b
86. Nelson DW, Nyström H, MacCallum RM, et al. Extended analysis of early computed tomography scans of traumatic brain injured patients and relations to outcome. *J Neurotrauma* 2010;27(1):51–64; doi: 10.1089/neu.2009.0986
87. Raj R, Siironen J, B. Skrifvars M, et al. Predicting outcome in traumatic brain injury: development of a novel computerized tomography classification system (Helsinki Computerized Tomography Score). *Neurosurgery* 2014;75(6):632–647; doi: 10.1227/neu.0000000000000533
88. Maas AI, Steyerberg EW, Butcher I, et al. Prognostic value of computerized tomography scan characteristics in traumatic brain injury: results from the IMPACT study. *J Neurotrauma* 2007;24(2):303–314; doi: 10.1089/neu.2006.0033
89. Vehviläinen J, Skrifvars M, Reinikainen M, et al. External validation of the NeuroImaging Radiological Interpretation System and Helsinki

- computed tomography score for mortality prediction in patients with traumatic brain injury treated in the intensive care unit: a Finnish intensive care consortium study. *Acta Neurochir (Wien)* 2022; doi: 10.1007/s00701-022-05353-0
90. Wintermark M, Li Y, Ding VY, et al. Neuroimaging radiological interpretation system for acute traumatic brain injury. *J Neurotrauma* 2018; 35(22):2665–2672; doi: 10.1089/neu.2017.5311
 91. Yuh EL, Jain S, Sun X, et al. Pathological computed tomography features associated with adverse outcomes after mild traumatic brain injury: a TRACK-TBI study with external validation in CENTER-TBI. *JAMA Neurol* 2021;78(9):1137–1148; doi: 10.1001/jamaneurol.2021.2120
 92. Ommaya AK, Gennarelli TA. Cerebral concussion and traumatic unconsciousness. Correlation of experimental and clinical observations of blunt head injuries. *Brain* 1974;97(4):633–654; doi: 10.1093/brain/97.1.633
 93. Miley JT, Rodriguez GJ, Qureshi AI. Traumatic intracranial aneurysm formation following closed head injury. *J Vasc Interv Neurol* 2008; 1(3):79–82
 94. Schicho A, Luerken L, Meier R, et al. Incidence of traumatic carotid and vertebral artery dissections: results of cervical vessel computed tomography angiogram as a mandatory scan component in severely injured patients. *Ther Clin Risk Manag* 2018;14:173–178; doi: 10.2147/tcrm.S148176
 95. Vande Vyvere T, De La Rosa E, Wilms G, et al. Prognostic validation of the NINDS common data elements for the radiologic reporting of acute traumatic brain injuries: a CENTER-TBI Study. *J Neurotrauma* 2020; 37(11):1269–1282; doi: 10.1089/neu.2019.6710
 96. Harburg L, McCormack E, Kenney K, et al. Reliability of the NINDS common data elements cranial tomography (CT) rating variables for traumatic brain injury (TBI). *Brain Inj* 2017;31(2):174–184; doi: 10.1080/02699052.2016.1225989
 97. Creeden S, Ding VY, Parker JJ, et al. Interobserver agreement for the computed tomography severity grading scales for acute traumatic brain injury. *J Neurotrauma* 2020;37(12):1445–1451; doi: 10.1089/neu.2019.6871
 98. Nielson JL, Cooper SR, Yue JK, et al. Uncovering precision phenotype-biomarker associations in traumatic brain injury using topological data analysis. *PLoS One* 2017;12(3):e0169490; doi: 10.1371/journal.pone.0169490
 99. Richter S, Winzeck S, Kornaropoulos EN, et al. Neuroanatomical substrates and symptoms associated with magnetic resonance imaging of patients with mild traumatic brain injury. *JAMA Network Open* 2021; 4(3):e210994–e210994; doi: 10.1001/jamanetworkopen.2021.0994
 100. Maas AIR, Menon DK, Manley GT, et al. Traumatic brain injury: progress and challenges in prevention, clinical care, and research. *Lancet Neurol* 2022;21(11):1004–1060; doi: 10.1016/S1474-4422(22)00309-X
 101. Steyerberg EW, Wieggers E, Sewalt C, et al. Case-mix, care pathways, and outcomes in patients with traumatic brain injury in CENTER-TBI: a European prospective, multicentre, longitudinal, cohort study. *Lancet Neurol* 2019;18(10):923–934; doi: 10.1016/S1474-4422(19)30232-7
 102. Zeiler FA, Mathieu F, Monteiro M, et al. Diffuse intracranial injury patterns are associated with impaired cerebrovascular reactivity in adult traumatic brain injury: a CENTER-TBI validation study. *J Neurotrauma* 2020;37(14):1597–1608; doi: 10.1089/neu.2019.6959
 103. Czeiter E, Amrein K, Gravesteijn BY, et al. Blood biomarkers on admission in acute traumatic brain injury: relations to severity, CT findings and care path in the CENTER-TBI study. *EbioMedicine* 2020;56; doi: 10.1016/j.ebiom.2020.102785
 104. Whitehouse DP, Monteiro M, Czeiter E, et al. Relationship of admission blood proteomic biomarkers levels to lesion type and lesion burden in traumatic brain injury: a CENTER-TBI study. *EbioMedicine* 2022;75
 105. Riemann L, Mikolic A, Maas A, et al. Computed Tomography Lesions and Their Association With Global Outcome in Young People With Mild traumatic brain injury. *J Neurotrauma* 2023;40(11-12):1243–1254; doi: 10.1089/neu.2022.0055
 106. Yue JK, Yuh EL, Korley FK, et al. Association between plasma GFAP concentrations and MRI abnormalities in patients with CT-negative traumatic brain injury in the TRACK-TBI cohort: a prospective multicentre study. *Lancet Neurol* 2019;18(10):953–961; doi: 10.1016/S1474-4422(19)30282-0
 107. Yue JK, Winkler EA, Puffer RC, et al. Temporal lobe contusions on computed tomography are associated with impaired 6-month functional recovery after mild traumatic brain injury: a TRACK-TBI study. *Neurol Res* 2018;40(11):972–981; doi: 10.1080/01616412.2018.1505416
 108. Caterino, J.M., Raubenolt, A. and Cudnik, M.T. (2011), Modification of Glasgow Coma Scale Criteria for injured elders. *Acad Emerg Med* 18: 1014–1021; doi: 10.1111/j.1553-2712.2011.01164.x
 109. Borg J, Holm L, Cassidy JD, Peloso PM, Carroll LJ, von Holst H, Ericson K; WHO Collaborating Centre Task Force on Mild Traumatic Brain Injury. Diagnostic procedures in mild traumatic brain injury: results of the WHO Collaborating Centre Task Force on Mild Traumatic Brain Injury. *J Rehabil Med*. 2004 Feb;(43 Suppl):61–75; doi: 10.1080/16501960410023822.
 110. Carroll LJ, Cassidy JD, Holm L, Kraus J, Coronado VG; WHO Collaborating Centre Task Force on Mild Traumatic Brain Injury. Methodological issues and research recommendations for mild traumatic brain injury: the WHO Collaborating Centre Task Force on Mild Traumatic Brain Injury. *J Rehabil Med*. 2004 Feb;(43 Suppl):113–125; doi: 10.1080/16501960410023877
 111. Hu T-T, Yan L, Yan P-F, et al. Assessment of the ABC/2 method of epidural hematoma volume measurement as compared with computer-assisted planimetric analysis. *Biol Res Nursing* 2016;18(1):5–11; doi: 10.1177/1099800415577634
 112. Won S-Y, Zagorcic A, Dubinski D, et al. Excellent accuracy of ABC/2 volume formula compared with computer-assisted volumetric analysis of subdural hematomas. *PLoS One* 2018;13(6):e0199809; doi: 10.1371/journal.pone.0199809
 113. Webb AJS, Ullman NL, Morgan TC, et al. Accuracy of the ABC/2 Score for intracerebral hemorrhage. *Stroke* 2015;46(9):2470–2476; doi: 10.1161/STROKEAHA.114.007343
 114. Mahan M, Rafter D, Casey H, et al. tbiExtractor: a framework for extracting traumatic brain injury common data elements from radiology reports. *PLoS One* 2020;15(7):e0214775; doi: 10.1371/journal.pone.0214775
 115. Pons E, Braun LM, Hunink MG, et al. Natural language processing in radiology: a systematic review. *Radiology* 2016;279(2):329–343; doi: 10.1148/radiol.16142770
 116. Kuo W, Häne C, Mukherjee P, et al. Expert-level detection of acute intracranial hemorrhage on head computed tomography using deep learning. *Proc Natl Acad Sci* 2019;116(45):22737–22745; doi: 10.1073/pnas.1908021116
 117. Lin E, Yuh EL. Computational approaches for acute traumatic brain injury image recognition. *Front Neurol* 2022;13:791816; doi: 10.3389/fneur.2022.791816
 118. O'Neill TJ, Xi Y, Stehel E, et al. Active reprioritization of the reading workload using artificial intelligence has a beneficial effect on the turnaround time for interpretation of head CT with intracranial hemorrhage. *Radiol Artif Intell* 2020;3(2):e200024; doi: 10.1148/ryai.2020200024
 119. Monteiro M, Newcombe VFJ, Mathieu F, et al. Multiclass semantic segmentation and quantification of traumatic brain injury lesions on head CT using deep learning: an algorithm development and multicentre validation study. *Lancet Digit Health* 2020;2(6):e314–e322; doi: 10.1016/S2589-7500(20)30085-6
 120. Jain S, Vande Vyvere T, Terzopoulos V, et al. Automatic quantification of computed tomography features in acute traumatic brain injury. *J Neurotrauma* 2019;36(11):1794–1803
 121. Mathieu F, Gueting H, Gravesteijn B, et al. Impact of antithrombotic agents on radiological lesion progression in acute traumatic brain injury: a CENTER-TBI propensity-matched cohort analysis. *J Neurotrauma* 2020;37(19):2069–2080; doi: 10.1089/neu.2019.6911
 122. Koschmieder K, Paul MM, van den Heuvel TLA, et al. Automated detection of cerebral microbleeds via segmentation in susceptibility-weighted images of patients with traumatic brain injury. *Neuroimage Clin* 2022;35:103027; doi: 10.1016/j.nicl.2022.103027
 123. van den Heuvel TLA, van der Eerden AW, Manniesing R, et al. Automated detection of cerebral microbleeds in patients with traumatic brain injury. *Neuroimage: Clinical* 2016;12:241–251; doi: 10.1016/j.nicl.2022.103027
 124. Kamnitsas K, Ledig C, Newcombe VFJ, et al. Efficient multi-scale 3D CNN with fully connected CRF for accurate brain lesion segmentation. *Medical Image Analysis* 2017;36:61–78; doi: https://doi.org/10.1016/j.media.2016.10.004

125. Gale SD, Baxter L, Roundy N, et al. Traumatic brain injury and grey matter concentration: a preliminary voxel based morphometry study. *J Neurol Neurosurg Psychiatry* 2005;76(7):984–988; doi: 10.1136/jnnp.2004.036210
126. Newcombe VF, Correia MM, Ledig C, et al. Dynamic changes in white matter abnormalities correlate with late improvement and deterioration following TBI: a diffusion tensor imaging study. *Neurorehabil Neural Repair* 2016;30(1):49–62; doi: 10.1177/1545968315584004
127. Siqueira Pinto M, Winzeck S, Kornaropoulos EN, et al. Use of support vector machines approach via ComBat harmonized diffusion tensor imaging for the diagnosis and prognosis of mild traumatic brain injury: a CENTER-TBI Study. *J Neurotrauma* 2023;40(13-14):1317–1338; doi: 10.1089/neu.2022.0365
128. Ledig C, Heckemann RA, Hammers A, et al. Robust whole-brain segmentation: Application to traumatic brain injury. *Med Image Anal* 2015;21(1):40–58; doi: 10.1016/j.media.2014.12.003
129. Bickart K, Sheridan C, et al. A systematic review of resting-state fMRI in traumatic brain injury across injury age, severity, mechanism, chronicity, and imaging methods. *Neurology* 2023; 100(17); doi: <https://doi.org/10.1212/WNL.000000000020377>
130. Newcombe V, Richter S, Whitehouse DP, et al. Fluid biomarkers and neuroimaging in mild traumatic brain injury: current uses and potential future directions for clinical use in emergency medicine. *Emerg Med J* 2023;40(9):671–677; doi: 10.1136/emered-2023-213111